UC Davis
UC Davis Electronic Theses and Dissertations

Title

The Grapes of Math: Catalyzing the Migration to Single Vine Irrigation Management

Permalink

https://escholarship.org/uc/item/11p3g499

Author

Jenkins, Matthew

Publication Date

2023

Peer reviewed|Thesis/dissertation

eScholarship.org Powered by the California Digital Library
University of California

The Grapes of Math:
Catalyzing the Migration to Single Vine Irrigation Management

By

MATTHEW R. JENKINS
DISSERTATION

Submitted in partial satisfaction of the requirements for the degree of

DOCTOR OF PHILOSOPHY

in

Horticulture and Agronomy

in the

OFFICE OF GRADUATE STUDIES

of the

UNIVERSITY OF CALIFORNIA

DAVIS

Approved:

_____
David E. Block, Chair

_____
Brian N. Bailey, Co-Chair

_____
J. Mason Earles

_____
Megan K. Bartlett

Committee in Charge
2023

Acknowledgements

It would simply not be possible to thank everyone who supported the creation of this dissertation, so instead I would like to highlight a few of the most important people who helped me get here.

First and foremost, I would like to thank my advisor David Block. The genuinely kind spirit with which Dave approaches everything in his life is an inspiration, and has been a reliable grounding force throughout my graduate studies. Over the years Dave remains the most trustworthy critic of my work, always offering insightful perspective when others might not look hard enough. Even more, Dave helped me see my potential when I could not, opening my future to opportunities I may not have been confident enough to pursue with such determination otherwise.

I also owe a great deal to the former contributors to this project, who paved the way for those of us that followed. Andrew McElrone, who first accepted me into his lab as a Research Assistant, gave me a chance to pursue my passion for agricultural science while also earning a natural segue into this dissertation work. Konrad Miller has been a huge asset to this project from even before its official beginning, helping me build what I personally believe to be the most interesting and promising HRI model. I cannot say enough about the three undergraduate students I worked with during this project, Autumn Mannsfeld, Dylan Lenczewski-Jowers, and Fabiola Lizett Chavez Lamas. It was humbling to watch each of these students latch onto some part of this project, make it their own and take off running. It opened my eyes to how gratifying it is to help others learn.

Thank you to all of my QE committee members–Emilio Laca, M. Andrew Walker, Maciej Zwieniecki, Mason Earles and Kenneth Shackel–for offering me the opportunity to share my work and explore exciting questions with feedback from some of my favorite scientists. My memories related to this day will be some of my favorites from this whole process.

I would not be here without the guidance and feedback of my dissertation committee members, Brian Bailey, Mason Earles and Megan Bartlett. The ideas and feedback they shared were vital to the development of this project and my development as a scientist. Early on in my time here at UC Davis, Mason helped me publish my first paper and in doing so gave me the courage to start using coding to try to build tools for research and industry (Théroux-Rancourt *et al.,* 2020). These formative experiences shaped all of my work since and I will be forever grateful.

The support of friends made this graduate school experience not just survivable, but deeply enjoyable. Without the help of Sasha Mikhailova and Daniel Friedman, I may never have been drawn out of my shell (Mikhailova and Friedman, 2018). In addition to some unforgettable pen play, thank you both for always being ready to share a warm meal and a wild conversation. I hope we can continue our tradition of camping, over the years. Even though I'm still just a plant guy, albeit somewhat more officially, thank you to all my neuroscience and immunology friends for entertaining my company for all these years. And to my dear friend Qais Hanifi, thank you for giving me constant reminders of what matters most, and, of course, for all the long days we shared at the farm.

It seems an impossible task to sufficiently thank my family for all they have done to clear a manageable path for me through this life. My mother, Gay Young, my father, Peter Jenkins, and my sister, Eleanor Jenkins, all helped in their own important way to give me a childhood filled with wonder and exploration, cultivating a deep appreciation for the sciences that sent me on this trajectory. My wife's family including her mother, Debbra Heim, her brother, Sean Prendergast, and his partner, Anna Thisius, deserve more gratitude than I can muster here, and have been incredibly supportive throughout this process, especially in the hardest of times. A massive thank you to my great friend and mentor, my father in-law, Franklyn Prendergast, who continues to be a steadfast reminder of the value of education. His generosity changed my life, allowing me to explore academic interests to my heart's desire.

This dissertation is dedicated to my wife, Kathryn Prendergast, who is a constant source of support for everything that brings me joy and fulfillment. Completing our graduate work at the same time, helping one another work stepwise through what at once seemed like an insurmountable series of achievements, has been one of the best experiences of my life. This dissertation is equally dedicated to our late cat, Bean Prenkins, who saw Kathryn and I through not only our time in Madison, but also Boulder, and then graduate school. She was our guiding light, a companion of immeasurable importance, a reliable warm ball of impossibly soft black fur in my lap and my best friend. Thank you, Bean, for teaching me the wisdom of a loving kindness spirit.

Visual Abstract

Research Goal: Develop a comprehensive single plant water use **sensing** and **delivery** system.

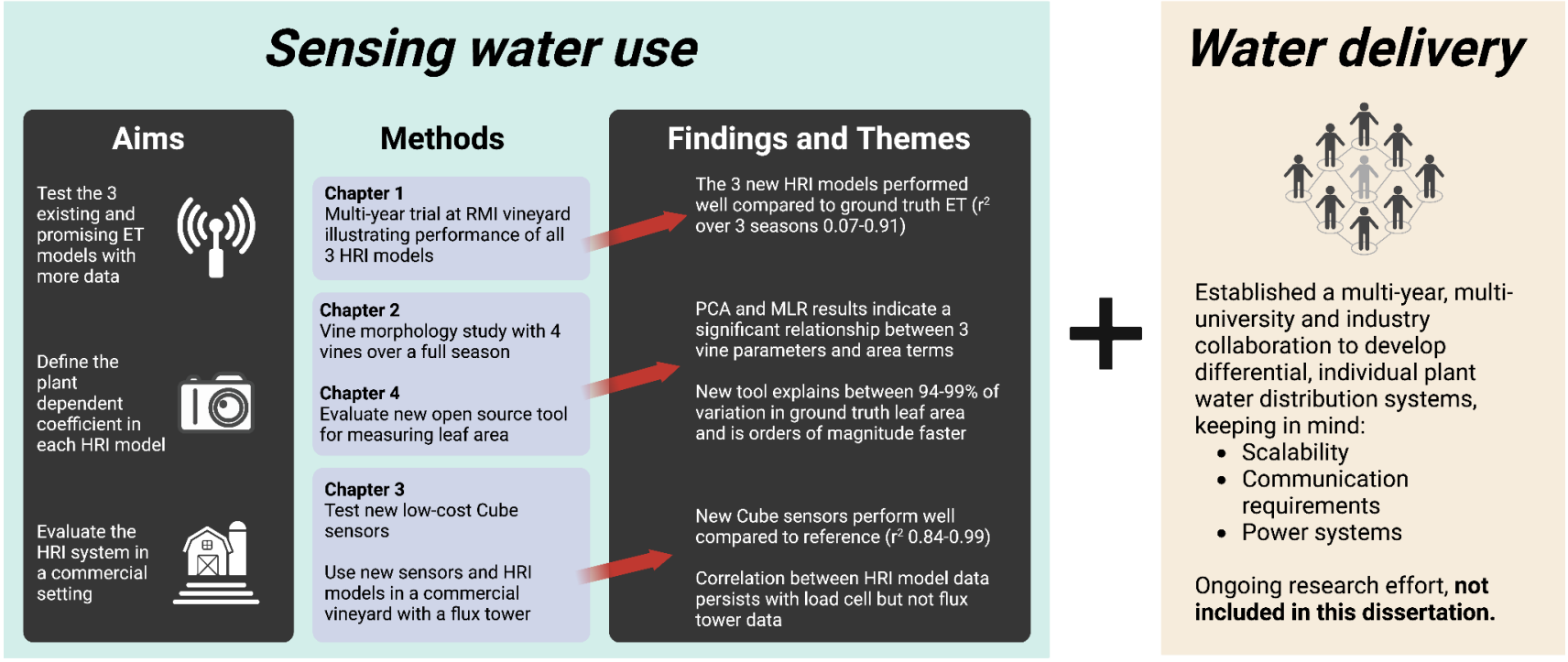

Visual abstract for, *The Grapes of Math: Catalyzing the Migration to Single Vine Irrigation Management (Jenkins, M. R., 2023)*

Abstract

As the global human population grows, the water demands of agriculture will likewise increase. Currently, over half of the world's water consumption is due to crop irrigation. Therefore, improving irrigation is essential to alleviating the effects of these rising demands. Developing low-cost technology for custom water delivery to individual or small groups of vines is a critical next step to advance precision irrigation. Current systems for estimating evapotranspiration (ET), or plant water use, work on the scale of a full vineyard (e.g., 3-5 acres) or the scale of a single vine, but at a cost that prohibits monitoring past a small number of representative vines. An ideal irrigation system, on the other hand, would rely on measurements of water demand—defined by both water use and water status indicators—and provide water to plants in response to these measurements.

Meeting this challenge would require a multidisciplinary effort over multiple years, but that is the goal of this dissertation, to develop a comprehensive single plant water use sensing and delivery system. First, three new ET models based on first principles or simple correlations are introduced and the results of a multi-year trial at RMI vineyard are presented to illustrate the performance of each of the novel High Resolution Irrigation (HRI) models. Results suggest the three models perform well, with single vine ET measurements from all three models consistently showing a strong relationship with ground truth ET measurements. Though these early results showed HRI is possible (range in r^2 = 0.07 - 0.92), in order to make this technology generalizable to any vine, it must be possible to measure the area term in each model directly from observations. This is the focus of the second chapter, in which vine physical characteristics were measured on a weekly basis throughout the season, then compared to area terms experimentally calculated periodically throughout the season using ground truth data and HRI model estimates. Multiple linear regression and principal component analyses suggest a significant relationship (p-value < 0.05, r^2 = 0.58 - 0.80) between two of the model area terms

and vine physical parameters including canopy superficial area, canopy polygon area and fraction of absorbed photosynthetically active radiation (fPAR). With these results it is possible to test the HRI ET models in a commercial agriculture context. Then a new low-cost biometeorological sensor is introduced, tested against reference sensors, then used to test the three HRI models in a commercial vineyard alongside research grade flux tower sensors. The Cube sensors showed strong correlation with the research grade reference sensors, fulfilling one of the early project goals of developing a low-cost biometeorological sensor for HRI and testing it in a commercial context. In the final chapter the new Leaf Area Tool image analysis pipeline is introduced, supporting HRI with new tools for extracting vine parameters related to model area terms from raw data. This field ready, fast (300x to 1400x faster than other methods tested) and accurate (r^2 = 0.94 - 0.99) method for the quantification of leaf area from digital images is tested on a diverse dataset of broad leaves.

Table of Contents

The Grapes of Math: Catalyzing the Migration to Single Vine Irrigation Management……..i

Acknowledgements…….ii

Visual Abstract……v

Abstract……vi

Table of Contents……..viii

Introduction: ***A review of evapotranspiration estimation methods for high-value crop applications*……1**

Abstract……2
Introduction……3
Coarse scale ET estimates……..……...10
Fine scale ET estimates……25
Distribution systems……...35
Discussion...……..……39

Chapter 1: ***Novel algorithms for high resolution prediction of canopy evapotranspiration in grapevine*……46**

Abstract……46
Introduction……..……47
Materials and methods……..……...52
Results……...……59
Discussion……..……..67

Chapter 2: ***Quantifying vine size and morphology for the High Resolution Irrigation evapotranspiration models*……72**

Abstract……72
Introduction……...73
Materials and methods……..……...76
Results……..……81
Discussion……..……..87

Chapter 3: ***Comparing novel single vine sensors and High Resolution Irrigation algorithms for ET to lysimetric and flux tower ET*……...….92**
Preface……..92
Introduction……..93
Materials and methods……...98
Results……102
Discussion……..106

Chapter 4: ***Leaf Area Tool, open source pipeline for automated leaf area detection*…….112**
Preface……112
Introduction……113
Materials and methods……119
Results……122
Discussion……..127

Summary……133

Bibliography……..141

Introduction

A review of evapotranspiration estimation methods for high-value crop applications

Matthew Jenkins, David E. Block

Preface

Typically a Graduate Group in Horticulture and Agronomy (GGHA) dissertation "Introduction" section is composed of an in-depth literature review complementing the relevant literature reviewed in each subsequent chapter. While the following manuscript (**ready for submission**) meets this criteria, it is also written as a stand alone journal article situated in the context of the field and modern global conditions. As such, it thoroughly covers the topics of plant water use sensing and water status sensing, as well as relevant recent publications in these areas; however, it does not fulfill the GGHA requirement to include a final section guiding the dissertation reader through the material to be presented. In lieu of this, a short discussion follows, introducing the overarching research question as well as the logic and organization of the chapters:

The overall goal of the HRI project is to develop a comprehensive single plant water use sensing and delivery system. In each chapter at least one of the aims proposed in my Qualifying Exam (QE) is explored through significant, often collaborative research efforts. The three QE aims were designed to address the central research question. In the first dissertation chapter the three novel High Resolution Irrigation (HRI) models are presented in a multi-year trial at the Robert Mondavi Institute (RMI) vineyard, addressing QE aim 1 which relates to testing the HRI models. The second dissertation

chapter deals with the area term in each of the three HRI models, and also addresses QE aim 2. The third dissertation chapter features an example of the HRI method being tested in a commercial context, thereby addressing QE aim 3. Thus, the organization of the chapters is quite logical up to this point. Then, in the fourth dissertation chapter a new software tool for leaf area analysis is introduced, complementing the entire HRI pipeline. The final dissertation section is a summary, focused on synthesizing all the results from all chapters in the context of the research goals formed at the outset of this project.

Abstract

More than half of global water use can be attributed to crop irrigation, and as human population grows so will the water requirements of agriculture. Improved irrigation will be critical to mitigating the impact of increased requirements. An ideal irrigation system is informed by measurements of water demand–a combination of water use and water status signals–and delivers water to plants based on this demand. In this review, examples of methods for monitoring water status are reviewed, along with details on stem and trunk water potential measurements. Then, methods for monitoring evapotranspiration (ET), or water use, are described. These methods are broken into coarse and fine scale categories, with a 10 meter spatial resolution threshold between them. Fourteen crop ET technologies are presented, including examples of successful estimation of ET in research and field settings, as well as limitations. The focus then shifts to water distribution technologies, with an emphasis on the challenges associated with the development of systems that achieve dynamic single plant resolution. Some attention is given to the process of choosing ET and water status sensing methods as well as water delivery system design given site characteristics and agronomic goals. The review concludes with a short discussion on the future directions of ET research and the importance of translating findings into useful tools for growers.

Introduction

As the global population continues to grow, so do the water demands of civilization (Jägermeyr *et al.,* 2017). These demands are driven principally by agriculture, which over the last decade accounted for approximately 70% of freshwater withdrawals from surface and subsurface water systems worldwide; and in developing countries this percentage may be as high as 90% (Foley *et al.,* 2011; Siebert *et al.,* 2010). Irrigation as defined by the Food and Agriculture Organization of the United Nations is by far the largest consumer of global water, accounting for 90% of all agricultural water use and more than 63% of overall water use (Zhang *et al.,* 2022). Given these statistics, it is difficult to predict the impact of continually increasing irrigated agricultural land throughout the world, which has almost doubled since the 1970s and now accounts for more than 40% of the total area used for agricultural production (FAO, 2014). In 2015, irrigated agricultural land was estimated to be about 3.14 million km^2 globally, but this figure is sensitive to many sources of error and has continued to rise for almost a decade since (Salmon *et al.,* 2015; Meier *et al.,* 2018). Irrigation's rapid acceptance over the last 70 years is the result of the proliferation of knowledge about the importance of irrigation for increasing agricultural production and reducing vulnerability of crops to failures, both critical to supporting growing populations (Smith, 2012). While irrigation technology and ancillary infrastructure principally address crop survival and yield, these resources also empower farmers to grow high value crops which can be more sensitive to water (Llamas and Martínez-Santos, 2005).

High value crops, like grapes or tree fruits and nut crops with structured canopies, are more water intensive than some seasonal crops such as wheat, corn and soy, as examples. For instance, though water footprints of all crops exhibit large spatial and temporal variation, producing 1 kilogram of almonds in California has been reported to require approximately 10,000 liters of water (Fulton et al., 2019), while producing 1 kilogram of wheat in Iraq, a similarly arid environment, has been reported to require approximately 1,876 liters of water

(Ewaid et al., 2019). Due to their significant water demands, nearly all commercial almond orchards in regions without ample rainfall, such as the Central Valley of California, are irrigated (Schwankl et al., 2020). Adequate rainfall poses an issue for viticulturists as well. While water needs vary greatly by region, varietal, and production style, it is estimated vineyards require about 650 millimeters of rainfall per year (Geisel et al., 2002). In recent years, these rainfall needs have not been met in many key viticultural areas such as California, South Australia, and parts of Southern Europe. As a result, drip irrigation is increasingly used in viticulture to make up the gap between vine water demand and what is available to vines in subsurface water systems from natural rainwater. In addition, it should be noted that vine water demand will be a strong function of the desired yield, with larger fruit yield demanding larger water uptake by the plant. While drip irrigation systems are designed to sustain crops, more importantly, they sustain agricultural industries, the economic importance of which cannot be understated.

The presence of widespread, sophisticated irrigation technology, while useful, requires abundant freshwater resources in order to achieve the parallel goals of agricultural and economic sustainability. The 2012 to 2017 drought in California underscores what happens when a region depending on agriculture for the majority of its economic activity is faced with immutable natural resource limitations. Howitt *et al.,* 2015 estimated the total drought impact on the California economy at $2.74 billion, with wide ranging effects on the environment, economy and society. Those in the agricultural industry bore the brunt of the effect, contending with a severe decrease in water resources that lead directly to nearly 3% losses in crop revenue, and a 75% increase in the cost of water pumping (Howitt *et al.,* 2015). Over time, the economic pressure created by the multi-year drought led to a 45% increase in idle land in California, over 21,000 lost jobs, and created the ideal conditions for the intense 2017 wildfires that caused unprecedented property and environmental damage (Kogan *et al.,* 2018). This sombering example is a salient reminder of the importance of natural water resources. Clearly, the

management of freshwater is paramount to a successful future trajectory of our agriculture industries, if not civilization itself.

One of the ways regions like California can manage water use is to focus on optimizing agricultural water use, the majority of which is accounted for by irrigation. The importance of optimizing irrigation is not only in minimizing water use by eliminating unnecessary overwatering, but also creating optimal conditions for crop development. Generally speaking, when root zone moisture is ideal throughout a plant's life cycle all crops will see improved yield, decreased disease pressure and improved vigor compared to plants grown in less than ideal conditions (Smith, 2012). Despite this knowledge the most common form of irrigation used by commercial growers of high value crops are drip systems that treat all plants in a management zone identically, even though it is known all plants do not require the same amount of water. Water demand heterogeneity can arise from cultivar differences, complex topography, canopy orientation, soil structure and composition, or roguing practices for disease control, as examples (Bambach et al., 2022b). When this variability is combined with complex deficit irrigation strategies, optimization of irrigation schemes becomes quite challenging.

If high value crop growers can meet this challenge head-on, by implementing effective irrigation strategies that can account for the complexity of plant water demand, or even approximate it, the possibility of simultaneously reducing unnecessary water use while maintaining or improving crop quality could become a reality (Stewart et al., 2011). For example, in 2017 researchers reported a two treatment experiment using grapevines at an E&J Gallo vineyard in Galt, California, USA. In the study, one block of "stressed" vines was irrigated with 69% of the amount of water applied to the grower standard irrigation treatment block. Not only were no significant yield differences observed between stressed and standard treatments, but the only significant qualitative difference was an increased concentration of malic acid content (Ko-Madden et al., 2017).

This review presents a comprehensive overview of the methods available to growers of high value crops for estimating evapotranspiration (ET) and informing irrigation scheduling in commercial agriculture systems. While other reviews of methods for estimating ET exist (Gharsallah et al., 2013; Ghiat et al., 2021; Prenger et al., 2002; Subedi et al., 2015; Zhang et al., 2016), none are focused on applications specific to high value perennial, woody cropping systems. To address this gap in the literature, and in order to present ET estimation options for high value crops in an organized and digestible format, we have organized the methods into two distinct groups of coarse scale and fine scale estimations (Table 1). For the purpose of this manuscript, we have defined the threshold for coarse scale as 10 meter spatial resolution or lower, a decision influenced by the 10 meter resolution of images taken by the Sentinel-2A satellite (Li *et al.,* 2019b). We acknowledge many of the technologies mentioned in this manuscript could be considered either fine or coarse scale depending on the application context, but categorize them anyways for the sake of an organized discussion. In the following sections, we will first introduce the important nuance between *how much* water plants need, and *when* they need it. Then, we will discuss coarse and fine scale ET technologies. As each technology is introduced, related concepts are explored, the forms of data required for calculations are discussed, as well as some examples of the successful implementation and any known weaknesses or limitations. Then, water distribution systems are considered in the context of ET estimates, with an emphasis on high spatial resolution distribution systems. In the conclusion section, major themes are revisited and the future directions of ET research are discussed.

How much vs. when?

To achieve the abstract goal of watering a plant according to its needs requires two fundamental components: (1) an engineered system for targeted delivery of water to each plant, and (2) an understanding of the plant's water needs that can inform irrigation decisions. The second component, understanding a plant's water needs, requires knowing how much water to

apply and when to apply it. While this may seem a trivial distinction, the questions of *how much* and *when* to water a plant have two very different answers, and arriving at those answers requires collecting and analyzing different types of data.

While estimating ET can inform *how much* water to give a plant, determining the best time to give this water to a plant requires understanding something about the plants' water status (Shackel *et al.,* 1997). Water status refers to water potential, a thermodynamic concept describing the Gibbs free energy per unit volume of some phase of water relative to pure liquid water at 1 ATM. The magnitude of this value is a result of both the soil water content and evaporative demand of the atmosphere (Ortuño *et al.,* 2006). In practice water potential can be a useful signal for growers because it can indicate whether or not a plant is experiencing debilitating water stress that prevents transpiration and reduces growth or photosynthesis (Nobel, 2005). Water potential is most commonly measured using a pressure chamber device, but when using this kind of device it is important to consider the difference between stem and leaf water potential.

In woody plants, such as grapes or tree crops, leaf water potential is not a reliable indicator of the water status of the whole plant because physiological and micrometeorological differences can cause local differences in leaf water potential (Kisekka, 2023; Nobel, 2005). Stem water potential serves as a better indicator of whole plant vascular performance and can be easily measured using a leaf bagging method that allows time for the leaf and petiole to equilibrate with stem water potential before measurement with a pressure chamber (Shackel et al., 1997). Although stem water potential can be a useful measurement, it is also a labor intensive process and for this reason has not seen widespread adoption beyond research (Kisekka, 2023). Also, it is known that stem water potential fluctuates diurnally and seasonally, which makes it difficult to set absolute general water potential thresholds for irrigation management. In order to use stem water potential information to trigger an irrigation system, measurements on target plants need to be benchmarked against non-stressed plants of the

same type in the same environment. Another recent study suggests developing crop and cultivar specific thresholds for commercial irrigation scheduling based on trunk water status measurements (Pagay, 2022).

To overcome these challenges, several automated and continuous methods for measuring or inferring stem water potential have been developed, including trunk diameter fluctuation sensors, sap flow sensors and micro tensiometers. Measuring trunk diameter fluctuation on a daily basis allows the extraction of a maximum daily shrinkage factor that has been shown to be effective for estimating the water status of trees (Huguet *et al.,* 1992; Cabibel and Isberie 1997; Cohen *et al.,* 2001). Sap flow sensors, which measure the flow of water and nutrients through xylem via the compensation heat-pulse method (Green and Clothier, 1988), or tensiometer sensors may also be used to estimate plant water status (Blanco and Kalcsits, 2021; Lakso et al., 2022). In the heat-pulse method a small wire is heated, and the rate at which this heat dissipates is correlated with sap flow rate. Tensiometers work by measuring the pressure in the xylem directly via a pressure sensor embedded in the trunk. While many measurement options exist, it is important to consider when to collect stem water potential measurements, as midday or solar noon water values for the same plant may give different results than a pre-dawn measurement, and reflect different physical concepts.

The predawn stem water potential measurement aims to understand the soil water potential based on the assumption that the roots of well-watered plants will equilibrate with the soil water potential overnight (Donovan *et al.,* 2001). A midday or solar noon stem water potential measurement may be useful for measuring the stress experienced by the plant during the last few hours, but may not reflect how much water a plant has access to for transpiration. Despite some limitations, in commercial almond cultivation, for example, midday stem water potential is considered the best indicator of whole plant water status because the pressure signal integrates information from the entire soil-plant-atmosphere continuum, capturing the effects of root zone and environmental conditions in one measurement (Fulton et al., 2014).

While tools like pressure chambers, trunk diameter calipers, sap flow sensors or even observation can be useful for determining *when* plants are transpiring or *when* to apply irrigation, these tools cannot directly measure *how much* water plants need.

Measuring Evapotranspiration

Evapotranspiration is a fundamental component of the global water cycle, connecting water, carbon and energy systems, but it is also fundamentally difficult to measure and predict because it integrates evaporation and transpiration (Zhang et al., 2016). Evaporation is a passive process that occurs at the soil surface and other wet surfaces. Vegetation transpires principally because it allows the plant simultaneous access to carbon dioxide and a means of keeping itself cool under the heat load of the sun, but it is also essential for plant growth and drives the transport of nutrients throughout the plant (Nobel, 2005). Measuring the combined effect of the vaporization of liquid water from surfaces into the atmosphere and the vaporization of liquid water inside leaves, plus the transport of these water vapors away from the site of vaporization, is not straightforward. The evaporation aspect of this process is driven by incident solar energy while the water vapor transport aspect is driven by the vapor pressure difference between the water vapor near the evaporating surface and the water vapor in the atmosphere (Allen et al., 1998).

Over the years, numerous methods have been devised to measure ET but many share some common characteristics. Some can be classified as mechanistic models, and others empirical. Mechanistic models are based on physical laws, though they often include assumptions or simplifications. These models are thought to be more precise because they can account for crop related changes, such as the Penman-Monteith model which includes terms describing physiological responses to the environment (Katsoulas and Stanghellini, 2019). Empirical models are based on observed correlations between multiple concepts. While these methods may be simple and often require less data, they typically lack generalizability. The Hargreaves model, for example, is well suited to closed greenhouse environments but is not

validated for performance in open field settings (Srivastava et al., 2018). Another limitation of many of the approaches to measuring ET is the spatial resolution of estimates, which can vary widely from several hectares to several square meters. In this study, we will categorize each ET estimation method as either Coarse Scale (> 10 m spatial resolution) or Fine Scale (< 10 m spatial resolution).

Coarse scale ET estimates

In many cases it makes more sense to measure ET at a spatial scale greater than 10 meters. In fact, it is not uncommon for the scale of estimates to be orders of magnitude greater than this threshold. In some parts of the world there is limited or no access to field measurements of meteorological data, so satellite or other remote sensing based estimates are the best or only option for estimating ET. In other cases there is simply not enough funding for fine scale measurements of ET, which are relatively more expensive because of increased sensor requirements and frequency of consultations with experts for data collection and analysis. While rare, it is also possible an environment may be nearly homogeneous in terms of soil composition, topography and elevation. In these cases, a fine scale estimate of ET is not necessary for adequate management of irrigation.

Original Penman-Monteith

The Penman-Monteith model is one of the first and seminal methods for estimating ET, but it was actually the culmination of two scientists' work spanning decades and institutions. Working at the Rothamsted Experimental Station, Howard Latimer Penman approached modeling the evaporation of water from an open surface and devised an equation used to this day. This model is based on only physical drivers, though, and was originally validated for open water bodies, well-watered grass and bare soil (Penman, 1948). In the 1950 and 60's John Lennox Monteith revisited the problem of evaporation of water, but this time with a focus on plant transpiration. To improve estimates of evaporation over well-water grass, Monteith

measured the resistance of stomata in the field then added this diffusion resistance to Penman's model (Monteith et al., 1965). The first example of an application of Penman-Monteith to a two layer model, which separates energy exchange at the canopy and soil levels, marked an important shift towards next generation modeling (Shuttleworth and Wallace, 1985). Many later models also focused on simplification, eliminating collinear terms and reducing data collection requirements without major impacts on accuracy of estimates (Steiner et al., 1991). Given all the options, growers must choose which of the numerous Penman-Monteith models to use. When considering which model to use, it is important growers are well informed on which models were designed for and validated in meteorological settings closest to the field conditions in question.

The original Penman-Monteith equation [Equation 1] is composed of two main terms, the surface resistance and aerodynamic resistance terms (Allen et al., 1998).

$$\lambda ET = \frac{\delta(R_n - G) + \rho_a C_p \frac{(e_s - e_a)}{r_a}}{\delta + \gamma(1 + \frac{r_s}{r_a})}$$

The λ term is the latent heat of vaporization of water, δ is the slope of the saturation vapor pressure curve, ρ_a is the mean air density at isobaric conditions, C_p is the specific heat of air, $e_s - e_a$ is a vapor pressure deficit term, γ is the psychrometric constant, r_s and r_a are the surface and aerodynamic resistance terms, respectively. Surface resistance is the resistance of water vapor to movement through the leaf stomata and soil surface, while aerodynamic resistance is the resistance of vertical water vapor diffusion from the leaf to the surrounding air. Surface resistance can be further subdivided into terms for bulk stomatal resistance of a well-illuminated leaf and active leaf area index. The bulk stomatal resistance is highly dependent on the type of crop, meteorological conditions, soil moisture content, and solute concentration in water. Active leaf area index is a dimensionless measure of the upper side area of the leaf per unit area of the soil underneath it, and as a result depends on the plant type, leaf density and life-cycle stage. Aerodynamic resistance is estimated from wind speed

measurements and calculated roughness lengths. These abstract lengths represent aspects of the heat and vapor transfer process, and can be estimated as one tenth of crop height (Allen et al., 1998).

While Penman-Monteith is a pioneering model it also has remarkable longevity in the field, with many examples of successful applications spanning the last 20 years. As an example, a two layer Shuttle and Wallace inspired model with added sub-models for net radiation and soil heat flux was used in 2010 to estimate the ET of a Merlot vineyard in Chile (Ortega-Farais et al., 2010). The Penman-Monteith approach has also been validated on tropical savanna and an evergreen *Eucalyptus* forest in Australia, explaining up to 74% of the variation in ET (Cleugh et al., 2007). Some evidence, however, points to shortcoming in the Penman-Monteith model, such as the lack of a term to consider the salinity of water. In the situation in which ideal meteorological conditions and soil moisture conditions exist for transpiration, high enough salinity can reduce the magnitude of the pressure gradient driving water flow through the plant without affecting model estimates (Turan et al., 2009). One other major known drawback of the Penman-Monteith approach is its reliance on the assumption of a homogeneous local climate. This assumption may be appropriate for open field settings, but is problematic for greenhouse settings (Morille et al., 2013).

The Stanghellini approach, extending Penman-Monteith to greenhouses

The greenhouse environment presents a particular challenge for the Penman-Monteith method. In order to calculate the aerodynamic resistance term, homogeneous local climate must be assumed, but this assumption is violated in nearly all greenhouses. Greenhouse architecture and sparse environmental control equipment typically leads to a heterogeneous environment (Balendonck et al., 2014). To overcome the challenges associated with modeling ET in a greenhouse, Cecilia Stanghellini revised the Penman-Monteith approach to more accurately account for the processes associated with ET in a greenhouse, using tomatoes as a reference crop. The revised model [Equation 2] includes modifications to the radiation flux terms

in the equation, considering the effects of greenhouse components such as soil covering, surface materials, heating or cooling devices, or other electronic equipment (Stanghellini, 1987).

$$\lambda ET = \frac{\delta R_n + (\frac{2 \cdot LAI \cdot \rho_a C_p}{r_e} VPD)}{\gamma(1 + \frac{\delta}{\gamma} + \frac{r_i}{r_e})}$$

The VPD term is vapor pressure deficit, and the r_i and r_e terms are the canopy internal and external resistance terms, respectively. The model also includes a modified leaf area index (LAI) term which accounts for exchange of energy from multiple layers of the canopy (Villarreal-Guerrero et al., 2012). Notably, net radiation is described differently, giving separate weights to short and long wave radiation's effect on a multi-layered canopy such as those typically found in greenhouses (Prenger et al., 2002). Other differences include terms for radiation resistance, external and aerodynamic resistance that accounts for the non-logarithmic profile of wind as distance from canopy increases, and the internal resistance of a leaf in greenhouse settings (Yan et al., 2018, Yan et al., 2020).

Measuring ET using the Stanghellini method requires measuring many of the same terms as other Penman-Monteith derived methods. These include net solar radiation, vapor pressure deficit, leaf area index, air density, leaf surface temperatures, and the concentration of carbon dioxide in air. Due to the large number of data types that need to be collected, a revised Stanghellini method was developed, including a simplified irradiance term called Canopy Area Index (CAI) (Fynn et al., 1993).

The performance of the Stanghellini method in a greenhouse has been compared to other methods including the original Penman-Monteith method. While there was not a significant difference between the the performance of the two models, the Stanghellini model consistently explained more of the variation in crop ET (Villarreal-Guerrero et al., 2012). Researchers attributed this performance gap to the Stanghellini model's inclusion of terms which better consider the environmental factors affecting bulk stomatal resistance. In another study, the

Stanghellini method was compared to the original Penman-Monteith, the pure Penman approach, and the Fynn approach, using a Red Maple Tree (Acer rubrum 'Red Sunset') grown in a greenhouse as a subject. The Stanghellini model explained nearly 88% of the variance in the maple tree ET, likely due to relatively improved characterization of the environmental factors impacting ET, whereas the other models explained less than 50% (Prenger et al., 2002).

The Priestly-Taylor approach, a simplified Penman-Monteith model

There are situations, such as in rural areas with no access to sensors or where power is not ubiquitous, which preclude the measurement of the meteorological and climatological parameters for calculating the aerodynamic resistance terms in a Penman-Monteith ET model. To overcome these challenges, another similar approach was developed by C.H.B. Priestly and R.J. Taylor but with a simplified approach to aerodynamic resistance. This model [Equation 3] replaces the aerodynamic resistance term in the Penman-Monteith model with a dimensionless coefficient, alpha (α) (Priestley and Taylor, 1972).

$$ET = \frac{1}{\lambda}\delta\frac{R_n - G}{\delta + \gamma}\alpha$$

In the original Priestley-Taylor model, researchers validated an alpha value of 1.26 for open field systems, a value used even in modern research (Donatelli et al., 2006). Though 1.26 is generally accepted, researchers in 2011 showed an alpha value of 1.26 is too low for arid and cold environments like Iran, where a value in the range of 1.82 - 2.14 is more appropriate (Tabari et al., 2011).

When using this model, solar radiation, air temperature and relative humidity will need to be measured. However, because the aerodynamic term is approximated with the alpha term, wind speed is not measured and roughness lengths are not approximated. Even without this term, which proponents of the original Penman-Monteith approach might argue is critical to accurately describing the environment, the Priestley-Taylor model has been shown to successfully estimate monthly canopy and soil ET (Fisher et al., 2008). Though this method can

be effective on its own, several studies have demonstrated successful efforts to improve the accuracy of predictions by allowing the value of alpha to fluctuate. One method demonstrated an improved performance of the Priestley-Taylor method by introducing a term which lets the alpha value vary as a function of NDVI and leaf surface temperature (Pereira and Villa Nova, 1992). In another study, researchers working with Sorghum suggested estimates can be improved by calculating alpha based on an equation that considers daily mean vapor pressure deficit (Steiner et al., 1991).

Several more recent studies, however, have shown the Priestley-Taylor method underestimates ET rates under advective conditions (Subedi and Chávez, 2015). Advection is the movement of vapor, heat and air as conveyed by the wind. When advective conditions interact with the canopy, which is not uncommon in an open field setting, the Priestley-Taylor method cannot accurately consider the dynamic effect of aerodynamic resistance in the system (Tolk et al., 2006). Many studies have highlighted this sensitivity to using an appropriate alpha term, but the alpha term has also been shown to interact with soil moisture content, solar radiation, atmospheric pressure and other meteorological concepts (Tabari et al., 2011). For example, in one study researchers showed that as surface resistance increases or humidity decreases, the alpha coefficient increases (Lhomme, 1997).

The Hargreaves and Samani approach, an air temperature based Penman-Monteith model

In remote or logistically challenging environments, such as those without access to grid power, it may be difficult to collect any meteorological data. In these situations, if air temperature alone may be measured, then it is possible to estimate the regional ET from these values (Hargreaves and Samani, 1985). The development of this ultra-simplified Penman-Monteith inspired method for estimating ET [Equation 4] was originally motivated by the lack of readily available meteorological data in developing countries that can limit the applicability of methods including most of the Penman-Monteith methods developed at the time.

$$ET = 0.0023(\frac{T_{max} + T_{min}}{2} + 17.8)\sqrt{T_{max} - T_{min}R_a}$$

In order to estimate the regional ET without any solar radiation data, or with solar radiation data of questionable accuracy, researchers devised a method using only air temperature validated for open field settings. In this method, global solar radiation at the surface (R_a) is estimated through air temperature values and empirical relationships (Hargreaves and Allen, 2003).

With this approach, users measure air temperature throughout the day and night, recording daily maximum (T_{max}) and minimum (T_{min}) values. Empirical coefficients based on site location are also used, to adjust for regional differences. These coefficients are correlated with temperature, but are also typically lower for interior regions and higher for coastal regions. Air temperature may be measured or estimated using ground based sensors or extra-terrestrial sensors mounted on orbital or aerial devices. Though they were designed to improve estimates, in one study it was found the empirical site adjustment coefficient may lead to the Hargreaves and Samani approach overestimating ET rate in many situations, leading to excess irrigation (Kumari and Srivastava, 2020). While the tendency to overestimate ET poses some limitations to the applicability of the Hargreaves approach, some studies have shown calibration parameters may be used to reduce overestimation of ET by up to 16.3% (Berti et al., 2014).

Surface Energy Balance

Energy balance methods are based on the concept of conservation of energy, which states the energy in some problem domain is constant, and neither created nor destroyed. Due to its somewhat flexible footprint this can be a cost effective method for estimating ET on scales ranging from single plots (1-2 hectares) to entire regions (Talsma et al., 2018, Zhang et al., 2016). With multispectral image data from satellite or aerial observation, surface energy is computed by combining the surface energy balance equation [Equation 5] with land surface flux expressions and temperature sensing.

$$R_n = LE + G + H + \Delta S_{air} + \Delta S_{air} + \Delta S_{bm} + \Delta S_{ph}$$

The energy balance equation states that net radiation (R_n) must be in balance with the latent heat flux density (LE), ground heat flux density (G), sensible heat flux density (H), and other less significant energy sinks (ΔS terms). While remote sensing can be effective for estimating regional ET via estimates of NDVI, local effects and the effects of specific plant morphology may necessitate some proximal sensing as well. For example, the turbulent structure of air over a vineyard, which is strongly influenced by the geometry of the underlying canopy, may not be accurately modeled by remote sensing alone (Alfieri et al., 2022).

In the context of the plant-soil-atmosphere system, energy balance theory states net radiation must be in balance with the latent heat flux density, ground heat flux density, sensible heat flux density, and other less significant energy sinks. Ground heat flux density is the rate of heat storage into the soil and vegetation due to conduction, and is either measured directly or computed using information from Normalized Difference Vegetation Index (NDVI) measurements (Long et al., 2014). Sensible heat flux density is the energy lost to the air from the plant, soil and cover crops via convection and conduction. Multiple methods have been developed to estimate sensible heat flux including eddy covariance, Bowen ratio method, and surface renewal (Rienth and Scholasch, 2019). The energy stored in the air layer and in the biomass and chemical energy stored in the carbohydrate bonds of plant sugars, formed using ATP and NADPH from the light reactions of photosynthesis, are usually considered negligible compared to other terms and are therefore ignored (Anapalli et al., 2018). The latent heat flux density is the heat lost from the system due to the evaporation of water, and is calculated as a residual, once all other parameters in the model are determined. Dividing the latent heat flux by the latent heat of vaporization of water will give ET.

Generally, surface energy balance methods can be categorized as either one or two layer models, though there are recent examples of three layer models as well (Burchard-Levine

et al., 2022). Single layer models do not distinguish between soil and vegetation components of ET, but recognize contributions to ET from both (Kustas, 1990). Sensitivity to local calibration and relatively extensive local reference data requirements restrict the use of single source methods to several hectare or smaller scale applications (Zhang et al., 2016). The Surface Energy Balance for Land (SEBAL) overcomes these limitations by empirically estimating the essential meteorological parameters and can therefore be applied over much larger areas, but it may lack regional specificity (Bastiaanssen et al., 1998). Two source surface energy balance methods account for the individual contribution of soil and vegetation to total heat flux but require more data inputs (Kustas, 1990; Norman and Kustas, 1995). The three source model applies to cropping systems such as vineyards, where the row and inter row represent two distinct zones of vegetation. The row is the perennial vine crop but the inter row is typically composed of seasonally rotated cover crops. In three source models the contributions to ET are partitioned into the soil layer, the cover crop layer and the crop layer. Independent of the number of layers, energy balance models require frequent and spatially contiguous measurements using ground based sensors and potentially also orbiting satellites or airplanes mounted with multispectral cameras for detecting parameters affecting ET (Safre et al., 2022). If overhead sensing is being performed, leaf area index (LAI) data may also be remotely collected in parallel and this data can be used to improve Penman-Monteith directly, or other energy balance based ET estimates via empirical relationships between LAI and NDVI (Senay et al., 2007; Reyes-González et al., 2019; Mu et al., 2007; Cleugh et. al., 2007).

In one of the earliest studies quantifying large scale ET trends, researchers reported successful implementation of a satellite sensed NDVI based model called Process-based Land Surface Evapotranspiration/Heat Fluxes algorithm (P-LSH) that separately computes the contributions of canopy, soil and open water bodies to ET (Zhang et. al., 2009, Zhang et al., 2010). Then in 2021 researchers successfully used data-driven models to estimate ET rate, using physical energy balance models coupled with machine learning, regression and neural

networks (Hu et al., 2021). Three source models have also been shown to perform well in vineyards, except under extreme advective conditions (Burchard-Levine et al., 2022). However, methods requiring aerial and orbital data collection methods may be sensitive to cloud cover and dust which can impact estimates of parameters important for calculating ET (Yuan et al., 2020). Also, sensible heat flux is sensitive to factors impacting the distribution of energy sources in the canopy including wind speed and surface roughness, and is therefore affected by canopy size, structure, trellising, plant phenological stage and even ground surface heterogeneity (Rienth and Scholasch, 2019).

Reference ET and Crop Coefficients

In other regions of the world, reference ET systems and crop coefficients are one of the options for estimating local ET. In California, USA, for example, this is an important method for estimating ET which allows growers throughout the state to schedule irrigation based on proxy measurements along with correction factors known as crop coefficients, specific for the type of plant being grown nearby and management factors (Allan et al., 1998; Behboudian and Singh, 1998). These proxy ET values, known as reference ET, are calculated at one of over 200 California Irrigation Management Information System (CIMIS) weather stations distributed throughout the state (LAWR-UC Davis, 2021). Some other states in the USA have similar systems including Florida (Jackson et al., 2008), Colorado (Andales et al., 2014), Arizona (Brown and Yitayew 1988), and Washington (Badr et al., 2015), as well as other countries including Australia (Webb, 2010), India (Wani et al., 2016), and the United Kingdom (Hough and Jones, 1997); but the specific data types available from these systems may differ from CIMIS. At each CIMIS station, meteorological data is collected at a weather station 2 meters above well-watered clipped grass, and then fed into a modified version of the original Penman-Monteith known as FAO56 Penman-Monteith because it was introduced in the Irrigation and Drainage Paper 56 from the United Nations Food and Agriculture Organization (Allan et al., 1998). While FAO56 Penman-Monteith is generally used for CIMIS reference ET

estimates it is also possible to use the CIMIS-Penman model which is a modified version of the Pruitt/Doorenbus Penman-Monteith equation that includes wind speed and cloud cover parameters (Pruitt, 1977)

Once reference ET (ET_o) is known, it can be used to calculate true ET of crops grown nearby by multiplying by a scaling factor known as the crop coefficient [Equation 6].

$$ET = ET_o \cdot K_c$$

The crop coefficient (K_c) is an experimentally derived value, specific to cultivar, seasonal canopy development and vine spacing, and sometimes adjusted for other management factors (Bravdo et al., 1986). The work of Williams showed the crop coefficient may be a function of the shaded area under a grapevine, but this relationship has not been quantified (Williams, 2016). Other studies have explored a two part definition for the crop coefficient, splitting the coefficient into separate terms for the basal crop coefficient representing a factor for crop transpiration, and the soil evaporation coefficient representing a factor for evaporation from the soil surface.

Compared to the other approaches for ET estimation, this method has the distinct advantage of being virtually free for California growers and other growers in areas with similar programs. However, this approach is limited by its reliance on the assumptions of generalizable regional reference ET values and crop coefficients. As a result, this method can be quite effective at estimating regional reference ET but it can lack local specificity, not adequately accounting for or ignoring complex factors influencing slight differences in plant water demand such as management practices, phenological stage, topography, soil characteristics and many others (LAWR-UC Davis, 2021). One study found the difference between crop coefficients recommended by FAO56 Penman-Monteith methods and locally observed data can be greater than 40% (Gharsallah et al., 2013). Researchers in this study attributed the results to crop coefficients, which attempt to integrate several physical and biological concepts into one signal, leaving significant potential for error if they are estimated incorrectly. Due to its

Penman-Monteith origins, the reference ET approach is inherently sensitive to local climatic conditions at the reference ET measurement site which may differ from local conditions at the prediction site. When climatic variation exists between the reference and prediction site, it may be possible to use direct measurements of stomatal and boundary layer resistance to calibrate estimates (Li et al., 2019, Yan et al., 2020). Additionally, these methods do not perform well under deficit irrigation, when they cannot completely account for the response of plants to water stress, a common feature in high value viticulture operations (Hochberg et al., 2017).

Eddy Covariance

Eddy covariance methods are considered one of the only ways to directly measure ET, via estimates of the sensible heat flux density (H) term in the energy balance equation [see Equation 5]. In this method, a flux tower is used to measure changes in vertical air velocity while simultaneously measuring the concentrations of water vapor in air, in order to calculate the vertical flux of water vapor, giving an estimate of ET (Tanny, 2013). This method is validated for open field crops, vineyards, open water bodies and grasslands (Kustas et al., 2022; Tanny, 2013). Like other fundamentally energy balance concepts, the eddy covariance method is most suited to open, flat and homogeneous vegetation canopies, an uncommon motif in agricultural settings. The fluxes observed by sensors mounted on flux towers represent ET from a dynamic area that depends on wind and air stability. This area is called the “footprint” or “fetch” (Chu et al., 2021; Zhang et al., 2014). The uncertainty of the exact dimensions of this area propagates through calculations, contributing to the error observed in estimates of sensible heat flux and other parameters which often only account for 70-80% of total incident energy (Stoy et al., 2013; Eshonkulov et al., 2019). In the 2022 Grape Remote Sensing Atmospheric Profile and Evapotranspiration eXperiment (GRAPEX) project, for example, researchers employed the eddy covariance method and observed a mean energy closure of 75% across multiple sites and years in the North Coast and Central Valley of California, USA (Bambach et al., 2022).

In the eddy covariance method, data is recorded at a high frequency, usually about 20 hertz. Data includes wind speed and direction and is typically recorded using a sonic anemometer. Relative humidity and air temperature are also recorded with research grade sensors. Gas concentrations in air are measured using an infrared gas analyzer. Recording all of these data at high frequency quickly leads to large files which are difficult to store locally. Recent progress in computation and automated sensing capabilities was critical to bringing eddy covariance methods into practice (Bambach et al., 2022). Also, efforts have been made to improve data collection protocols in eddy covariance systems by separating monitoring systems for tall vegetation such as orchard trees and soil surfaces (Saugier et al., 1997; Wilson et al., 2000). In these approaches, independent estimates of soil evaporation and crop transpiration are calculated, but the footprint of ground sensors is typically much smaller than above canopy measurements (Baldocchi, 1997).

In one of the more innovative applications of the eddy covariance approach, researchers used the Keeling Plot technique to partition ET data measured at the ecosystem level into soil and vegetation sources (Williams et al., 2004). This work was accomplished using spatially distributed flux towers which in addition to measuring parameters for estimates of ET, were able to detect the portion of heavy isotopes (^{2}H, ^{18}O) in the evaporating water inside their respective footprint. It is known that water evaporated from soil is depleted in heavy isotopes relative to other liquid water at Earth's surface (Allison et al., 1983). Some other literature reports the eddy covariance method as logistically challenging due to the necessity of high frequency meteorological measurements and complex data processing procedures which usually require experts (Ghiat et al., 2021).

The eddy covariance method, while favored by researchers for its ability to directly estimate ET, is very challenging to validate. The large scale and high variability of the flux footprint, as well as the open boundary layer of the volume studied, both affected by the degree of advection, create issues for those seeking to make direct comparisons of other ET estimates

to the estimates generated by eddy covariance methods (Kustas et al., 2022; Stanhill, 2019). The issue of the flexible footprint, which results in energy imbalance between the total available energy and turbulent fluxes calculated by the eddy covariance technique, can lead to overuse of water in agricultural settings. Different approaches for computationally distributing this imbalance to create pseudo-balance can lead to uncertainty in daily ET estimates up to 50% (Bambach et al., 2022). The Bambach et al., 2022 team of researchers went on to show over the growing season this uncertainty can amount to up to a third of the total annual applied irrigation.

Soil Moisture Sensors

Unlike indirect energy balance methods, soil moisture sensors directly measure the moisture content of the soil environment. Many different techniques have been developed, but two of the most commonly used categories in high value crop agriculture are volumetric and tensiometric sensors. Volumetric moisture sensors, such as neutron probes, capacitance sensors, and time-domain-reflectometry sensors measure the way a signal behaves in the soil, then estimate the percent of water in the soil by volume using known correlations (Townend et al., 2001). Tensiometric sensors, on the other hand, directly measure capillary tension, the physical force holding the water in the soil (Mullins, 2001).

Soil moisture sensors have the benefit of automation and continuous data collection, but these advantages are outweighed by myriad practical disadvantages, including a fundamental sensitivity to the heterogeneous distribution of moisture in the soil environment. Soil moisture sensors are also immobile once placed, and therefore what a sensor measures is often not what is perceived by the deep, diffuse roots of vines and trees, which can explore soil space over time. Most importantly though, there is no simple or direct way to estimate plant water status or ET using soil moisture content (Lavoie-Lamoureux et al., 2017).

Despite no direct method for calculating ET, soil moisture sensors may be used for irrigation management provided there is some knowledge about the water balance properties of

the growing medium. Water balance is a concept referring to the range between the maximum water holding capacity of a growing medium, or field capacity, and the level at which the plant can no longer transpire, also known as the wilting point (Datta et al., 2017). The field capacity and wilting point of a growing site may be determined via laboratory tests, sensor based estimates, or using the Rosetta model, which exploits pedotransfer equations to estimate the terms indirectly (Schapp et al., 2001). It is not uncommon for researchers to simply assume a field capacity soil matric potential of -33 kPa, though some studies suggest an assumption of -10 kPa may be more generalizable (Van Lier, 2017). Wilting point may also be assumed, and the generally accepted value is -1500 kPa, though this value is a function of soil texture, crop type and other local factors which may impact the true wilting point (Tolk, 2003).

Pan Evaporation Method

With the pan evaporation method it is possible to use nothing more than a standardized pan of open water, a scale and a watch to estimate local crop ET. While the most basic of pan evaporation approaches can achieve the aforementioned elegance of nearly optimal operational efficiency, modern examples of this method typically require the collection of supplemental meteorological data for model building purposes. Other approaches involve calculating a pan coefficient (K_p) that when multiplied by pan evaporation (E_p) yields an estimate of reference and then crop ET [Equation 7].

$$ET = K_p \cdot E_p$$

The most widely used method for determining a pan coefficient value is a table from the United Nations Food and Agriculture Organization which categorizes different values based on the composition of the ground surrounding the pan, the local climate type and the size and type of vegetation near the pan (Doorenbos and Pruitt, 1977).

The pan evaporation method is effective because it takes advantage of the correlation between pan evaporation and reference ET, which in turn has a known correlation with crop ET.

To reduce error caused by differences between pans, there is a standard pan called the “class A evaporation pan” issued by the United States National Weather Service which allows for more accurate comparisons between sites. While the relationship between pan evaporation and reference ET is valid under many conditions, there can be conditions causing differences in energy fluxes and heat storage in an open water pan relative to vegetation. This effect is pronounced at night when energy stored in the pan during the day increases the overnight evaporation rate of water in the pan, while canopy resistance to transpiration will cause little to no nighttime ET (Snyder et al., 2005).

Nevertheless, properly used, the pan evaporation method can produce useful estimates of crop ET. In one study, researchers developed a method wherein pan coefficient values can be estimated, eliminating the need for wind speed and relative humidity data. With a scale, the pan evaporation can be measured and this alone was shown to be a strong predictor of the pan coefficient value (Snyder et al., 2005). In another recent study, researchers in the central Himalayas trained machine learning models using multiple types of data including pan evaporation, air temperature, relative humidity, wind speed, and illuminated hours. Of the five artificial intelligence models trained, the neural network and the inference models were best performing in terms of estimating crop ET, further demonstrating the relevance of the pan evaporation technique (Malik et al., 2017).

Fine scale ET estimates

For many years the methods for fine scale ET estimation have been relegated to research applications, but recently several options designed for commercial use have come to fruition, opening the door to widespread acceptance (Jenkins *et al.,* 2023; *FloraPulse*, Davis, CA; *LI-COR Biosciences*, Lincoln, NE). The development of these tools was driven by the need for technology that allows for irrigation management at smaller spatial scales, specifically addressing the spatially heterogeneous water demand of high value crops grown in

topographically complex and heterogeneous environments. Intra-vineyard spatial variability, for example, poses a particularly difficult challenge and has been well characterized as a nearly ubiquitous feature which has been linked to vine performance (Gatti *et al.,* 2022; Gatti *et al.,* 2017; Brillante *et al.,* 2016; Matese and Di Gennaro, 2015). When irrigated with a conventional drip system controlled by coarse scale ET estimates, the consequence of this spatially heterogeneous water distribution is a non-uniform ripening of berries. Ultimately non-uniform ripening results in an increased fraction of the resulting must being composed of immature and over-ripe berries compared to a more uniformly ripened harvest from the same vineyard (Bramley *et al.,* 2005).

In grapes and other high value crops, water balance contributes directly to overall fruit quality, not just yield and ripening, layering additional complexity into its management. For example, in perennial woody crops well-timed water stress can help control vegetative vigor and may increase fruit quality at harvest (Chaves *et al.,* 2007; Van Leeuwan and Seguin, 2006). Conversely, moderate to severe water stress caused by extreme deficit irrigation can damage cellular components for light harvesting, limiting photosynthesis. If this water stress is prolonged, delays in ripening, sudden plant collapse and reduced fruitfulness can negatively impact yield and quality (Dayer *et al.,* 2007). These constraints can create a problem, however, because the irrigation manager's goal is finding this narrow range of applied water by considering the plant's needs, but these needs usually vary in a complex way through space and time. Fine scale ET estimates seek to reveal this complex patchwork of variable plant water needs.

Lysimeters

Lysimeters directly measure ET by sensing changes in the mass of soil and vegetation inside of a container mounted on a scale. These complex devices were designed by researchers to study the process of ET, develop ET models, measure precipitation and dew and water flow in the unsaturated zone of the soil profile (Kandra et al., 2023; Jenkins *et al.,* 2023; Hirschi et al., 2017). A properly designed lysimeter replicates the natural environmental

conditions of the target environment and vegetation combination. Generally this means the overall size, pruning habit and other management factors applied to the lysimeter plant are comparable to the management strategies applied to vegetation of the same type in the local area (Ghiat et al., 2021). Some lysimeters are buried underground to protect sensory equipment and ensure vegetation is maintained at a plausible height, and soil is maintained at a plausible temperature, but examples of above ground lysimeters demonstrate this is not a necessity for achieving good results (Jenkins *et al.,* 2023). Lysimeters may also be equipped with an adjustable ground water level watering system maintaining soil hydration at levels equal to the surrounding soil (Umwelt-Geräte-Technik GmbH, 2023). Typically, all soil plant and meteorological sensors are mounted on the potted plant infrastructure and then all of this is mounted on a three or four point load cell with a sensitivity of at least 0.01 kg. The surface area of the lysimeter soil may be used to translate mass units of water into spatial units of millimeters per area.

If the lysimeter is a closed system, in other words if it has no drain, then ET is calculated by taking the integral of the derivative of load cell mass with respect to time, ignoring irrigation and precipitation events [Equation 8].

$$ET = \int_0^t \frac{d}{dt} mass$$

If, however, the lysimeter has a drain to allow for excess water to flow out the bottom of the potted soil enclosure, mimicking groundwater recharge, then in order to calculate the ET this overflow must be measured in addition to the mass of the load cell. ET can then be calculated by taking the integral of the derivative with respect to time of the load cell data, adjusted for groundwater recharge. Though calculating ET may be slightly more complicated, the advantage of lysimeters with drains is they can provide information about soil water retention and percolation of excess irrigation water that no other methods can provide (Stanhill, 2019).

The high cost of installation and maintenance of lysimeters limit their applicability to research applications and some particularly high value crops (Ghiat et al., 2021). Typically lysimeters are used to validate other forms of ET estimates that are less difficult to move to new areas. For example, in 2017 lysimeters were used by researchers in Switzerland to validate eddy covariance for ET estimates using well-watered grass as a research subject (Hirschi et al., 2017). Measurements were taken hourly from 2009 to 2015, and using lysimeter data as reference researchers were able to show eddy covariance performs well to estimate ET, especially on the annual time scale. In this study, direct comparison to lysimeter ground truth ET allowed researchers to demonstrate eddy covariance underperforms during and immediately after precipitation events. This finding highlights the limitations of eddy covariance sensors under rainfall conditions, contributes to researchers' understanding of why eddy covariance methods underestimate ET and how this impacts the energy balance gap, and demonstrates the value of lysimeters for model validation.

Sap Flow Sensors and Microtensiometers

Sap flow sensors are another promising technology, with several advantages over other fine scale methods. These sensors directly measure the movement of fluid inside the xylem from the roots to stems and to leaves, where water is transpired through stomata—a process called sap flow. Sap flow is essential for the maintenance of the hydraulic continuum from soil to plant to atmosphere, thus monitoring this process can yield important information about the hydraulic function or dysfunction of the plant (Steppe *et al.,* 2015). Various methods for estimating sap flow rate have been developed, including thermal dissipation probes and the steam heat balance method (Granier, 1985; Lascano, 2000; Lascano *et al.,* 2016). Both are based on the concept of measuring the difference between a heated element and a non-heated reference element; as sap flow rate increases the temperature difference between the two elements decreases (Fernández and Testi, 2017). A variation of this method is also used for standard flow meters in pipes.

Microtensiometer sensors are based on the same principles as soil tensiometers but have been designed to suit the purpose of measuring plant water status. While no direct method for estimating ET from water status is known, microtensiometers can be used to assess whether or not a plant is transpiring and estimate how much. Sensors such as the flagship model from *FloraPulse* in Davis, California, are based on a microelectromechanical design that allows measurement of plant stem water potential continuously with a high degree of precision (Lakso et al., 2022b). They are also small, low cost, consume very little power, allow for wireless data transmission, and like sap flow sensors are fully automated once installed. These sensors, mounted on the plant using a custom drill bit and mounting kit, have been tested extensively, and in one recent study they were used in *Vitis vinifera* L. cv. Shiraz and Cabernet Sauvignon and compared to pressure chamber measurements. Trunk water potential measurements from the microtensiometers generally agreed with seasonal and diurnal patterns of stem water potential measured by pressure chamber (Pagay, 2022).

While the sap flow and microtensiometer methods will fundamentally achieve single plant resolution, individual sensors are very expensive and require skilled labor for installation and routine maintenance. As a result, sensors are typically mounted on only 1 to 3 plants per management zone. Plants are chosen to represent the range of variability; a problematic assumption that can ignore many sources of heterogeneity.

Gas Exchange Measurement Systems

Portable gas exchange systems give direct measurements of parameters at the leaf level, and thereby give estimates of leaf level gas exchange including carbon dioxide and water vapor. In these systems at least one leaf of the target plant is isolated from the environment, usually by sealing it inside of a clear chamber with several micrometeorological sensors and a regulated carbon dioxide gas supply (Parkinson et al., 1980). Gasses including carbon dioxide and water vapor concentrations are measured at the inlet and outlet of the sealed chamber

using an infrared gas analyzer that can determine the concentration of gasses in air based on the characteristic absorption of infrared radiation by different gasses (PP Systems, 2023).

When portable gas exchange measurement systems were first introduced in the 1970s, their adoption was limited to research applications largely due to the size and complexity of the necessary equipment. These early devices measured the concentrations of carbon-14 dioxide in air within plexiglass domes to determine the photosynthesis rate of grasses (Tiezen et al., 1974). In the 2000s portable gas exchange systems became much smaller and easier to use, engendering an era of non-research applications. Despite vast improvements in the size and portability of these technologies with innovations from companies such as *LI-COR Biosciences*, their substantial price which was $50,000 USD in 2018, prohibits many growers from being able to use these systems (Salter et al., 2018). Furthermore, this technology provides leaf level estimates of gas exchange and photosynthesis rates, and extrapolating these rates to whole plants or groups of plants may not be straightforward.

In one recent study, researchers used portable gas exchange measurements to measure leaf level photosynthesis and gas exchange rates then successfully upscaled these estimates to calculate whole plant fluxes. Though the efforts to understand canopy level fluxes were successful, researchers noted up-scaling was sensitive to the accuracy of the leaf area index and photosynthetic light curve data used in calculations (Martínez-Maldonado et al., 2022). Many of the applications of this technology aim to improve ET estimates with other technologies that are more easily generalized over areas relevant to commercial agriculture. For example, infrared gas analysis was used to estimate the effect of increasing carbon dioxide concentration on the stomatal resistance of plants. Researchers found elevated carbon dioxide concentrations reduce transpiration per unit leaf area, and also water use efficiency may be improved but only because photosynthesis rate is increased, not because transpiration is reduced (Allen, 1990). These findings are vital for understanding and anticipating the effects of increasing atmospheric carbon dioxide on Earth.

Infrared Temperature Measurement Systems

It is also possible to increase the resolution of coarse scale ET estimates using infrared temperature sensors, though this technology alone will not provide enough data to calculate estimates of ET (Xue et al., 2022). These sensors take advantage of the cooling effect that happens when leaves are transpiring water through their stomata, in which the temperature difference between ambient air and the surface of the leaf reflects the transpiration rate (Nobel, 2005). If the temperature of the leaf is lower than the ambient temperature then the leaf is transpiring, but if the temperature of the leaf is equal to or higher than the ambient temperature then the leaf is not transpiring and is experiencing acute stress (Still et al., 2019). With leaf surface temperature data, it is possible to add another term to other ET estimation models, such as one of the surface energy balance models. This new term accounts for when leaves are actually transpiring instead of assuming this is a constant process during sunlight hours.

Though it is a straightforward concept, the measurement of leaf temperature is non-trivial. Leaves are not static in space, because of wind, growth over time and other factors, and are subject to the meteorological uncertainty associated with an outdoor environment. The thermocouple approach to measuring leaf temperature involves the direct contact of a thermocouple to the leaf surface, a design that presents many challenges to the user. Physical contact with the leaf may be interrupted at any time for numerous unpredictable reasons, and even when perfect contact is maintained throughout the duration of measurement windows the thermocouple may absorb solar radiation, causing error (Tarnapolsky and Seginer, 1999). Despite these challenges, thermocouples are quite a popular method for measuring leaf temperature because of their low cost, simple operation and relatively fast measurement time (Yu et al., 2016). Recently, infrared sensors have gained popularity for measuring leaf surface temperature because of their fast measurement time, accuracy and reliability over longer measurement windows such as full seasons. However, infrared leaf temperature sensors are

sensitive to changes in the quality of air that affect the way light travels, and as a result dust, mist or smoke may impact the quality of measurements with these sensors (Yu et al., 2016).

High Resolution Irrigation Models

The High Resolution Irrigation (HRI) models were developed as algorithms along with low-cost sensors designed to provide growers with up to single plant ET resolution in vineyard and orchard cropping systems (Jenkins *et al.,* 2023). These methods utilize non-destructive, largely automated proximal sensing and a computation pipeline, feeding data from biometeorological sensors to the models. In this process, wind speed, air temperature and relative humidity are measured in or near the plant canopy. There are three HRI models which can be used to calculate estimated ET rate per area, or mass flux ($\dot{m}_e$ in Equation 9).

The Convective Mass Transfer (CMT) model is one of two HRI models inspired by first principles. CMT relates transpiration to theory describing the convective mass transfer from a flat surface of water into moving air. This theory is based on an application of the Reynolds analogy, which suggests a simple relationship between different transport phenomena (Cussler, 2009). Using convective heat transfer from a flat solid plate into a fluid with laminar flow over its surface as an analogy, transpiration is defined as convective mass transfer from a flat surface of liquid or a gas saturated with water vapor into a gas with laminar flow over its surface (Cussler, 2009). From this theory the estimated mass transfer flux depends on the mass transfer coefficient and the difference between the partial pressure of water in air at the saturated surface, and in the air in the greater atmosphere.

The CMT model maintains three assumptions. First, all transpiring leaf surfaces are saturated with water vapor, perfectly flat and having a uniform temperature equal to the temperature of the air in the canopy. Second, it is assumed the boundary layer is maintained at a constant level of saturation, and finally, it is assumed a laminar flow of air exists at the leaf surface which carries water vapor away from the boundary layer. While most agricultural systems violate some or all of these assumptions, the CMT model has been shown to perform

well in *Vitis vinifera* L. cv. Zinfandel vines, explaining up to 86% of the variation in lysimeter ET rate over three seasons (Jenkins *et al.,* 2023).

The second first principles inspired HRI model, the Mass Balance (MB) model, is based on the concept of conservation of mass, which states in any closed system mass is constant. In the case of a plant canopy, this means the mass flow rate of water out of the canopy is equal to the mass flow rate of water into the canopy plus the mass flow rate from the plant. However, in order for this theory to be used for estimating ET rate, it is assumed the cross-sectional area of the canopy is constant, as is the velocity of wind through the plant. With these assumptions, the ET rate can be calculated as a product of the bulk velocity of air, the cross-sectional area of the canopy, and the difference between the absolute humidity outside and inside the canopy. To capture the characteristics of air flowing out of the canopy and air flowing into the canopy, meteorological sensors are mounted both inside and outside of the canopy but the ideal location of these sensors, specifically the sensor outside the canopy, is not obvious. Typically the outside of canopy sensors are mounted downwind of the canopy, given the prevailing wind direction. This is a problematic assumption though, that does not consider the seasonal and diurnal variability of wind speed and direction (Jenkins *et al.,* 2023). Researchers suspect the sensitivity to sensor placement to be the reason the MB model was observed to be the most variable over three seasons, explaining between 7% and 91% the variability in lysimeter ET rate (Jenkins *et al.,* 2023).

The third HRI model is called the Empirical Model (EM) because it was selected by researchers using only statistical methods from a set of more than 25 candidate models, exploring mass flux as a function of various combinations of biometeorological parameters. The goals of EM model development were generalizability and dimensional reduction. In addition to computational efficiency, dimensional reduction has the added benefit of reducing the number of sensors that would need to be included in the low-cost sensors being developed in tandem with the HRI project. The final EM model was selected because in addition to achieving reduced

dimensionality, it also performed well in terms of ET predictions when compared to other candidate models (Jenkins *et al.,* 2023).

Unlike the other HRI models, the EM model only includes bulk wind speed and air temperature parameters as well as the interaction of these parameters. This approach assumes humidity measurements and related parameters are not strong enough predictors of ET rate to be included in a model designed to explain variation in mass flux and inform irrigation decisions. Despite having no physical meaning, researchers observed the EM model to perform well in a viticulture setting, explaining between 57% and 92% of the variation in lysimeter ET over a three year period (paper1).

Once mass flux has been calculated using one of the three HRI models, it is possible to calculate ET. Each HRI model generates an estimated instantaneous mass flux for every two minute interval. This mass flux ($\dot{m}_e$) is integrated over time and multiplied by a plant scaling coefficient (A_s) giving estimated ET [Equation 9].

$$ET = A_s \cdot \int_0^t \dot{m}_e \, dt$$

In Jenkins *et al.,* 2023 the researchers calculated model estimated ET over the span of a single hour surrounding solar noon and a full day, then compared this to lysimeter measurements. Together, the models explained nearly 63% of the variability in hourly lysimeter ET and 82% of the variability in daily lysimeter ET. Compared to eddy covariance and crop coefficient methods, the HRI method explains a similar amount of the variation in reference ET.

While the observed correlations with ET persisted over multiple plants and multiple seasons, results indicated accurate prediction of ET depends on accurate calculation of the plant scaling term, which varies with plant and over time. The area terms for two of the models, CMT and MB, have an actual physical meaning (leaf area for CMT and canopy cross-sectional area for MB), but the area term in the EM does not. In order to expand the generalizability of

HRI estimates and encourage industry adoption it will be essential for researchers to develop methods for direct calculation of area terms from physical data such as ground based imagery collected during normal tractor passes. Downstream image analysis could be automated using a deep learning approach, similar to the approach used in Olenskyj *et al.,* (2022), to extract physical parameters of the vine that are well correlated with model area terms.

Distribution systems

Fine scale ET estimates and automated water status sensing may shed light on the previously undetectable heterogeneity of water demand at small spatial scales, even individual plants (Jenkins *et al.,* 2023; Lakso *et al.,* 2022) but this knowledge is not very useful without an irrigation system that can accomplish differential water delivery based on this information. Recent research has shown remotely sensed data including LAI and NDVI may be used to identify areas of relative homogeneity within an overall heterogeneous growing area (Ohana-Levi *et al.,* 2022). These sub-areas of homogeneous conditions are considered management zones, and may be identified from LAI and NDVI data using time-series clustering if fine scale ET estimates and high density automated water status are not available. However, not all agricultural areas are appropriate for broad subdivision of growing areas into several or even tens of management zones. In some growing areas the landscape is too uneven and heterogeneous to identify any areas larger than 10 square meters with consistent conditions. In others, management practices such as roguing for disease control, or the spatial dynamics of water demand over time, may necessitate higher resolution irrigation control to achieve optimal plant health.

Once information about the spatial distribution of water demand is available, through fine scale ET estimates and automated water status sensing or via remotely sensed approximations, it is important to choose an appropriate water delivery system. If time-series clustering results indicate the growing area in question is characterized by a temporally stable patchwork of a

small number of homogenous areas it may be optimal to use an irrigation zoning technology such as the one from Verdi that allows growers to monitor the health of each zone and adjust settings remotely (*Verdi*, Vancouver, BC). If, however, time-series clustering results indicate the growing area in question consists of a small number of homogenous areas but these areas are not stable through time, a more dynamic approach may be needed. If there are several distinct seasonal stable states of stable homogeneous zones, then perhaps a Verdi Ag style system could be developed for all seasons and adapted from season to season. However, if the dynamism of the location of homogenous areas is not predictable, then a system that allows for irrigation delivery at the single plant level may be most appropriate. It is also possible in some extremely heterogeneous environments or in particularly high value cropping systems such as some vineyards or indoor cannabis or cut flower farms, that fine scale individual plant control will be the most appropriate choice for achieving highly valuable yield and quality outcomes.

Any system designed to deliver water to plants based on their individual needs, or the needs of small groups of plants, would consist of a high density of water delivery equipment such as valves and flow sensors. In order to be useful, this armada of water delivery hardware must have access to power, a system for harmonious and reliable communication, and sufficient computational power.

To be functional at scale, high precision water delivery equipment would need to be low powered, but still operate 24 hours a day in harsh conditions and often in remote locations without access to grid power. In these situations, researchers have had success using portable solar energy harvesting panels as well as large capacity lead-acid batteries to power field equipment (Kustas et al., 2022; Jenkins et al*.,* 2023). Miniaturized versions of this technology could be used to power groups of valves, though choosing the location of solar panels would be important to ensure sufficient sun coverage while also not interfering with plant management practices. Also, batteries will need to be resistant to outdoor environmental conditions including many extreme temperature cycles as well as having high energy density. Thanks to recent

advances in lithium iron phosphate battery technology including improved thermal stability, long lifespan, and low risk of combustion, this may be possible (Hassoun et al., 2014). However, changings thousands of batteries may require too many natural resources and labor to be sustainable, especially if the batteries cannot be easily recycled. In situations where grid power is available at growing sites, it could also be possible to use irrigation lines with incorporated low voltage power lines providing a constant supply of power to valves and other devices mounted along the lines.

Even if power is available to all the irrigation equipment, in order for this equipment to function properly and deliver water only when conditions warrant, it is essential that spatially distributed devices can rapidly and reliably communicate with each other. In the case of powering irrigation valves with wires embedded in tubing, it would be possible to also include communication wiring in this tubing. This method would ensure devices communicate with each other and any central nodes, and data could be sent from any central nodes to control each device or many simultaneously. However, in the absence of irrigation tubing with embedded wires or a similar wired solution, low power wide area networks may provide the best option. Low power wide area networks are an ideal option for low power IoT devices in agricultural settings.

Several low power wide area networks have been investigated for their applicability to large scale deployment of networks of devices in rural settings. The Long Range Wide Area Network (LoRaWAN) is a low data rate communication protocol specifically designed for minimum energy budget applications and the longest range coverage for communication (Marini et al., 2022). Another popular low power wide area network technology, called Narrowband IoT (NB-IoT), was developed for efficient connectivity in cellular IoT networks and to optimize for minimal power consumption (Marini et al., 2022). A third option, Sigfox, was designed for IoT applications operating with only small infrequent data packets. This technology transmits in the sub-gigahertz range allowing for extremely low power consumption, and because sensor

networks are managed by Sigfox, infrastructure management is relatively simple compared to other options (Lalle et al., 2019; *Sigfox,* Labège, France).

Overall, while each of these technologies show great potential to support development in different areas of IoT innovation, research has shown the NB-IoT option may be the most promising for agriculture applications. With NB-IoT there is the distinct advantage of being able to connect massive numbers of devices, more than fifty thousand, to a single node, whereas LoRaWAN and Sigfox are limited to thousands of connections per node (Liberg et al., 2017). Furthermore, because it supports larger numbers of devices with low packet error rate, NB-IoT is thought to have better scalability properties than LoRaWAN (Persia et al., 2017). In terms of coverage, NB-IoT seems to be the frontrunner. In one study, it was found LoRaWAN could not provide sufficient indoor coverage, while NB-IoT achieved connectivity with less than a 5% error rate (Vejlgaard et al., 2017). Another study demonstrated NB-IoT has the best coverage probability, even though link loss with devices was slightly higher when compared to LoRaWAN (Lauridsen et al., 2017). Perhaps the most compelling evidence for NB-IoT's promise was a comparative study in rural and urban areas in 2020 which showed in a real-life scenario that NB-IoT outperformed LoRaWAN. Researchers attributed the relatively better performance of NB-IoT to directional antennas that allowed for better coverage to devices (Ribeiro et al., 2020).

Beyond the energy and communications needs of the irrigation distribution system are the computational needs. Though irrigation control and status monitoring would likely require very little onboard computation, if any, it is possible the data communication and analysis centers used for irrigation control could also be used for meteorological data storage and processing, as described in Jenkins *et al.,* 2023. Whether or not this is the case, onboard computation hardware would include a low power consumption design, low power communication protocol compatibility and the ability to control low power and valves. However, ideally onboard computation hardware would also include the ability to receive and store data from flow, meteorological sensors and water status sensors, and sufficient computation power to

perform some onboard analysis. Especially if fine scale ET sensors such as those in the HRI approach are used in combination with a single plant or a high spatial density of irrigation control, then it will be important to strike a balance between onboard computation and transmission of raw data in order to achieve optimal energy efficiency.

Discussion

Capitalizing on the potential for ET sensing technologies to improve irrigation management will be crucial to sustaining agricultural industries amidst rising global competition for water resources. Especially in high value cropping systems such as grapes or tree fruits and nuts, ET sensing will be important to reducing water use without preventing growers from continuing to hit economically important yield and quality targets (Stewart et al., 2011), that is higher water use efficiency. Beyond higher efficiency, in some high value crops like grapes proper timing of deficit irrigation can improve quality at harvest. Given this knowledge, in order to fully realize the water use reduction and quality outcomes associated with a well designed irrigation management system, growers need to be able to understand and measure water demand. In this case water demand represents the integration of two concepts, *how much* water plants are using and *when* plants need this water to be replaced. Combining water use and water status signals, growers can understand the water demand of crops but the resolution of this understanding is fundamentally defined by the resolution of ET and water status measurements (Table 0.1).

Many of the ET estimation options available to growers were designed for performance at spatial resolutions greater than 10 meters. These technologies were originally developed for situations in which a host of field level research grade sensors are available, as is the case with

	Model	Resolution		Time step	Application
		Footprint	***Number of plants***		
Coarse	Surface Energy Balance, remotely or proximally sensed	10 meter or greater	Multiple	Monthly, weekly, daily, hourly	Open field
	Original Penman-Monteith	10 meter or greater	Multiple	Daily	Open field
	Stanghellini	10 meter or greater	Multiple	Hourly	Greenhouse or indoor
	Priestly-Taylor	10 meter or greater	Multiple	Daily	Open field
	Hargreaves and Samani	10 meter or greater	Multiple	Daily	Open field
	Reference ET and Crop Coefficients	100 meter or greater	Multiple	Hourly	Open field
	Eddy Covariance	10 meter or greater	Multiple	Hourly	Open field
	Soil Moisture Sensors	10 meter or greater	Multiple	Hourly	Open field, greenhouse or indoor
	Pan Evaporation	10 meter or greater	Multiple	Daily or hourly	Open field
Fine	Lysimeters	Area of Lysimeter	Single or Multiple	Two minutes or less	Open field, greenhouse or indoor
	Sap Flow Sensors	1 - 6 meters	Single	Hourly	Open field, greenhouse or indoor
	Gas Exchange Measurements	Less than 1 meter	Single	Two minutes or less	Open field, greenhouse or indoor
	Infrared Temperature Measurements	Less than 1 meter	Single	Hourly	Open field, greenhouse or indoor
	High Resolution Irrigation Models and Low Cost Sensors	1 - 6 meters	Single or Multiple	Two minutes	Open field

Table 0.1: ET models are organized into coarse and fine scale categories, and summarizing information is given on the number of plants considered by each model, the time step of ET estimates and the appropriate applications.

the original Penman-Monteith approach (Penman, 1948), or alternatively for situations where there is little or no access to field level meteorological data, as is the case with some remotely sensed methods (Talsma et al., 2018, Zhang et al., 2016). While most of the methods for estimating coarse scale ET are adaptations of the original Penman-Monteith model, others rely on direct measurements of the environment and empirical correlations for estimating parameters and then ET. Independent of their origin, each of the coarse scale approaches relies on some assumptions that limit their generalizability.

For example, in order to calculate estimates of ET using the SEBAL approach researchers must assume the conditions impacting measurements are not significantly affecting the accuracy of measurements and therefore ET estimates. In practice this assumption is often violated, as orbiting satellites with spectral cameras routinely encounter obstructions such as clouds, dust, or other airborne particles (Yuan et al., 2020). In the Penman-Monteith approach, many of the factors influencing ET are taken into account, but some soil characteristics are not included, such as salt stress. The assumption that salt stress can be ignored, negatively affects this model's accuracy in situations where salt stress is limiting root uptake of otherwise available water (Turan et al., 2009). The foundation of the Priestley-Taylor model is rooted in an assumption that the aerodynamic resistance term in the original Penman-Monteith model can be well represented by a dimensionless constant. While the use of this constant expands the utility of the Priestley-Taylor approach beyond the scope of other Penman-Monteith style approaches, it also restricts the model to situations without advective conditions (Tolk et al., 2016). The reference ET and crop coefficient approach is similarly dependent on the acceptance of at least one assumption. In this case, it is assumed crop coefficients are generalizable despite reports of up to a 40% difference between crop coefficient adjusted FAO56 Penman-Monteith based reference ET estimates and local estimates (Gharsallah et al., 2013). Despite the fundamental concept of energy balance in a closed system, in the eddy covariance approach for estimating ET the average observed energy closure is reported to be about 75% in vineyards.

Furthermore, when growers apply methods to redistribute the residual energy to other terms in the energy balance model, this can lead to uncertainty in daily estimates of ET up to 50% (Bambach et al., 2022).

Other methods for estimating ET were developed for performance at fine spatial scales of less than 10 meters. These methods are especially useful in high value cropping systems where heterogeneity of terrain is a common feature of growing areas. Landscape heterogeneity such as soil differences, slope angle, shade and edge effects, as examples, as well as genetic and phenotypic heterogeneity can all lead to differences in water demand. Even more, in some high value cropping systems such as vineyards and orchards it is common to observe roguing or replacement as disease control and recovery management strategeies. In situations such as these, fine scale ET methods along with water status sensing, will empower growers with knowledge of the spatially heterogeneous water demand in their growing areas. However, like the methods for coarse scale ET estimates, fine scale methods also rely on assumptions that limit their applicability.

For example, informing irrigation decisions with sap flow and microtensiometer data requires accepting the assumption of generalizable crop and cultivar based trunk water status thresholds (Pagay, 2022). When using leaf level gas exchange measurement systems to estimate whole plant ET, it is assumed upscaling methods are accurate, even though these methods include empirical relationships between plant morphology and measurements of LAI and light response which have not been extensively validated (Martínez-Maldonado et al., 2022). Even simple methods such as using infrared sensors to measure leaf surface temperature rely on the assumption of adequate conditions for measurement, otherwise measurement error caused by particles in air like dust or smoke may be ignored (Yu et al, 2016). The HRI models also rely on assumptions of environmental conditions in order to calculate estimates of ET. The CMT model assumes satured boundary layer conditions of all

leaves and laminar flow of air over these surfaces, while the MB model assumes a constant cross-sectional area of the whole plant.

Each of these approaches to ET estimation show great potential for improving irrigation management in different sectors of agriculture, but determining the most appropriate method for a particular setting can be challenging. Choosing how to measure ET requires striking a balance between achieving yield and quality goals while also minimizing overhead and operational costs. Though some landscapes are highly heterogeneous, planted with very high value crops, and represent ideal use cases for high resolution irrigation systems along with fine scale ET sensing technologies, economic limitations or knowledge access may prohibit the use of these technologies, especially as they are still being developed. Also, the correlation between increasing spatial resolution of ET estimates and increasing costs associated with installing and operating them leads many growers towards compromising on spatial resolution and accuracy in order to achieve low costs. According to a recent survey conducted by the Almond Board of California, 89% of farmers in California still use the hand feel method for scheduling irrigation, though a notable fraction reported using science based methods, too (Kisekka, 2023). Crop ET estimates were used by 75% of respondents, soil moisture sensors were used by 61%, and 23% reported using water district estimates. Another 43% of respondents reported measuring water status with sap flow sensors or microtensiometers and 31% reported monitoring water status with pressure chambers.

Ultimately, the choice of ET and water status sensing method must be compatible with irrigation system design. If the growing area in question is mostly homogeneous in terms of landscape and will be planted with an isogenic or a morphologically stable crop, then a low cost per area coarse scale estimate of ET would likely be sufficient. For areas such as these that do not require a high spatial resolution of control over water delivery, the current industry standard approach of block based irrigation would likely be sufficient to achieve agronomic goals. However, if the environment necessitates sub-block level control, growers may benefit from

choosing a fine scale estimate of ET along with a plant level or sub-block level irrigation system design.

The future of ET research looks promising. The potential for operational applications of several new and innovative technologies is substantial and will address growing need for higher resolution, lower cost and more reliable ET sensing and water delivery systems. Single plant ET methods have recently been advanced, with important findings that will improve how growers determine water status or *when* to apply water (*FloraPulse*, Davis, CA) and water use or *how much* water to replace (Jenkins *et al.,* 2023). There is also research being done to improve high resolution water delivery systems. Even with recent advances in variable rate drip irrigation (AL-agele et al., 2021), systems will need to be developed which can simultaneously measure dispensed water and modulate water flow, to achieve the ideal of truly single plant resolution delivery. Coarse scale ET technologies are improving as well, with recent advances in eddy covariance based estimates and remote sensing technologies. For example, a two source energy balance approach including the eddy covariance technique was recently successfully applied in an environment with significant advective conditions (Kustas et al., 2022b). Also, remote sensing was recently shown to be an effective means of estimating daily ET, and identifying distinct irrigation management zones within a larger block of crops (Safre et al., 2022; Ohana-Levi et al., 2021).

Unfortunately though, honing the spatial resolution of ET technologies and improving the accuracy of estimates will not be sufficient for achieving widespread acceptance in commercial agriculture. Technologies simply delivering utility may earn acceptance among the scientific community, but the alleged target audience of our work in the irrigation space, the grower, has historically been more challenging to engage. To bridge the gap between the scholars and the growers, the future workforce in this space will need to seriously consider how to make water use and water status information available to growers in a practical, digestible format. Eliminating friction at all steps–from acquisition, installation and operation of hardware, to

dealing with routine maintenance or troubleshooting, as well as in user interfaces where carefully curated results may be absorbed or just as easily ignored–will be essential to driving the acceptance of ET technologies beyond the borders of the ivory tower.

Acknowledgements

This manuscript was made possible through financial support from Till Guldimann and the Ernest Gallo Endowed Chair in Viticulture and Enology.

Author contributions

M.R.J. wrote the paper with revisions from all authors.

Chapter One

Novel algorithms for high-resolution prediction of canopy evapotranspiration in grapevine

Matthew Jenkins, Autumn Mannsfeld, Shayla Nikzad, Jean-Jacques Lambert, Konrad Miller, Mark Burns, J. Mason Earles, David E. Block

Preface

The following manuscript (**published September 2023, Oeno One**) is printed here with the same content as the journal edition, apart from necessary formatting differences. This chapter addresses the first aim outlined in my QE, “test the three existing and promising models using additional data”.

Abstract

Developing low-cost technology for custom water delivery to individual or small groups of plants is a critical next step to advance precision irrigation. Current systems for estimating evapotranspiration (ET), or plant water use, work on the scale of a full vineyard (e.g., 3-5 acres) or the scale of a single vine, but at a cost that prohibits monitoring past a small number of representative vines. To develop and evaluate low-cost ET sensors for individual grapevines, we used three head-pruned Zinfandel vines in pots and placed them on load cells to collect continuous weights indicative of actual ET. We mounted research-grade sensors for humidity, temperature, and wind speed on each vine and saved data at 2-minute intervals during three growing seasons. We developed three models based on first principles (Convective Mass Transfer or Mass Balance approaches) or simple correlations to predict actual single-plant ET

from these data. We present here the results of a multi-year trial at the UC-Davis RMI vineyard to illustrate the performance of each of the models for ET estimation. Relative model performance was assessed by comparing model predictions to ground truth data provided by measurements from load cells–including assessments of estimated instantaneous ET rate, estimated cumulative water use over a one-hour window surrounding solar noon, and estimated cumulative water use over a full 24-hour period. The three algorithms developed consistently performed well, with single vine ET rate predictions showing a strong linear relationship with ground truth (range in r^2 over three seasons CMT r^2 = 0.61 - 0.86; MB r^2 = 0.07 - 0.91; EM r^2 = 0.57 - 0.92). The MB approach, which includes two measurements of relative humidity and temperature, was the most variable, likely due to the impact of sensor placement. In all seasons, we also examined the trend in the plant scaling factor found in each model, deemed A_s, which, based on model theory, is a function of vine size. Taken together, these results suggest that high-resolution irrigation (HRI) models are a promising new method for ET estimation at the single plant level.

Introduction

In California, recurrent droughts and water shortages have led to competition between agricultural, urban and conservation water needs (Diffenbaugh *et al.,* 2015). Even in the face of these challenges, there are still about 355,000 acres of grapes being cultivated throughout the state (CDFA and USDA, 2022). These vineyards typically use drip irrigation practices, which treat all plants in a management zone identically, even though it is clear that all plants do not require the same amount of water. Water demand heterogeneity can arise from cultivar differences, complex topography, canopy orientation, soil structure and composition, or roguing practices for disease control, as examples. As a consequence of this variability, treating all plants in a management zone as identical will generally lead to some plants receiving excessive

or inadequate water. Beyond the needs of the plant, water balance contributes to fruit quality and yield, layering additional complexity into its management. For example, in perennial woody crops like grapes and almonds, well-timed water stress can help control vegetative vigour and may increase fruit quality (Chaves *et al.,* 2007; Van Leeuwan and Seguin, 2006). Conversely, moderate to severe water stress caused by extreme deficit irrigation can damage cellular components for light harvesting, limiting photosynthesis. If this water stress is prolonged, delays in ripening, sudden vine collapse and reduced fruitfulness can negatively impact berry yield and quality (Dayer *et al.,* 2007). These constraints can create a problem, however, because the irrigation manager's goal is finding this narrow range of applied water by considering the plant's needs, but these needs usually vary in a complex way through space and time. When this variability is combined with complex deficit irrigation schemes, optimization of water use can be nearly impossible using existing technology.

1. Existing methods for measuring evapotranspiration

Current methods for measuring crop ET (ET_c) are powerful, and various approaches have already been commercialised. Some of the most widely used methods to measure ET are energy balance technologies, sap flow sensors, and the more traditional approach of reference ET (ET_o) and crop coefficients, but all of these methods come with significant limitations.

1.1. Energy balance technologies

Energy balance methods are based on the concept of conservation of energy, which states that the energy in some problem domain is constant. For the plant-soil-atmosphere system, then, energy balance theory states that net radiation must be in balance with the latent heat flux density, ground heat flux density, sensible heat flux density, and other less significant energy sinks. Ground heat flux density is the rate of heat storage in the soil and vegetation due to conduction and is either measured directly or computed using information from Normalized Difference Vegetation Index (NDVI) measurements. Sensible heat flux density is the energy lost

to the air from the plant, soil and cover crops via convection and conduction. This term is sensitive to factors impacting the distribution of energy sources in the canopy, including wind speed and surface roughness, and is, therefore, affected by canopy size, structure, trellising, plant phenological stage and even ground surface heterogeneity (Rienth *et al.,* 2019). Researchers have developed multiple methods to estimate sensible heat flux density, including eddy covariance, Bowen ratio method, and surface renewal (Li *et al.,* 2008; Paw U *et al.,* 1995). The energy stored in the air layer, in the biomass, and chemical energy stored in the carbohydrate bonds of plant sugars are usually considered negligible compared to other terms (Anapalli *et al.,* 2018). The latent heat flux density is the heat lost from the system due to the evaporation of water and is calculated as a residual once all other parameters in the model are determined. Latent heat flux density divided by the latent heat of vaporisation of water will give ET.

While energy balance technologies for estimating ET_c are some of the most widely employed, they are also limited to coarse spatial resolutions, are expensive and can be sensitive to many different sources of error.

1.2. Sap flow sensors

Sap flow sensors are another promising technology, with several advantages over energy balance methods. These sensors directly measure the movement of fluid inside the xylem from the roots to stems and to leaves, where water is transpired through stomata—a process called sap flow. Sap flow is essential for the maintenance of the hydraulic continuum from soil to plant to atmosphere; thus, monitoring this process can yield important information about the hydraulic function or dysfunction of the plant (Steppe *et al.,* 2015). Various methods for estimating sap flow rate have been developed, including thermal dissipation probes and the steam heat balance method (Granier, 1985; Lascano, 2000; Lascano *et al.,* 2016). Both are based on measuring the difference between a heated element and a non-heated reference

element; as the sap flow rate increases the temperature difference between the two elements decreases (Fernández and Testi, 2017). While the sap flow method will fundamentally achieve single-plant resolution, individual sensors are expensive and require skilled installation and routine maintenance labour. As a result, sensors are typically mounted on only 1 to 3 plants per management zone. Plants are chosen to represent the range of variability; a problematic assumption that can ignore many sources of heterogeneity.

1.3. Reference ET and crop coefficients

Another important method for estimating ET_c is by a proxy measurement along with correction factors known as crop coefficients, specific for the type of plant being grown nearby (Allan *et al.,* 1998; Behboudian and Singh, 1998). These proxy ET values, known as ET_o, are calculated at one of over 200 California Irrigation Management Information System (CIMIS) weather stations distributed throughout the state (LAWR-UC Davis, 2021); some other states have similar systems. Each station measures local weather parameters over a reference crop (well-watered grass), and these parameters are fed into a Penman-Monteith model which predicts hourly ET_o. Once ET_o is known, it can be used to calculate the true ET_c of crops grown nearby by multiplying by a scaling factor known as the crop coefficient (K_c). The crop coefficient is an experimentally derived value specific to the cultivar and is sometimes adjusted for other management factors (Bravdo *et al.,* 1987). Compared to the other approaches for ET_c estimation, this method has the distinct advantage of being virtually free for California growers. However, this approach is limited by its reliance on the assumptions that regional ET_o values and crop coefficients are generalisable. As a result, this method can be quite effective at estimating regional ET_c but it can lack local specificity, ignoring complex factors that influence slight differences in vine-to-vine water demand, such as management practices, phenological stages, topography, soil characteristics and many others (LAWR-UC Davis, 2021). Additionally,

these methods do not perform well under deficit irrigation when they cannot completely account for the response of plants to water stress (Hochberg *et al.,* 2017).

2. The High-Resolution Irrigation method

Our work addresses the complexity of modern irrigation management by outlining a system for delivering water differentially to each plant according to its needs—in other words, High-Resolution Irrigation (HRI). From the outset, we understood achieving HRI would require developing two fundamental components: (1) an engineered system for the targeted delivery of water to each plant and (2) an understanding of the plant's water needs that can inform irrigation decisions.

The second component, understanding a plant's water needs, requires knowing how much water to apply and when to apply it. The scope of this investigation is limited to exploring the question of how much water to apply, which is defined as evapotranspiration (ET) from a single plant.

Here we introduce the development and theoretical basis of three novel HRI models for predicting ET rate. To illustrate the performance of each of the models, we present the results of a three-year trial at the UC Davis RMI vineyard. We assessed relative model performance, comparing instantaneous ET rate, cumulative water use over a one-hour window surrounding solar noon and cumulative water use over a full 24-hour period. Throughout the 2020, 2021 and 2022 growing seasons, we also examined the trend in the plant scaling factor found in each model, deemed A_s. Together, these observations strongly support the utility of the new HRI models for ET_c estimation.

Materials and methods

1. Collecting single vine data

We collected data from three head-trained *Vitis vinifera* L. cv. Zinfandel vines grafted on St. George rootstock (*V. rupestris*), planted in 1.1 m3 plastic containers filled with Yolo County, CA sourced sandy loam. Zinfandel scion was grafted onto rootstock in Davis, CA in 2009, and then vines were transplanted into containers in 2016. Yolo County sandy loam has been shown to have an available water holding capacity of about 10-15% by volume (Schwankl and Prichard, 2009). Vines were located in the Robert Mondavi Institute (RMI) vineyard in Davis, California (*Figure 1.1*).

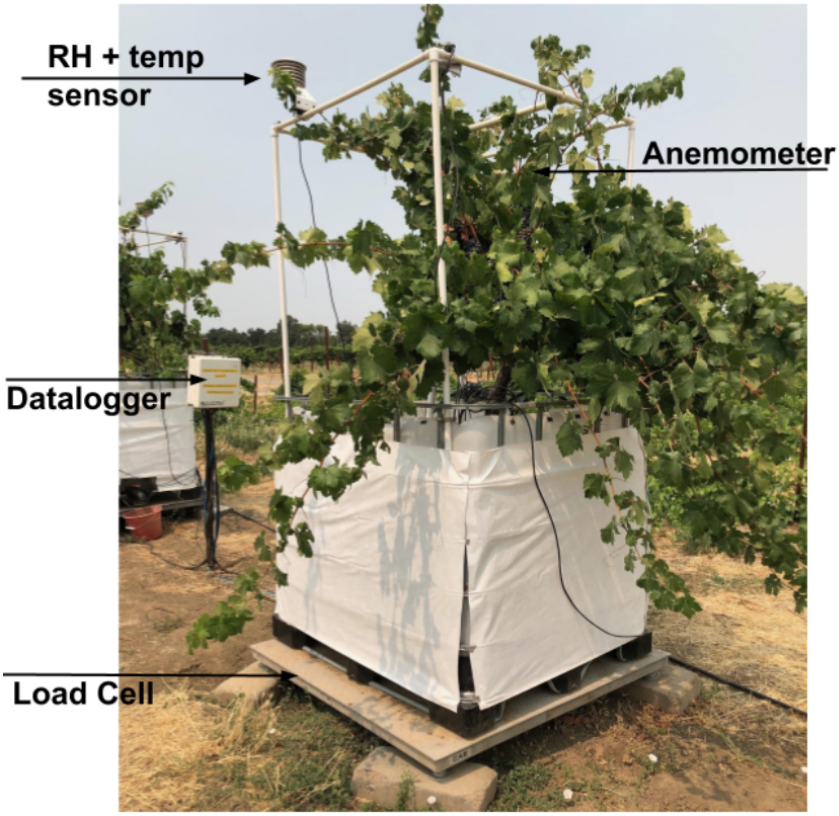

Figure 1.1: Potted grapevine lysimeter used for HRI model validation. Note: a second relative humidity (RH) and temperature (temp) sensor is out of view, in the centre of the canopy.

We irrigated vines using a dedicated programmable drip irrigation and fertigation system, composed of 8 equally spaced 2 L/H Woodpecker pressure compensating drippers (*Netafim*, model 01WPC2) in a 1.5-meter circumference ring around the base of each vine. Irrigation events ranged in duration from 30 to 180 minutes and were programmed to occur before dawn every 24 to 72 hours during periods of normal irrigation, and no irrigation was done during dry-down periods. Vines received the same pest management and fertiliser regimen as other vines at RMI, per the direction of the vineyard manager. Data were collected from two vines during the 2020 and 2021 seasons and three vines in the 2022 season.

To predict the ET rate (units = $kg \cdot s^{-1}$) and then calculate single plant ET (units = kg), we measured the wind speed, air temperature and relative humidity in vine canopies by mounting each vine with a suite of research-grade sensors. We measured wind speed (units $m \cdot s^{-1}$) inside the vine canopy using a single needle anemometer (*East 30 Sensors*; Pullman, WA) that took instantaneous wind speed measurements every 10 seconds and recorded the average of the previous 12 instantaneous measurements for every 2-minute interval. We measured temperature (units ^{o}C) and relative humidity (units %) using HMP60L sensors (*Campbell Scientific*; Logan, UT) mounted both inside and outside of each vine canopy and recorded instantaneous measurements at each 2-minute interval. We filtered all biometeorological data using a 3-hour moving average to remove noise without causing any significant over or under-approximation of daily maxima and minima.

To measure ground truth ET (units = kg), we placed each potted vine and attached sensor suite on a commercial load cell, model HFS 405 (2270 kg capacity, 0.01 kg resolution, *CAS Corporation*; Seoul, South Korea), which recorded instantaneous mass at each 2-minute interval. The load cell was calibrated each year in February using manufacturer guidelines. ET was then calculated by difference. From this point forward, ground truth ET will be referred to as

load cell-measured ET. ET rate (units = $kg \cdot s^{-1}$) is calculated by taking the derivative of mass with respect to time.

We automated all data collection using two CR1000 data loggers (*Campbell Scientific*; Logan, UT), with 1 or 2 vines and associated sensors per logger, using custom CR1 programs. A single 30 W solar cell and 12 V lead acid battery powered the entire vine-sensor system.

2. Predicting ET rate for single grapevines

If the ET rate of water through the canopy of a plant could be measured, then calculating ET would be relatively straightforward. As current technology cannot accurately measure the ET rate directly at this scale, we have developed three novel models for predicting the ET rate using common biometeorological measurements. These models estimate ET but do not include a term for soil evaporation as a first approximation because early experiments showed the effect of soil surface evaporation was small, averaging less than 5-10% of daily water loss. Our methods use non-destructive, largely automated proximal sensing and a computation pipeline, feeding data from biometeorological sensors to the models. In this process, we measure wind speed, air temperature and relative humidity in or near the plant canopy. Using only these parameters, we have created three models, described in detail in the following sections, which can be used to calculate the estimated ET rate per area ($\dot{m}_e$, units $kg \cdot s^{-1} \cdot m^{-2}$) for single plants. Hereafter, we refer to the ET rate per area as mass flux.

2.1. Convective Mass Transfer mass flux model

The Convective Mass Transfer (CMT) model is one of two HRI models inspired by first principles. CMT relates transpiration to theory describing the convective mass transfer from a flat surface of water into moving air. This theory is based on applying the Reynolds analogy, which suggests a simple relationship between different transport phenomena (Cussler, 2009). In

this case, we use an analogy to the well-described process of convective heat transfer from a flat solid plate into a fluid with laminar flow over its surface. Using this analogy, we can define transpiration as the convective mass transfer from a flat surface of liquid or a gas saturated with water vapour into a gas with laminar flow over its surface (Cussler, 2009). From this theory, the estimated mass transfer flux depends on the mass transfer coefficient (K_m) and the difference between the partial pressure of water in the air at the saturated surface (P_{sat}) and in the air in the greater atmosphere (P_∞) [*Equation 1*].

$$\dot{m}_e = K_m \cdot (P_{sat} - P_\infty)$$

In this case, the mass transfer coefficient (K_m) is a function of the mass diffusivity of air, the Reynolds number, the Schmidt number, and a scalar term. The Reynolds number can be expressed as a function of the bulk velocity of air and kinematic viscosity, while the Schmidt number can be expressed as a function of kinematic viscosity and mass diffusivity. Note that in a pure gas, the diffusion coefficient and viscosity are proportional to $T^{3/2}$ and $T^{1/2}$, respectively (Bird *et al.,* 2006). When the pure gas condition is assumed to be true, and all other constants are included in the scalar (k_{cmt}) term, the full CMT model can be reduced to [*Equation 2*]:

$$\dot{m}_e = v_\infty^{\frac{1}{2}} \cdot T^{\frac{11}{12}} \cdot k_{cmt} \cdot \Delta P$$

where v_∞ is the bulk velocity of air ($m \cdot s^{-1}$) measured inside the canopy, T is canopy air temperature (K), and Δ P ($g \cdot m^{-2}$) is the difference between partial pressure of water in air in the boundary layer and the greater atmosphere. The saturation pressure of water in the air is calculated using Antoine's Equation, which relates vapour pressure to air temperature; and partial pressure is calculated by multiplying this value by relative humidity in the canopy. This model maintains three assumptions: first, all transpiring leaf surfaces are saturated with water vapour, perfectly flat and with a uniform temperature equal to the temperature of the air in the canopy. Second, stomata are assumed to remain in the open state, to maintain constant

boundary layer saturation, and finally, it is assumed that a laminar flow of air exists at the leaf surface which carries water vapour away from the boundary layer. Consistent with CMT theory, the area term (A_s) associated with this flux would be equal to the total saturated surface area of the transpiring leaves in the canopy. As k_{cmt} is a constant and not easily calculated *a priori*, here we will include this parameter with A_s to get a new modified area term, A_s', which will not affect the remainder of the analyses. Hence, in our calculations, *Equation 2* is used without the k_{cmt} term.

2.2. Mass Balance mass flux model

The Mass Balance (MB) model is based on the concept of conservation of mass, which states that in any closed system mass is constant and is neither created nor destroyed. In the case of a plant canopy, this means the mass flow rate of water out of the canopy ($\dot{m}_{out}$) is equal to the mass flow rate of water into the canopy ($\dot{m}_{in}$) plus the mass flow rate from the plant (i.e. evapotranspiration rate, $\dot{m}_p$). With rearrangement, this equation states the ET rate is equal to the difference between the mass flow rate out of the canopy and into the canopy, as seen in [*Equation 3*].

$$\dot{m}_p = \dot{m}_{out} - \dot{m}_{in} = \left(A_s \cdot v_{\infty,\, out} \cdot H_{out} \right) - \left(A_s \cdot v_{\infty,\, in} \cdot H_{in} \right)$$

However, here we assume that the cross-sectional area of the canopy is constant, as is the velocity of wind through the plant (verified experimentally). With these assumptions, the ET rate can be calculated as a product of the bulk velocity of air (v_∞, units $m \cdot s^{-1}$) measured inside the canopy, the cross-sectional area of the canopy (A_s, units m^2) and the difference between the absolute humidity (H, units $g \cdot m^{-3}$) outside and inside the canopy. Thus, by dividing both sides of *Equation 3* by the area term, the full MB model for mass flux can be reduced to [*Equation 4*]:

$$\dot{m}_e = v_\infty \cdot \Delta H$$

where Δ H is the difference between H of the air outside the canopy and the air inside the canopy. Absolute humidity, a function of air temperature, is computed using a formula derived from the Ideal Gas Law and an equation for Saturation Vapor Pressure (Snyder, 2005). As stated above, based on the mass balance concepts underlying this model, the area term (A_s) would equal the cross-sectional area of the vine canopy.

2.3. Empirical mass flux model

We selected the Empirical Model (EM) using only statistical methods from a set of more than 25 candidate models exploring mass flux as a function of various combinations of measured biometeorological parameters, as well as the interactions of these parameters. The goals of EM model development were generalisability and dimensional reduction. In addition to computational efficiency, dimensional reduction has the added benefit of reducing the number of sensors needed in the low-cost sensors being developed as part of this project.

We selected the full EM model [*Equation 5*] because in addition to achieving reduced dimensionality, it also performed well in terms of ET predictions when compared to other candidate models.

$$\dot{m}_e = k_1 \cdot v_\infty + k_2 \cdot T + k_3 \cdot (v_\infty \cdot T)$$

The EM includes only bulk wind speed (v_∞, units $m \cdot s^{-1}$) measured inside the canopy and air temperature (T, units ^oC) parameters as well as the interaction of these parameters, and unit fixing constants (k_1, k_2 and k_3). This approach assumes humidity measurements and related parameters (e.g., partial pressure) are not strong enough predictors of ET rate to be included in a model designed to explain variation in mass flux and inform irrigation decisions. Due to its empirical nature, the area term (A_s) in this model does not have a clear physical meaning.

3. Calculation of model area terms

To calculate ET_e (units = kg) from mass flux, the magnitude of the model-associated area term must first be measured or calculated; here, we calculated A_s experimentally. During any given time window we achieved this calculation by dividing the load cell measured ET rate by the model-estimated mass flux. Throughout all seasons thus far we used two to four continuous days of data to fit a new A_s term, then used this term to make projected predictions for the next 10-12 days. Based on data collected in 2020, we found that it is helpful to recalculate a new A_s term for each model every 10-14 days, at least until canopies are fully established.

4. ET_e from mass flux

Once mass flux has been calculated using one of the three novel models and A_s terms have been determined, it is possible to move on to ET calculation. Each HRI model generates an estimated instantaneous mass flux for every two-minute interval. This mass flux is integrated over time (t, units s) and multiplied by a plant scaling coefficient (A_s, units m^2), giving estimated ET_e [*Equation 6*]:

$$ET_e = A_s \cdot \int_0^t \dot{m}_e dt$$

ET rates are found by simply multiplying mass flux estimates by the A_s terms without integration. While early data suggests that all models perform well in terms of correlating estimated ET rate with measured ET rate, we have only started investigating methods for directly estimating the area term from physical measurements.

5. Programming and data analysis

For the following results, we used R v3.5.1 for all analysis and visualization (R Core Team, 2018). Model statistics, including r^2, p-value and RMSE, were generated using the ‘stats’

package, a part of R. For all computation we used a 2021 Apple MacBook Pro with 16 gigabytes of random access memory.

Results

From May 2020 through August 2022, we collected three seasons of data with our sensors and load cells. All biometeorological parameters are characterised by a strong diurnal pattern (*Figure 1.2*). Ground truth ET data, generated from load cell measurements, were recorded at 2-minutes intervals. When viewed over time, this data reveals periods of evapotranspiration as well as irrigation events (*Figure 1.3*).

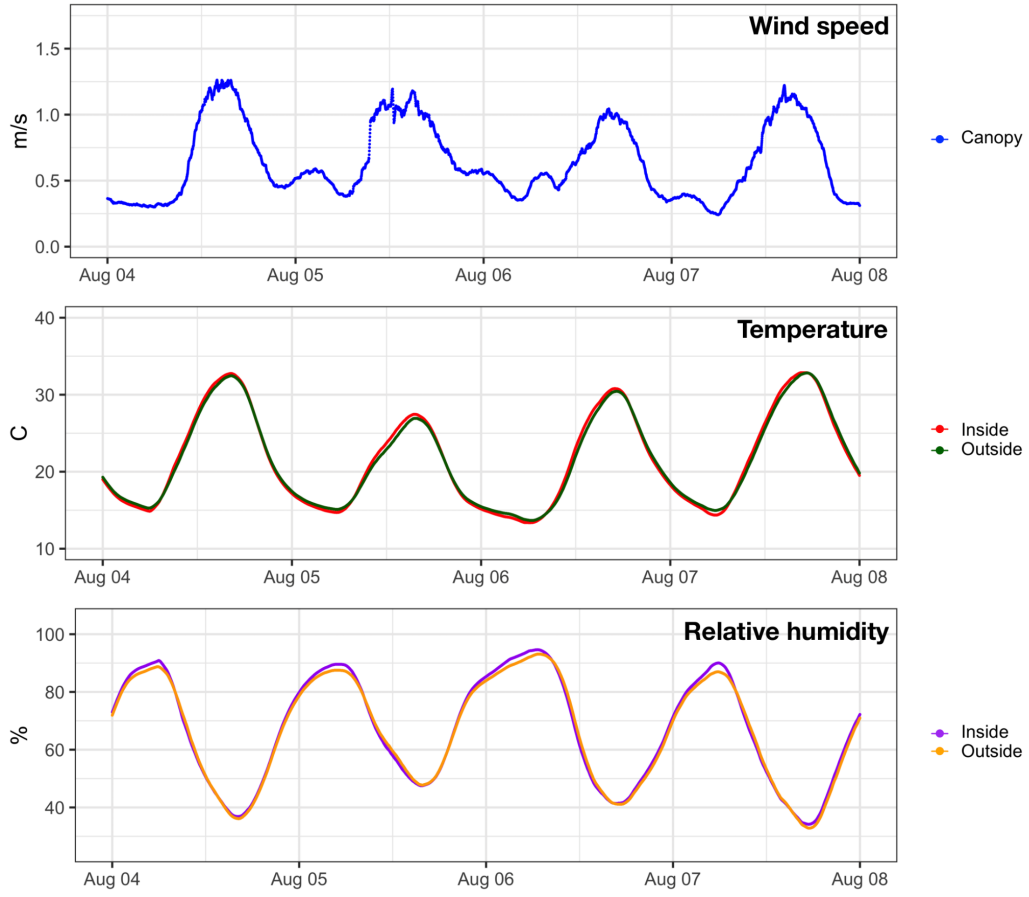

Figure 1.2: (top) Wind speed inside the canopy, over time, with spikes during daylight hours and mild wind at night. (middle) Air temperature inside and outside the canopy, over time, with maxima around solar noon and minima just before sunrise. (bottom) Relative humidity inside and outside the canopy, over time, with maxima just before sunrise and minima around solar noon. Data from August 2020.

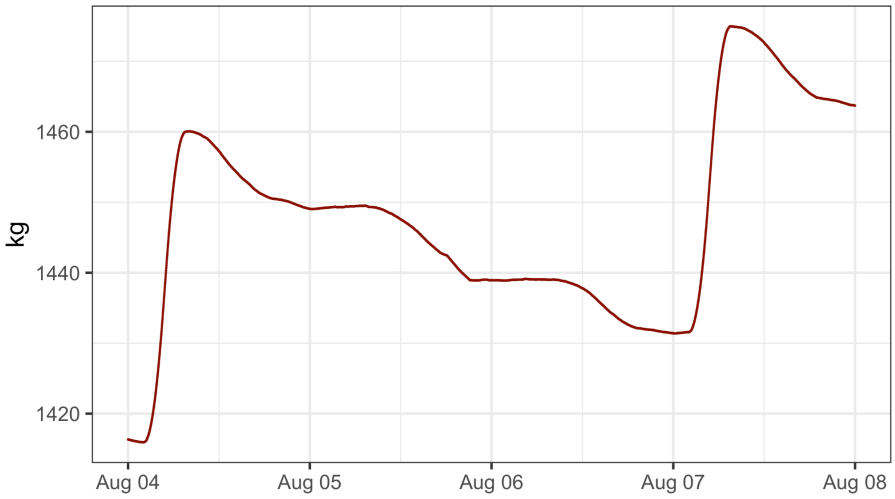

Figure 1.3: Data from the load cell, smoothed using a 180 minute moving average filter to remove noise. The periods of high positive (+) slope are irrigation events, the flat periods are nighttime when little to no ET is occurring, and the periods of negative (-) slope are daytime when ET rate is highest. Data from August 2020.

The measured ET rate is computed from the load cell data by taking the derivative of mass with respect to time (*Figure 1.4*). It can be seen that the evapotranspiration is highest during times with peak temperature, which occurs around solar noon each day. While these data are reported only for a single vine, other vines exhibited very similar behaviour. Overall, we observed vines using about 30 litres of water per day, which falls within the range of

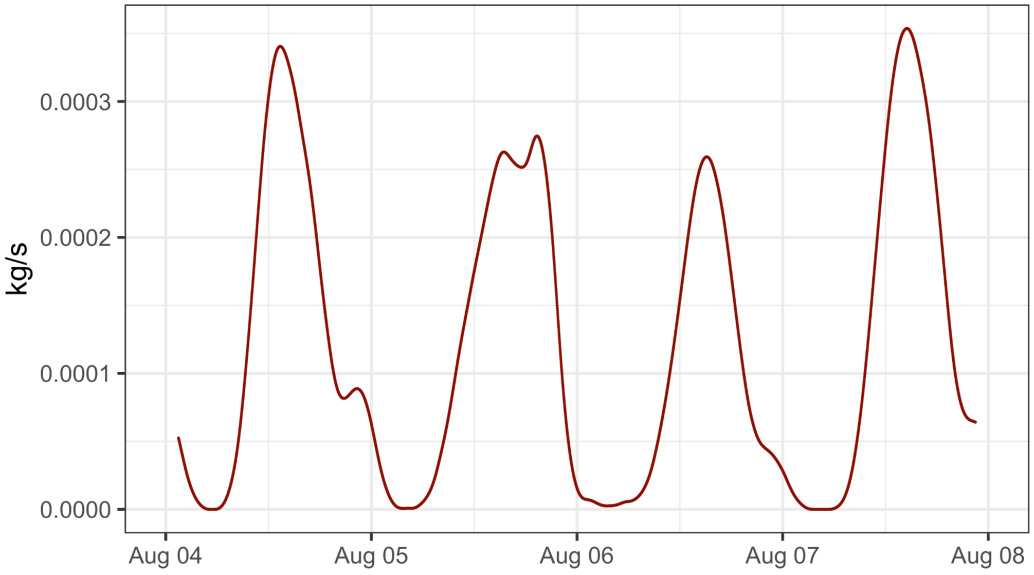

Figure 1.4: Measured ET rate is computed by taking the derivative of load cell mass with respect to time. Irrigation events were ignored using a filter. Data from August 2020.

observations from UC ANR in 2002, which measured 22.7 to 37.9 litres of water used per day for mature, vigorous grapevines in the Central Valley of California (Geisel *et al.,* 2002).

We used filtered biometeorological parameters to make ET rate predictions using our three models. In *Figure 1.5*, the load cell measured ET rate is plotted alongside model-predicted ET rate over a 5-day period in June 2022. We found a strong linear relationship between model-predicted and load-cell-measured ET rates. The CMT predicted ET rate r^2 values were 0.89 for Vine 1, 0.85 for Vine 2 and 0.66 for Vine 3; MB predicted ET rate r^2 values were 0.78 for Vine 1, 0.22 for Vine 2 and 0.45 for Vine 3; and EM predicted ET rate r^2 values were 0.87 for Vine 1, 0.89 for Vine 2 and 0.74 for Vine 3 (*Figure 1.5*).

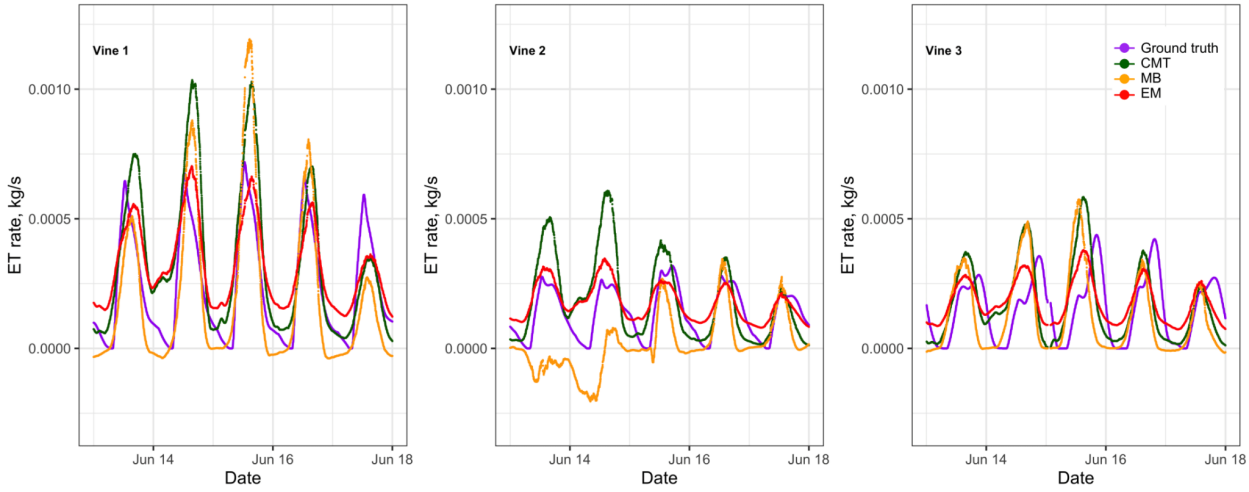

Figure 1.5: Each plot shows the ET rate of water as determined by the load cell and by one the HRI models for a 5-day period in June 2022. In all figures the purple line represents the load cell measured ET rate. The p-value for all linear regressions was less than $2 \cdot 10^{-16}$. The CMT r^2 values ranged from 0.66 to 0.89, the MB r^2 values ranged from 0.22 to 0.78, and the EM r^2 values ranged from 0.74 to 0.89.

We observed similar agreement over the course of the full 2020, 2021, and 2022 seasons (*Table 1.1*). At most times of the day the CMT model tends to overpredict and the EM model tends to underpredict during the daytime and overpredict during night-time hours. The MB model was both under and overpredicted and was more prone to error. Importantly, we collected some of these data during extended periods of drought stress as well as during

Vine	Model	June 2020	July 2020	August 2020	June 2021	July 2021	August 2021	June 2022	July 2022	August 2022
1	*CMT*	$r^2 = 0.73$ RMSE = $1.04 \cdot 10^{-4}$ p-value < $2 \cdot 10^{-16}$	**Drydown** $r^2 = 0.84$ RMSE = $1.20 \cdot 10^{-4}$ p-value < $2 \cdot 10^{-16}$	$r^2 = 0.82$ RMSE = $1.03 \cdot 10^{-4}$ p-value < $2 \cdot 10^{-16}$	$r^2 = 0.78$ RMSE = $1.65 \cdot 10^{-4}$ p-value < $2 \cdot 10^{-16}$	**Drydown** $r^2 = 0.75$ RMSE = $2.38 \cdot 10^{-4}$ pp-value < $2 \cdot 10^{-16}$	$r^2 = 0.68$ RMSE = $2.49 \cdot 10^{-4}$ p-value < $2 \cdot 10^{-16}$	**Drydown** $r^2 = 0.86$ RMSE = $1.20 \cdot 10^{-4}$ p-value < $2 \cdot 10^{-16}$	$r^2 = 0.78$ RMSE = $1.82 \cdot 10^{-4}$ p-value < $2 \cdot 10^{-16}$	$r^2 = 0.73$ RMSE = $1.73 \cdot 10^{-4}$ p-value < $2 \cdot 10^{-16}$
	MB	$r^2 = 0.78$ RMSE = $9.21 \cdot 10^{-5}$ p-value < $2 \cdot 10^{-16}$	**Drydown** $r^2 = 0.91$ RMSE = $9.20 \cdot 10^{-5}$ p-value < $2 \cdot 10^{-16}$	$r^2 = 0.87$ RMSE = $8.33 \cdot 10^{-5}$ p-value < $2 \cdot 10^{-16}$	$r^2 = 0.74$ RMSE = $1.70 \cdot 10^{-4}$ p-value < $2 \cdot 10^{-16}$	**Drydown** $r^2 = 0.66$ RMSE = $2.40 \cdot 10^{-4}$ p-value < $2 \cdot 10^{-16}$	$r^2 = 0.55$ RMSE = $2.81 \cdot 10^{-4}$ p-value < $2 \cdot 10^{-16}$	**Drydown** $r^2 = 0.75$ RMSE = $1.61 \cdot 10^{-4}$ p-value < $2 \cdot 10^{-16}$	$r^2 = 0.71$ RMSE = $1.47 \cdot 10^{-5}$ p-value < $2 \cdot 10^{-16}$	$r^2 = 0.90$ RMSE = $1.47 \cdot 10^{-5}$ p-value < $2 \cdot 10^{-16}$
	EM	$r^2 = 0.75$ RMSE = $9.88 \cdot 10^{-5}$ p-value < $2 \cdot 10^{-16}$	**Drydown** $r^2 = 0.85$ RMSE = $1.19 \cdot 10^{-4}$ p-value < $2 \cdot 10^{-16}$	$r^2 = 0.83$ RMSE = $9.98 \cdot 10^{-5}$ p-value < $2 \cdot 10^{-16}$	$r^2 = 0.81$ RMSE = $1.52 \cdot 10^{-5}$ p-value < $2 \cdot 10^{-16}$	**Drydown** $r^2 = 0.83$ RMSE = $1.93 \cdot 10^{-4}$ p-value < $2 \cdot 10^{-16}$	$r^2 = 0.80$ RMSE = $1.94 \cdot 10^{-4}$ p-value < $2 \cdot 10^{-16}$	**Drydown** $r^2 = 0.86$ RMSE = $1.21 \cdot 10^{-4}$ p-value < $2 \cdot 10^{-16}$	$r^2 = 0.84$ RMSE = $1.56 \cdot 10^{-4}$ p-value < $2 \cdot 10^{-16}$	$r^2 = 0.81$ RMSE = $1.45 \cdot 10^{-4}$ p-value < $2 \cdot 10^{-16}$
2	*CMT*	$r^2 = 0.61$ RMSE = $2.15 \cdot 10^{-4}$ p-value < $2 \cdot 10^{-16}$	**Drydown** $r^2 = 0.73$ RMSE = $1.01 \cdot 10^{-4}$ p-value < $2 \cdot 10^{-16}$	$r^2 = 0.61$ RMSE = $1.07 \cdot 10^{-4}$ p-value < $2 \cdot 10^{-16}$	$r^2 = 0.78$ RMSE = $1.33 \cdot 10^{-4}$ p-value < $2 \cdot 10^{-16}$	**Drydown** $r^2 = 0.72$ RMSE = $1.32 \cdot 10^{-4}$ p-value < $2 \cdot 10^{-16}$	$r^2 = 0.70$ RMSE = $1.47 \cdot 10^{-4}$ p-value < $2 \cdot 10^{-16}$	**Drydown** $r^2 = 0.83$ RMSE = $6.75 \cdot 10^{-5}$ p-value < $2 \cdot 10^{-16}$	$r^2 = 0.83$ RMSE = $7.01 \cdot 10^{-5}$ p-value < $2 \cdot 10^{-16}$	$r^2 = 0.83$ RMSE = $6.95 \cdot 10^{-5}$ p-value < $2 \cdot 10^{-16}$
	MB	$r^2 = 0.16$ RMSE = $2.57 \cdot 10^{-4}$ p-value < $2 \cdot 10^{-16}$	**Drydown** $r^2 = 0.35$ RMSE = $1.56 \cdot 10^{-4}$ p-value < $2 \cdot 10^{-16}$	$r^2 = 0.15$ RMSE = $1.59 \cdot 10^{-4}$ p-value < $2 \cdot 10^{-16}$	$r^2 = 0.22$ RMSE = $2.35 \cdot 10^{-4}$ p-value < $2 \cdot 10^{-16}$	**Drydown** $r^2 = 0.07$ RMSE = $2.41 \cdot 10^{-4}$ p-value < $2 \cdot 10^{-16}$	$r^2 = 0.19$ RMSE = $2.41 \cdot 10^{-4}$ p-value < $2 \cdot 10^{-16}$	**Drydown** $r^2 = 0.42$ RMSE = $1.28 \cdot 10^{-4}$ p-value < $2 \cdot 10^{-16}$	$r^2 = 0.48$ RMSE = $1.24 \cdot 10^{-4}$ p-value < $2 \cdot 10^{-16}$	$r^2 = 0.41$ RMSE = $1.33 \cdot 10^{-4}$ p-value < $2 \cdot 10^{-16}$
	EM	$r^2 = 0.65$ RMSE = $2.02 \cdot 10^{-4}$ p-value < $2 \cdot 10^{-16}$	**Drydown** $r^2 = 0.67$ RMSE = $1.04 \cdot 10^{-4}$ p-value < $2 \cdot 10^{-16}$	$r^2 = 0.57$ RMSE = $1.12 \cdot 10^{-4}$ p-value < $2 \cdot 10^{-16}$	$r^2 = 0.86$ RMSE = $9.85 \cdot 10^{-5}$ p-value < $2 \cdot 10^{-16}$	**Drydown** $r^2 = 0.88$ RMSE = $8.38 \cdot 10^{-5}$ p-value < $2 \cdot 10^{-16}$	$r^2 = 0.89$ RMSE = $8.65 \cdot 10^{-5}$ p-value < $2 \cdot 10^{-16}$	**Drydown** $r^2 = 0.87$ RMSE = $5.93 \cdot 10^{-5}$ p-value < $2 \cdot 10^{-16}$	$r^2 = 0.92$ RMSE = $4.87 \cdot 10^{-5}$ p-value < $2 \cdot 10^{-16}$	$r^2 = 0.89$ RMSE = $5.79 \cdot 10^{-5}$ p-value < $2 \cdot 10^{-16}$

Table 1.1: Data are shown for Vine 1 (V1) and Vine 2 (V2) for the months of June, July and August in 2020, 2021 and 2022 growing seasons. Each cell gives the r^2, RMSE and p-value for the relationship between model predicted ET rate and load cell measured ET rate. The cells marked "**Drydown**" included a 10-day drydown. Two vines were used because only two vines of data were available for all three seasons

periods of typical irrigation. Including stressful periods, noted in *Table 1.1*, provides additional evidence that the models generate estimates of crop ET_c and not another concept like reference ET_o which is more related to evaporative demand. In this experiment, each dry-down event represents 10 consecutive days without receiving any applied irrigation. Note the relatively poor performance of Vine 2 in the MB model in all growing seasons, exhibited in *Figure 1.5* and *Table 1.1*. This can be attributed to errors when calculating absolute humidity differences from temperature and individual relative humidity, especially when these differences are small. Sometimes, when absolute humidity inside and outside the canopy is very close, a negative ET rate can be calculated, which is unlikely for grapevine, and is probably a result of a lack of sensitivity in the methods used to sense and calculate absolute humidity. Absolute humidity error could also be the result of sensor placement. We noted the outside canopy relative humidity sensors for Vine 2 were placed upwind of prevailing winds relative to Vine 2, while the outside canopy humidity sensors for Vine 1 and 3 were placed downwind relative to their respective vines, thus indicating the importance of proper sensor placement for the successful use of the MB approach. Both the CMT and EM models give generally good predictions of the ET rate. Neither of these approaches uses the external relative humidity sensors on the experimental vines, which means none of the effects seen on Vine 2 are present in these calculations.

Given their physical bases, we hypothesised that the trend in the CMT and MB associated A_s terms over each season could have a consistent relationship to the seasonal trend in other plant physical parameters, such as Leaf Area Index (LAI) or cross-sectional area of the canopy (Orlando *et al.,* 2016; *Figure 1.6*). In 2020 and 2022, the CMT model A_s values displayed an overall trend that somewhat or very much resembles annual cycles in canopy physical parameters like LAI, with an increase until approximate veraison with subsequent levelling out, but this trend was reversed in 2021. While in 2022 the MB model A_s trend was

somewhat like the expected trend, the trends observed in 2020 and 2021 were not what we would expect for plant growth during a growing season. In several instances during 2020 and 2021, the MB model A_s values were below zero, indicating erroneous predictions likely due to sensitivity issues with sensing and calculating absolute humidity. After these observations, we now believe that the A_s term relationship to physical measurements, such as LAI, is more nuanced and is likely mediated by other factors, such as physiological changes caused by the senescence of older leaves, fruit set, or other seasonal processes.

With the calculation of A_s terms, we can now directly compare the load cell measured and model predicted ET. Load cell measured ET, ET_c, is calculated by integrating load cell measured

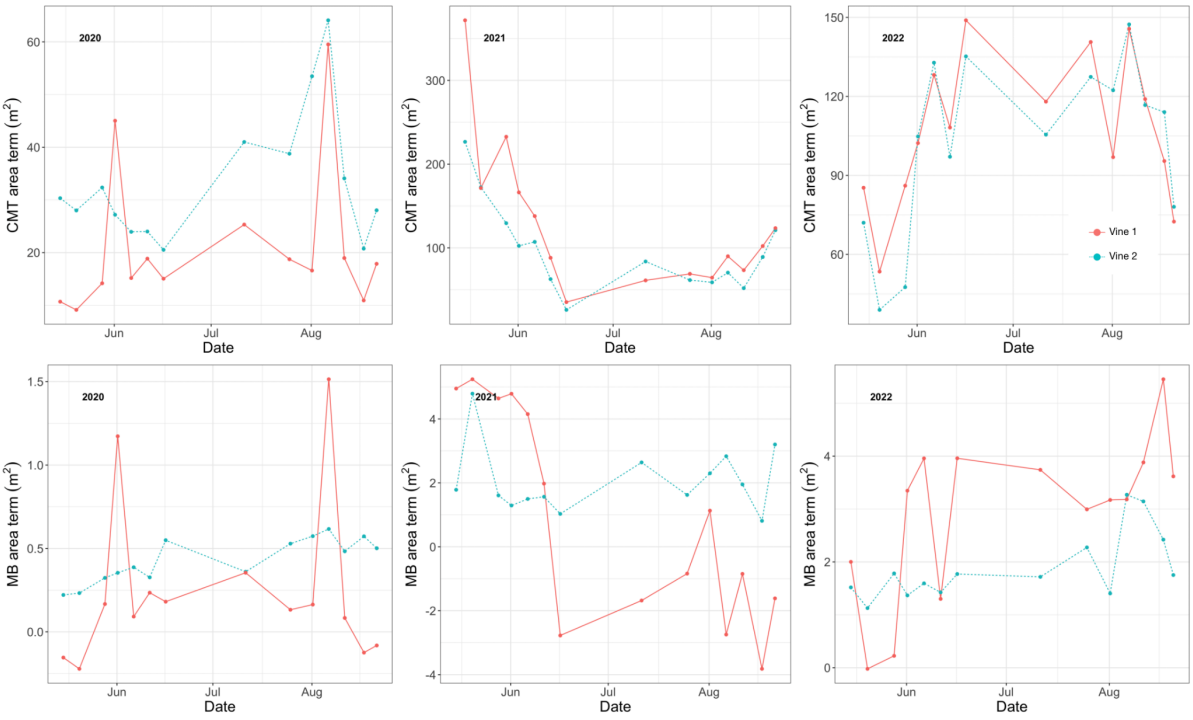

Figure 1.6: Example of trend in experimentally determined area term (A_s) values for CMT (top row) and MB (bottom row) models over the 2020 (left column), 2021 (middle column), and 2022 (right column) growing seasons. Legend in top, right panel.

ET rate over time. For all vines, we computed the model predicted ET_e and load cell measured ET_c over a 1-hour window from 13:00-14:00 PST, daily using 56 days for Vine 1, 42 days for Vine 2 and 23 days for Vine 3, distributed approximately evenly from May to August, 2022 (*Figure 1.7*). The days used to calculate model predicted ET_e and load cell measured ET_c were chosen based on the availability of a continuous set of data for a full 24-hour period. The main challenge to finding a full 24 hours of measurements every 2 minutes was frequent gaps in wind speed data, a result of the unprotected needle design of the anemometers. If the anemometer needle comes into contact with anything, such as a leaf, insect or debris, during the measurement window, it will record a zero, negative or unreasonably large value. These erroneous recordings are considered to be gaps or missing data. To understand how the models performed relative to one another over short periods of time during the day, we performed multiple linear regression analyses on all 1-hour vine and model data. The multiple r-squared is 0.6292, suggesting a good overall fit, and all model p-values are significant at the 0.001 level, indicating a significant relationship between all model predictions and ground truth.

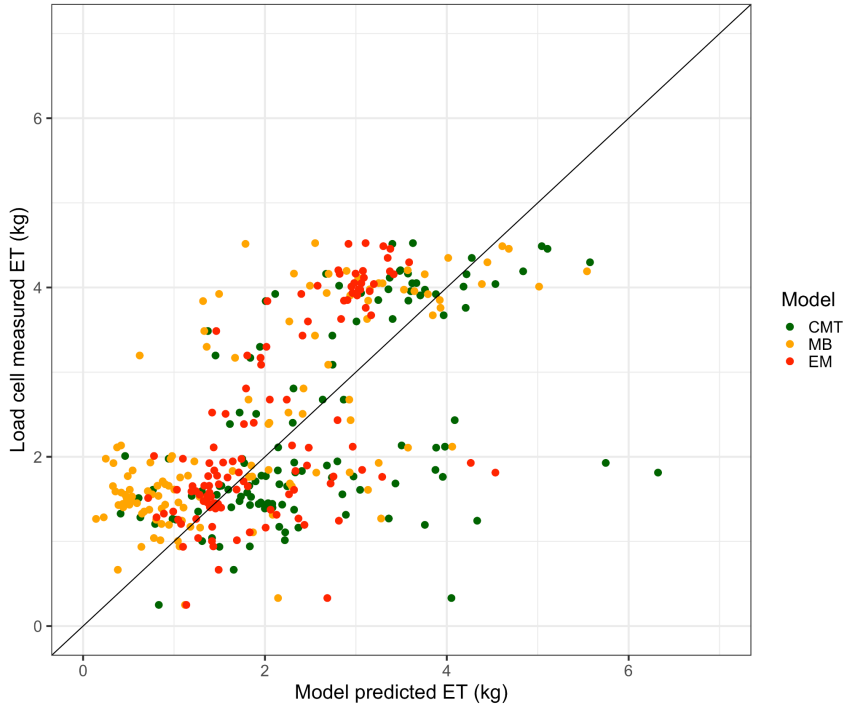

Figure 1.7: Plot comparing the predicted ET_e from all of the HRI models, and ground truth ET_c from the load cells during a 1 hour window from 13:00-14:00 each day (units = kg). Data are from Vines 1-3 using dates May-August in the 2022 season. Data were fit with a multiple linear regression model, and a 1:1 reference line is shown in black. The multiple r-squared is 0.6292, and all model associated p-values are significant at the 0.001 level of significance.

We also computed the model predicted ET_e and load cell measured ET_c over a 24-hour window, daily for the same 23, 42, or 56 days distributed approximately evenly from May to August, 2022 (*Figure 1.8*). With the inclusion of night in this multiple linear regression analysis, when little to no ET is occurring, and all models predict more accurately than during the day, the linear relationships between model predicted and ground truth ET now explain up to 82% of the variation in crop ET_c over a wide range of phenological stages and environmental conditions. The increase in explained variation could also be due to small shifts in prediction compared to ground truth. These shifts have a relatively large effect on the accuracy of predictions during some times of day, but over longer integration periods this effect is significantly reduced. Overall, only the CMT and EM model p-values are significant at the 0.001 level. MB model predictions are associated with a p-value of 0.17 suggesting a non-significant relationship between MB-predicted ET and ground truth ET over full 24-hour periods.

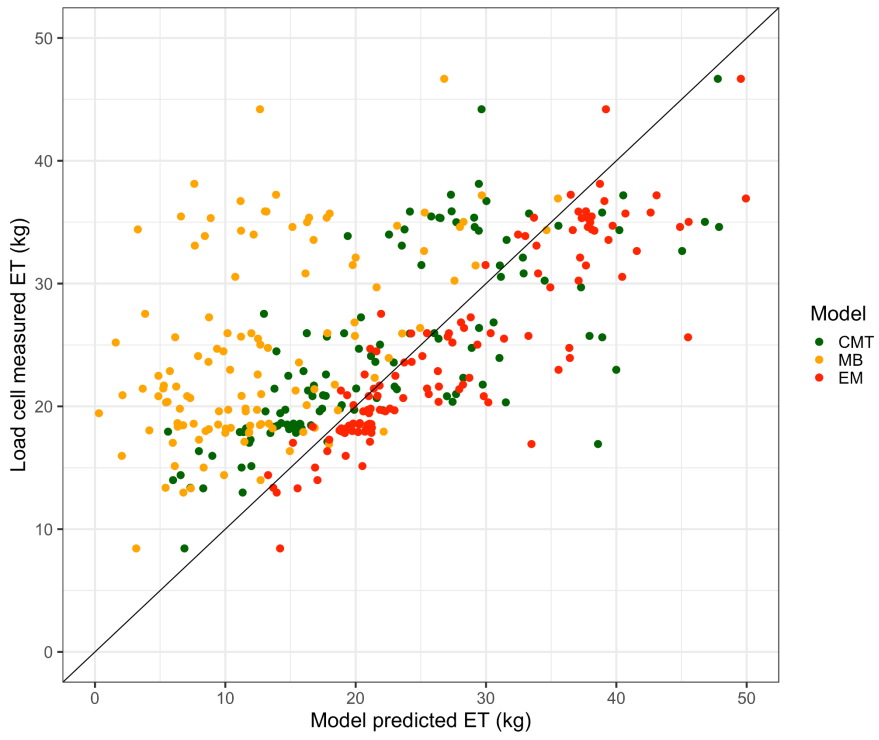

Figure 1.8: Plot comparing the predicted ET_e from all of the HRI models, and ground truth ET_c from the load cells during a 24 hour window each day (units = kg). Data are from Vines 1-3 using dates May-August in the 2022 season. Data were fit with a multiple linear regression model, and a 1:1 reference line is shown in black. The multiple r-squared is 0.8232, and the CMT and EM model associated p-values are significant at the 0.001 level of significance. The MB model p-value is 0.17.

We suggest, based on these results, that crop ET can be modelled effectively using HRI techniques and biometeorological data measured in vine canopies, though accurate calculation of A_s values may be critical to improving these predictions and enhancing generalisability.

Discussion

Given the generally consistent results over multiple seasons, we believe the three novel HRI models for predicting the ET rate of a single vine are a promising new method. With this fine-scale understanding of the water use of individual plants, irrigation managers could, for the first time, adjust water application rates to ensure plants are receiving what they need and nothing more. This vital step towards improved efficiency of applied irrigation, which accounts for the vine-to-vine water use variability that results from the heterogeneity of vineyards, will support further development of important technology capable of addressing the growing problem of water scarcity while maintaining or improving grape quality.

The data presented here is strong evidence that the ET rate can be well described using only simple biometeorological measurements and either first principles or empirical models. Based on the performance criteria of r^2 and RMSE, the EM model consistently explained more variation in ET rate than other models. However, while the EM gave the best results for these vines, we believe that the CMT model or MB models, which are based on first principles, will prove to be more generalizable, especially to variable canopy architectures and seasonal changes.

Other technologies designed to estimate ET also face challenges but comparing other models to the HRI model is not straightforward because most other models make predictions at coarser time scales. Generally, data from other ET estimation methods, especially crop coefficient methods, is presented on the scale of months or seasons such as in Li *et al.,* (2008), not days or hours. However, in Gómez-Candón *et al.,* (2021), researchers captured

multispectral images of Durum wheat fields using UAVs and then calculated actual ET using a Two-Source Energy Balance, an application of energy balance which separates energy fluxes, and, therefore ET, from plant and soil into two components (Norman *et al.,* 1995; Kustas and Anderson, 2009). Using this method the remotely sensed estimates of ET calculated with the TSEB model only explained 50% of the variation in daily ground truth ET measurements. While these researchers exemplified how challenging applying ET sensing methods can be in the field, some studies have also reported better performance of the energy balance approach. Anapalli *et al.,* (2018) demonstrated energy balance ET predictions can explain as much as 82% of the variation in lysimeter ET; however, this study was focused on corn and the ET measurements were less frequent, at once per day. Still, comparing these correlations to those observed in *Table 1.1*, it is reasonable to conclude that the HRI models offer a viable alternative to existing methods for estimating ET.

While the observed correlations with ET rate persist over multiple vines and multiple seasons, accurate prediction of ET_e will depend on the accurate calculation of the A_s term, which may vary with plant and over time. The A_s terms for two of the models, CMT and MB, have an actual physical meaning, albeit with the CMT model term incorporating k_{cmt}, but measuring those parameters directly may not be straightforward and will require further exploration. Again, for a single vineyard, we may not need this term to make good predictions of ET, but to make these predictions generalisable, it will be essential, especially if vines are of different sizes because of replanting or heterogeneities in soil or topography. Calculation of A_s terms directly from physical data, such as ground-based imagery of the vines collected throughout the season during normal tractor passes, would be possible. Downstream image analysis could be automated using a deep learning approach, similar to the approach used in Olenskyj *et al.,* (2022), to extract canopy cross-sectional areas, total leaf area, or other physical parameters of the vine that are well correlated with the model A_s terms.

Because generalisability is likely a prerequisite for the viability of this technology, it is critical that we unravel the physical meaning of this term and how to measure it directly. Studying how the experimentally derived A_s terms change over the growing season provides early insights into how we might overcome this problem. As was previously mentioned, we believe the trend in the area term could have some consistent relationship to the trend of other plant physical parameters over the growing season, such as leaf area or leaf area index, which tends to increase until harvest (typically early September in California) when it begins decreasing until leaves are shed shortly thereafter (Netzer *et al.,* 2009). Given these observations, and the physical basis of two of the HRI models, we hypothesised that the A_s term will be proportional to other physical measurements such as LAI or canopy cross-section. However, the experimentally derived area terms from the 2021 season did not resemble the expected pattern. Due to the way humidity and temperature sensors were mounted in the centre of the canopy and not in a different or more dynamic position, we believe the calculations of true A_s were masked by other intracanopy effects such as physiological changes in transpiration rate caused by senescence of older leaves, fruit set, or other seasonal processes. In future studies, we aim to explore ways to mitigate the effect of these other variables.

Other challenges include issues with the relative placement of humidity sensors and vines, which can severely impact the accuracy of MB-predicted mass flux. In future seasons we will investigate more accurate methods for calculating absolute humidity, including methods that are not sensitive to the relative positioning of vines and sensors or, alternatively, finding the optimal location of sensors for a given vine geometry. This issue is exemplified in *Figure 1.2* and *Table 1.1* which both show the MB predicted ET rate for Vine 2 as underperforming relative to other vines. Moreover, note that in *Figure 1.3*, the A_s term for the MB predictions dips below 0 several times in 2020 and 2021, indicating a negative ET rate was erroneously calculated. This sensitivity to sensor and vine location reveals a fundamental weakness of the MB model, as it

requires twice as many sensors as the other models and ideal sensor placement, and therefore increases the likelihood of incorrect measurements.

In addition to these issues, implementation in a commercial vineyard presents other challenges. For example, it is possible that canopies with less radial symmetry, such as many common trellis systems in California, could be more difficult to measure. It is also possible that certain trellis systems, cultivars, regions, topographical features, or other factors we have yet to consider could limit the performance of the models. In addition, sensors used by the models will need to be inexpensive, especially if every vine or a high density of vines is to be monitored, and robust in an agricultural environment–both topics of further research.

Even with the remaining challenges of increasing generalizability, the algorithms' prediction of the ET rate of water from single vines is very promising as an inexpensive and high-resolution means of controlling irrigation. Applied correctly, the algorithms presented here provide an option to growers looking for greater efficiency of irrigation and improved crop quality. The HRI algorithms provide a theoretical and practical basis for growers to balance irrigation with the varied water demands of vines growing in heterogeneous environments, all using a noninvasive and automated process.

Acknowledgements

The authors thank Leticia Chacon Rodriguez for viticultural guidance and access to vineyard facilities, Guillermo Federico Garcia Zamora and Gonzalo Ruiz Gonzalez for assistance with vine care and equipment installation at the RMI Vineyard, and Kathryn Prendergast of the Graduate Writing Fellows at the University of California Davis for assistance with editing. This work was made possible through financial support from Till Guldimann and the Ernest Gallo Endowed Chair in Viticulture and Enology.

Author contributions

M.R.J., J.J.L., S.N., and D.E.B. designed and implemented the experimental field setup. K.M. and M.R.J. conceptualised the CMT model. D.E.B., S.N. and M.R.J. conceptualised the MB model. M.R.J. conceptualised the EM model. M.R.J. and A.M. wrote all the code for data capture, analysis and visualisation. M.R.J. and D.E.B. wrote the paper with revisions from all authors. D.E.B., M.B., J.J.L., and J.M.E. provided funding and access to materials.

Data availability

Some of the data used for this publication, including examples from all sensors and the load cell, is available as a CSV file on Zenodo at https://doi.org/10.5281/zenodo.7983157.

Chapter Two

Quantifying vine size and morphology for the High Resolution Irrigation evapotranspiration models

Matthew Jenkins, Dylan Lenczewski-Jowers, Fabiola Chavez Lamas, Konrad Miller, Shayla Nikzad, Matthew Gilbert, Mark Burns, David E. Block

Preface

In an important followup to chapter one, this manuscript (**ready for submission**) focuses on developing a better understanding of which vine morphological features correlate with model area terms. This study addresses the stated goals of QE aim 2, “define the plant-dependent coefficient in each of the models”.

Abstract

The development of methods for directly estimating vine scaling terms is a critical next step towards advancing high resolution irrigation (HRI) to a phase of commercial utility. Currently, evapotranspiration (ET), or plant water use, is estimated at the scale of a full vineyard (e.g. 3-5 acres) or on the scale of a single vine, but at a cost that prohibits monitoring past a small number of representative vines. Previous results have shown that HRI is possible, but in order to make this technology generalizable to any vine, it must be possible to measure or estimate site-dependent model terms (called area terms here) in each model directly from observations. To better understand which vine morphological features correlate with model area terms, we utilized four head-pruned Zinfandel vines in pots and placed them on load cells to collect continuous weights indicative of actual ET. We mounted research grade sensors for

humidity, temperature, and wind speed on each vine, and saved data at 2 minute intervals during the 2022 growing season. To test the hypothesis that model area terms can be measured directly, we measured vine physical characteristics on a weekly basis throughout the season, then experimentally calculated area terms periodically throughout the season using ground truth data. We observed a similar pattern in all the vine physical parameters and area terms over the season (multiple r^2 0.58 - 0.80). We also assessed the correlation between the parameters in these groups using multiple linear regression and principal component analysis. The results suggest a significant relationship between the MB and CMT area terms and the vine parameters of canopy superficial area, polygon area and fPAR. While this relationship is consistent in our data, further investigation will be required to extract an equation for direct calculation of CMT or MB area terms from vine observations. Overall, these results expand support for the HRI models for ET estimation at the single plant level.

Introduction

Even with a wetter than average 2023 spring season, much of California remains in a state of drought, further intensifying the competition between agricultural, urban and conservation water needs, especially in regions where high-value crops are grown (Diffenbaugh *et al.,* 2015). Despite growing pressure to conserve water in the region, California growers alone are irrigating 300,000 hectares of vineyards (CDFA and USDA, 2022). The drip irrigation systems used in these cropping systems typically treat all plants in a management zone identically, even though it is clear all plants do not require the same amount of water. This variability of water demand can arise from cultivar differences, complex topography, soil structure and composition, or roguing practices for disease control, as examples. Consequently, treating all plants in a single irrigation zone as identical will typically result in some excessively wet or dry soil conditions, which can affect crop quality and yield, layering additional complexity

into irrigation management. Even more, in some perennial woody crops like grapes and almonds, well-timed water stress can also help control vegetative vigor and may increase fruit quality (Chaves *et al.,* 2007; Van Leeuwan and Seguin, 2006). Stress caused by too much deficit irrigation, however, can lead to decreased yields and quality. Ideally, an irrigation system would allow the grower to maintain soil saturation in this narrow range of applied water, which would require understanding the spatially and temporally dynamic concept of individual plant water demand. In Jenkins *et al.,* 2023, we introduced three models, which along with low cost sensors, would empower growers to apply irrigation based on an individual plants' water use.

Because current technology cannot accurately measure evapotranspiration (ET) rate directly at the scale of individual plants, we developed three novel models for predicting ET rate using common biometeorological measurements. These high-resolution irrigation (HRI) models are all based on easily measured biometeorological parameters with the Convective Mass Transfer (CMT) and Mass Balance (MB) models inspired by first principles. The third model, the Empirical Model (EM) was selected from a set of candidate models based on purely statistical methods.

All of the HRI models generate a prediction of ET rate per area, which is then integrated over time to find ET per area. In order to scale the ET per area to the size of the vine, all models use an area term (A_s). To test the hypothesis that area terms can be measured directly, we considered the ways in which plant morphology is quantified in existing cropping systems. In many other horticultural contexts outside of irrigation, the quantification of plant size or vigor is important for informing the appropriate magnitude of an intervention. For example, when vineyard managers are making fertilizer recommendations for the upcoming season, the primary factor influencing calculations is the cluster pruning weight from the previous season, a proxy for vine size accounting for the largest sink of nutrients–the berry clusters (Arrobas *et al.,* 2014). In commercial viticulture, vine size may also be determined using remote and proximal methods. Light detection and ranging (LiDAR) sensors mounted on various vehicles, such as tractors or

aerial vehicles, are used to create detailed three dimensional point-cloud datasets representing plant and topographical dimensions, useful for estimating application rates of sprays, as one example (Bailey and Mahaffee, 2007). For remote areas or larger areas, satellite imagery is often the most practical option for determining size or distribution of plants. Downstream analysis of multi-band satellite imagery may be used to estimate the density and dimensions of vegetation, and has applications for determining changes in vegetation indices over time (Herman *et al.,* 2018).

Other modern methods used to estimate ET in commercial vineyards require the consideration of vine characteristics in order to scale predictions to the target environment or vine. When applying energy balance concepts in the context of an open field Eddy Covariance System, ET estimates are produced in the form of vertical flux of water vapor, which must be multiplied by an area (Tanny, 3013; Ghiat *et al.,* 2021). A closed system is fundamental to the idea of an energy balance, and therefore a bounding area is required for this calculation. This area, however, is highly variable and the assumption that its boundaries are fixed, is problematic (Stanhill, 2019). Sap flow technologies directly measure the movement of fluid inside the xylem from the roots to stems and to leaves, where water is transpired through stomata. In order to inform irrigation management or estimate ET using sap flow sensors, growers must perform seasonal in field calibration using lysimeters or other established methods for estimating ET, to adjust for site and plant vigor (Fernández and Testi, 2017). While a seasonal calibration can give growers the confidence to estimate local ET from sap flow measurements, these estimates may not be accurate in other plots where the calibration was not performed, and may not account for the variability caused by spatially heterogeneous aspects of the growing area, for example (Mancha, 2021). If growers opt to use reference ET_o to estimate local ET, then they will need to know the area over which they are estimating ET. The CIMIS system relies on the FAO56 Penman-Monteith model, a blend of mass transfer and energy balance concepts (CIMIS, 2021). Because of the nature of energy balance theory, the grower will need to input an

area that corresponds to the area illuminated by the sun in order to estimate ET. Once all other terms in the model are estimated, this area is used to calculate incident solar energy, and ET is calculated as a residual (Kyaw Tha Paw U *et al.,* 1995).

In this manuscript we will discuss the meaning of the area terms in the CMT and MB models for predicting ET rate. To illustrate the relationship between experimentally determined area terms and directly measured vine parameters, we present the results of a one-year trial at the UC-Davis RMI vineyard. We assessed the correlation between vine physical parameters and area terms through multiple regression and principal component analysis. Our observations suggest area terms could be measured directly, thereby empowering high resolution ET estimation using the HRI models.

Materials and methods

We collected data from three, head trained *Vitis vinifera* L. cv. Zinfandel vines grafted on St. George rootstock (*V. rupestris*), planted in plastic containers filled with Yolo County, CA sourced sandy loam; estimated available water holding capacity of about 10-15% by volume (Schwankl and Prichard, 2009). The Zinfandel scion was grafted onto rootstock in Davis, CA in 2009, then vines were transplanted into containers in 2016. Vines were located in the Robert Mondavi Institute (RMI) vineyard in Davis, California. We irrigated vines using a dedicated programmable drip irrigation and fertigation system, composed of 8 equally spaced 2 L/H Woodpecker pressure compensating drippers (Netafim, model 01WPC2) in a ring around the base of each vine. Irrigation events were programmed to occur before dawn every 24 to 72 hours during periods of normal irrigation. Vines received the same pest management and fertilizer regimen as other vines at RMI, per the direction of the vineyard manager.

To predict ET rate (units $kg \cdot s^{-1}$) and then calculate single plant ET (units kg), we measured the wind speed, air temperature and relative humidity in vine canopies by mounting each vine with a suite of research grade sensors. We measured wind speed (units $m \cdot s^{-1}$) inside

the vine canopy using a single needle anemometer (*East 30 Sensors*; Pullman, WA) that took instantaneous wind speed measurements every 10 seconds and recorded the average of the previous 12 instantaneous measurements for every 2-minute interval. We measured temperature (units ^{o}C) and relative humidity (units %) using HMP60L sensors (*Campbell Scientific*; Logan, UT) mounted both inside and outside of each vine canopy and recorded instantaneous measurements at each 2-minute interval. We filtered all biometeorological data using a 3-hour moving average to remove noise without causing any significant over or under-approximation of daily maxima and minima.

To measure ground truth ET (units kg), we placed each potted vine and attached sensor suite on a commercial load cell, model HFS 405 (2270 kg capacity, 0.01 kg resolution, *CAS Corporation*; Seoul, South Korea), which recorded instantaneous mass at each 2-minute interval. The load cell was calibrated each year in February using manufacturer guidelines.

We automated all data collection using two CR1000 data loggers (*Campbell Scientific*; Logan, UT), with 1 or 2 vines and associated sensors per logger, using custom CR1 programs. A single 30W solar cell and 12V lead acid battery powered the entire vine-sensor system.

Both the CMT and MB models utilize a non-destructive, largely automated proximal sensing and a computation pipeline, feeding data from biometeorological sensors to the models. In this process, we measure wind speed, air temperature and relative humidity in or near the plant canopy to calculate estimated ET rate per area ($\dot{m}_e$, units kg $\cdot$ s^{-1} $\cdot$ m^{-2}) for single plants. Hereafter we refer to the ET rate per area as mass flux.

Once mass flux has been calculated using one of the novel models and A_s terms have been determined, it is possible to move on to ET calculation. Each HRI model generates an estimated instantaneous mass flux for every two minute interval. This mass flux is integrated over time (t, units s) and multiplied by a plant scaling coefficient (A_s, units m^2), giving estimated ET_e [Equation 1]:

$$ET_e = A_s \cdot \int_0^t \dot{m}_e dt$$

While early data suggests all models perform well in terms of correlating estimated ET with measured ET, here we aim to expand the generalizability of HRI through investigating methods for estimating the area term directly from physical measurements.

For the purpose of this manuscript, we focus only on models with area terms having a physical basis. The EM model was selected through purely statistical processes, so the area term in this model has no physical definition. The CMT and MB models, on the other hand, are based on first principles theories and the area terms in these models have putative physical definitions. The CMT model relates transpiration to theory describing the convective mass transfer from a flat surface of water into moving air. This theory is based on an application of the Reynolds analogy, which suggests a simple relationship between different transport phenomena (Cussler, 2009). In this case we use an analogy to the process of convective heat transfer from a flat solid plate into a fluid with laminar flow over its surface. Using this analogy, transpiration is defined as convective mass transfer from a flat surface of liquid or a gas saturated with water vapor into a gas with laminar flow over its surface (Cussler, 2009). Consistent with CMT theory, the area term (A_s) associated with this flux would be proportional to the total saturated surface area of the transpiring leaves in the canopy. The Mass Balance (MB) model is based on the concept of conservation of mass. In the case of a plant canopy, this means the mass flow rate of water out of the canopy is equal to the mass flow rate of water into the canopy plus the mass flow rate from the plant. Based on mass balance concepts, the area term (A_s) is proportional to the cross-sectional area of the vine canopy.

To test the hypothesis that the area terms in the CMT and MB models can be measured directly, we experimentally calculated area terms and measured vine physical characteristics weekly throughout the season.

Experimental calculation of model area terms

During any given time window in the 2022 growing season we calculated A_s by dividing the load cell measured ET rate by the model estimated mass flux. In this study we used 10 hours of continuous data to fit each new A_s term. Even though data collected in 2020 showed that in order to make reasonable ET predictions it is only necessary to recalculate a new A_s term for each model every 10-14 days, we wanted to illustrate the change in A_s over the season at a higher frequency.

Measurement of vine physical parameters

During the 2022 growing season we measured the fraction of absorbed photosynthetically active radiation (fPAR), took digital images, and captured LiDAR scans on a weekly basis. We also estimated postseason ground truth leaf area using a destructive method. While some of these measurements were collected because of model theory, others were collected purely to enrich the characterization of the vines. In the end, any reliable method of measuring vine size or morphology that can be used to estimate the area terms, not just model predicted correlates, would expand the utility of the HRI models for estimated ET.

To capture fPAR, we used a custom ceptometer made by mounting 8 equally spaced light sensitive diodes in series on an aluminum rod. This sensor is connected to a CR850 data logger for computation and data storage (*Campbell Scientific*; Logan, UT). Each week, we measured the light intensity above and below the canopy three times, then recorded the average of each value. By measuring the photosynthetically active radiation above and below the canopy, we are able to estimate leaf area index (LAI) (Pokovai and Fodor, 2019).

After capturing fPAR, we used the Camera app on an Apple iPhone 13 Pro to capture 12 megapixel (3024 x 4032 pixels) digital images of vines. Each week, images were captured from the same location, 5 m North of potted vine boxes, with the camera fixed at a height 1 m above

the ground. Superficial area (SArea) was manually extracted using the selection tool using FIJI software (Schindelin *et al.,* 2019), tracing the largest possible rectangle around the vine foliage as it appeared in each image. We also extracted polygon area (PArea) using FIJI and the polygon selection tool, tracing the largest possible area around the visible edge of the vine foliage as it appears in each image. An example of the images used for SArea and PArea measurements can be found in *Figure 2.1*.

Figure 2.1: Example of a digital image of a grapevine. Note the two black marks on the proximal, rightmost PVC pipe post. The distance between the inside edges of these marks is 0.5 m, and allows researchers to extract superficial area (SArea) and polygon area (PArea) canopy measurements using image processing software.

Several recent smartphone models have added a built-in LiDAR sensor (*Alphabet Inc;* Mountain View, CA; *Apple Inc;* Cupertino, CA; *Samsung Electronic Co Ltd;* Suwon-si, South Korea). Using the onboard LiDAR sensor included with the iPhone 13 Pro along with a 3D Scanner App (*Laan Labs*; New York, NY), researchers scanned vines at weekly intervals. Creating a representative three-dimensional point cloud of the vines required one full 360º pass

with the scanner, while slowly sweeping the sensor in a vertical direction to fill in details on the underside and topside of the vine canopy. Once scans were captured and labeled, we used the 3DScannerApp measurement function to measure the 3 semi-axes required to calculate ellipsoid volume. The canopies were approximated as ellipsoids, as a first approximation, for early model development and because head trained vines do roughly resemble this shape. However, in future seasons, we are exploring automated methods for extracting more accurate measurements of canopy volume using a convex hull approach.

After the 2022 growing season, once leaves had naturally senesced, we carefully removed canes from each vine, keeping canes from each vine separated. Canes were counted, then nodes per shoot were counted and an average node per shoot ratio was determined for each vine. Using average node per shoot ratio and shoot number, we estimated leaf number for each vine. Then, using data from a 2013 Oregon State University extension study describing the average sizes of grapevine leaves, we estimated the total leaf area of each vine (units = m^2).

Programming and data analysis

For the following results, we utilized R v3.5.1 for all analysis and visualization (R Core Team, 2018). Model statistics, including r^2 and p-value, were generated using the 'stats' package, a part of R. For all computation we used a 2021 Apple MacBook Pro with 16 gigabytes of random access memory.

Results

Experimental area terms over time

Using data from May 2022 through August 2022, we calculated model area terms 164 times throughout the season for two vines (*Figure 2.2*). We used only two vines because in order to make calculations of area terms all other sensor data must be available, and for many periods of time throughout the season the anemometers on two of the vines were malfunctioning. Both Vine 1 and Vine 2 CMT area terms start small then increase rapidly in early

season. In early August we observed another slight increase in CMT area term growth rate, followed by a rapid decline. In the MB area term figure, Vine 2 appears smaller than Vine 1, but both vines display a similar pattern over the season. Early season growth of the MB area term is steady, until mid June when the value becomes essentially stable until early August. Vine 1 displays a late season increase in value followed by a sharp decrease in value, similar to the CMT area term trends for both vines. The similarity between these trends is likely due to the phenological stages of the grapevine growing season, which are punctuated by a significant decrease in canopy growth as the vines begin diverting more energy towards fruit development, and a dropoff in productivity at the end of the season as the vine shed older leaves due to heat and drought stress.

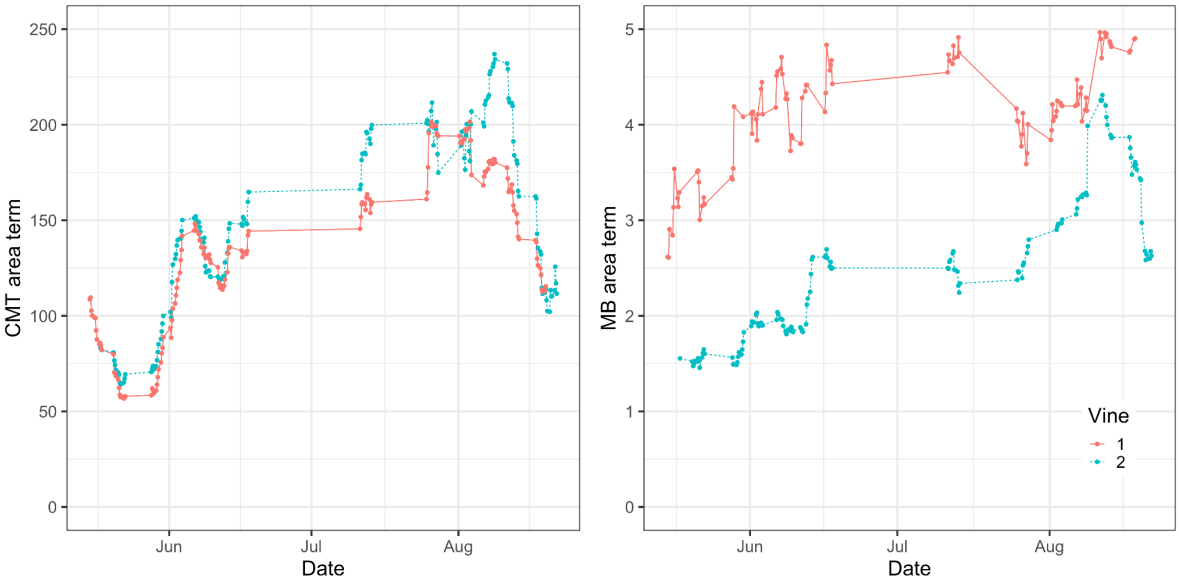

Figure 2.2: CMT and MB area terms (A_s) over time. Each point is calculated with 10 hours of continuous data.

We also compared postseason estimated leaf area to the post-veraison values of vine physical parameters (*Table 2.1*). Based on CMT model theory, the area term in this model is defined as leaf area. Given the observed late-season trend in the CMT panel of *Figure 2.2*, it would be reasonable to expect the estimated leaf areas for Vine 1 and 2 to be very similar, and this is what our estimates suggest. The trend in the MB panel of *Figure 2.2*, however, does not

seem to correlate with MB model theory. At the end of the season, the Vine 1 MB area term is much larger than the Vine 2 MB area term. Given MB theory, it would be reasonable to expect the SArea or PArea or Vine 1 would be larger than Vine 2, but this is not the case. Unexpectedly, the volume parameter seems to correlate with the end of season state of the MB area terms, with Vine 1's volume about 35% larger than Vine 2's volume.

Vine	Leaf Area (m^2)	Superficial Area (m^2)	Polygon Area (m^2)	fPAR (%)	Volume
1	3.10528512	0.9755	0.6687	78.92	0.5135
2	3.05599488	1.5225	0.8513	57.81	0.3779

Table 2.1: Postseason estimated leaf area and average post-veraison values of vine physical parameters.

Assessing correlation between area terms and vine parameters

In order to assess if there is a correlation between any of the vine physical parameters and experimentally calculated area terms, we extracted fPAR, SArea, PArea and Volume from canopy data (*Figure 2.3*). All parameters for all vines displayed a rapid increase in value through early June, followed by a prolonged period of slower growth stretching until early August. We plotted model predicted area terms against vine physical parameters to elucidate any obvious relationships (*Figure 2.4*). We also performed multiple linear regressions between all

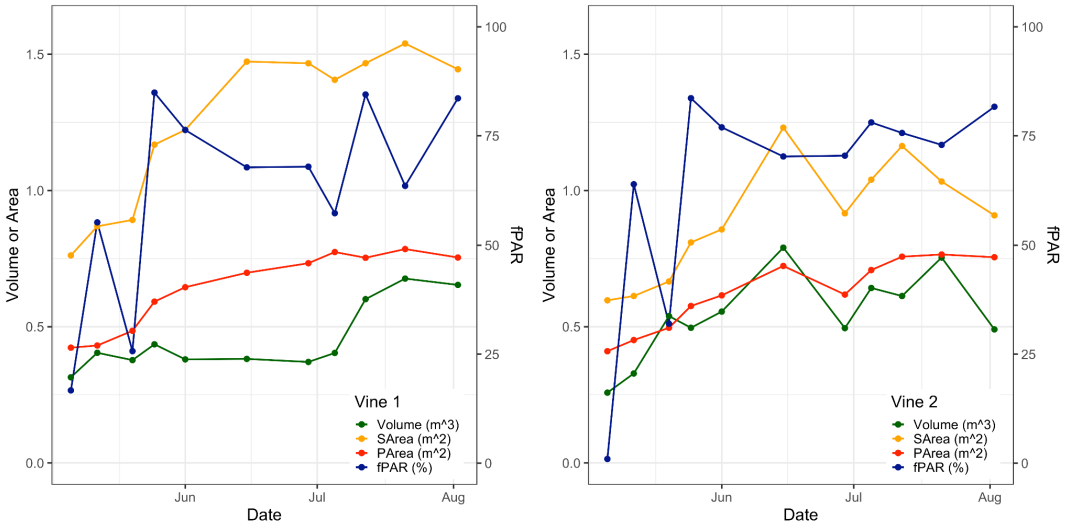

Figure 2.3: Vine physical parameters over time. Parameters were measured weekly throughout the season.

parameters and each of the model area terms. There is a strong relationship between multiple physical parameters and both of the area terms. When evaluating the CMT model, the multiple r-squared is 0.7986, which indicates that overall the vine physical parameters explain almost 80% of the variation in the CMT area term. Both the SArea and PArea p-values are significant at

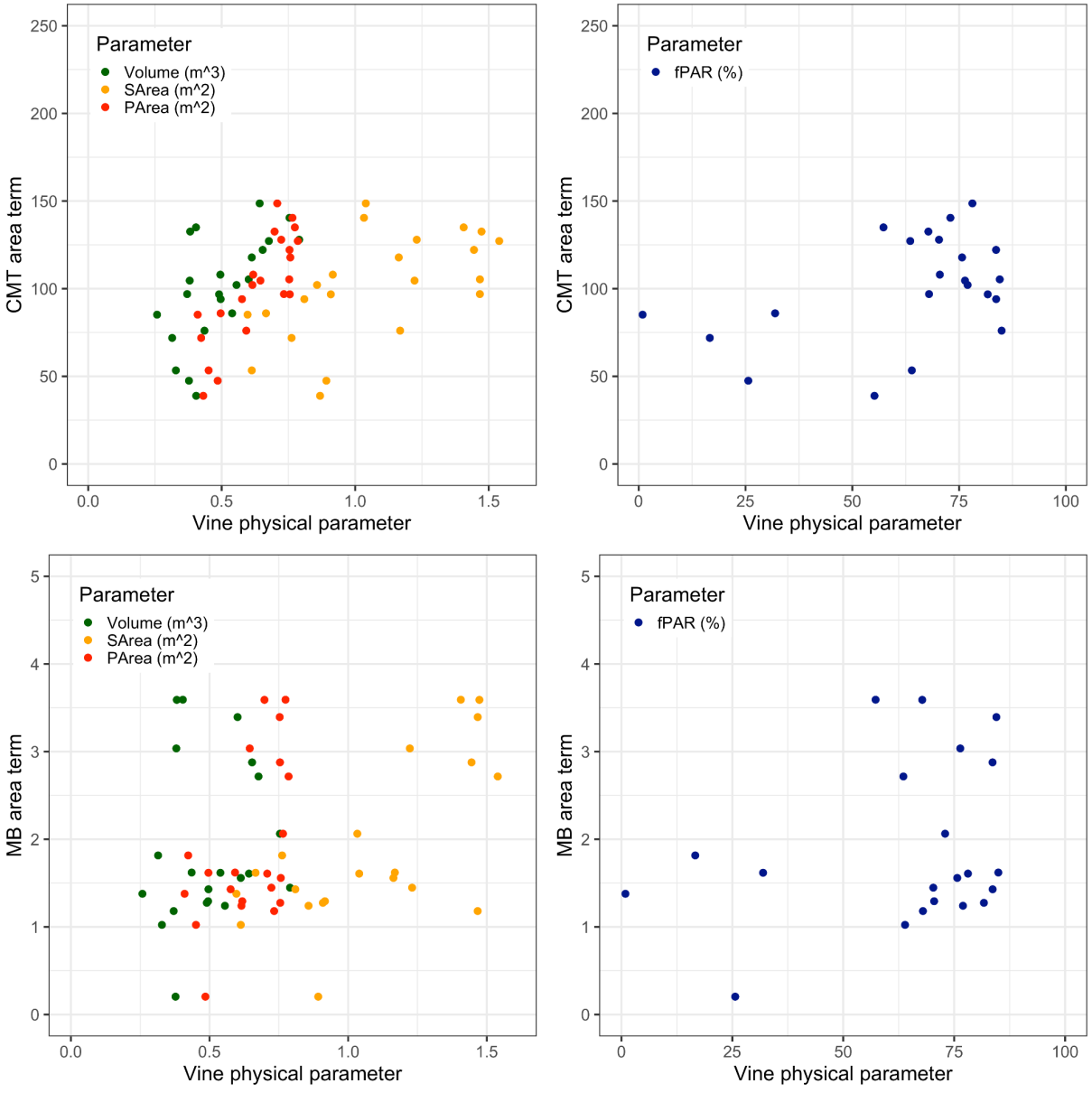

Figure 2.4: Vine physical parameters versus model area terms. The top two panels correspond to the CMT model and the bottom two panels represent the MB model. fPAR is plotted separately from SArea, PArea and Volume, because the range of observations is much larger than the range of these other parameters.

the 0.05 level, suggesting these terms have a significant relationship with CMT area term. The multiple r-squared corresponding to the MB model is 0.5842, indicating that the vine parameters explain less of the variance in the MB area term. Despite this, the superficial area and polygon area p-values were once again significant at the 0.05 level. We also built linear models between each of the vine parameters and each of the model area terms to assess the strength of each correlation (*Table 2.2*). P-value in this case gives information about the significance of the relationship between the independent variables, the vine parameters, and the dependent variables, the area terms. The r-squared value, on the other hand, sheds light on the goodness of fit between the trends in the two concepts. For the CMT model, all vine parameters had a significant relationship with the area term at the 0.05 level, but only the PArea parameter explained more than 50% of the variation in the CMT area term. In the MB model analyses, the SArea and PArea parameters were observed to have a significant relationship with the MB area term, and the SArea explained about 42% of the variation in the area term, the most of any of the parameters.

Model Area term	**Superficial Area (m^2)**	**Polygon Area (m^2)**	**fPAR (%)**	**Volume (m^3)**
CMT	$r^2 = 0.3088$ p-value = 0.004276	$r^2 = 0.6576$ p-value = $2.858 \cdot 10^{-6}$	$r^2 = 0.1540$ p-value = 0.04004	$r^2 = 0.3956$ p-value = 0.001713
MB	$r^2 = 0.4252$ p-value = 0.0006024	$r^2 = 0.2996$ p-value = 0.004933	$r^2 = 0.07422$ p-value = 0.2200	$r^2 = 0.02974$ p-value = 0.4428

Table 2.2: Statistical results, r-squared and p-value, of linear models between each of the vine parameters and each of the model area terms.

To further unravel the relationships between the vine physical parameters, and also between the vine physical parameters and experimentally determined area terms, we performed principal component analysis (PCA) on all vine physical parameters and each experimentally determined model area term, separately (*Figure 2.5*). The data used to generate each PCA

biplot includes measurements and estimates from four vines, from May to August, 2022. In both biplots, the black numbers represent weekly observations for each model:vine combination, and the red arrows are abstract representations of the vine parameter or area term concepts as projected on the first two principal components in each analysis. In the CMT biplot PCs 1 and 2

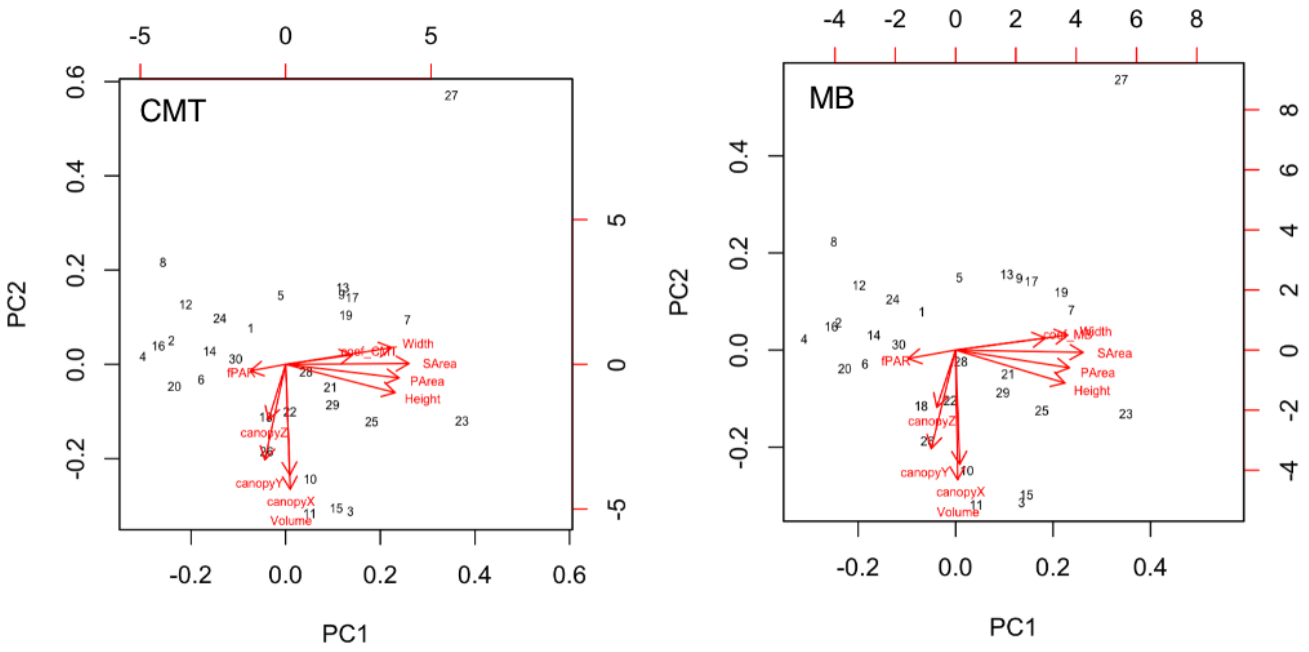

Figure 2.5: Biplots including all vine physical parameters and each model area term, projected onto principal components one (x-axes) and two (y-axes).

account for 61% of the variance, while in the MB biplot PCs 1 and 2 account for 63% of the variance. Note in both biplots the fPAR arrow is oriented 180° to both the CMT and MB area term arrows, and to a lesser extent vine width and superficial area arrows. This opposite relative orientation indicates some correlation between these parameters. Both biplots also feature two key groupings of nearly collinear arrows, representing parameter or area term concepts. The first group includes width, SArea, PArea, and Height and the second group includes canopyX, canopyY, canopyZ and Volume. Height refers to the vertical dimension which is measured and collected during the SArea measurement process, and the canopyX, canopyY, and canopyZ terms refer to the measurements made during LiDAR scan analysis, in order to calculate ellipsoid volume. While some of these groupings represent physical ideas that are conceptually

connected, it is important to remember that the connection between synthetic principal component dimensions and real world meaning is not straightforward, and therefore these groupings only reflect a relative relationship between variables in this dataset. The orthogonality of the first group to the second group indicates the parameters in the first group are not well correlated with the parameters in the second group. The slightly longer Euclidean distance of the MB area term arrow, relative to the CMT area term arrow, indicates that this area term is better represented on the first and second principal components in the MB biplot.

Overall, consistent evidence that superficial area, polygon area and fPAR have a relationship with CMT and MB area terms suggests that it may be possible to estimate area terms from vine measurements, though further research will be required to refine the approach to calculating A_s directly from images, scans or other sensor data.

Discussion

The ability to directly measure area terms of vines would allow growers to make ET predictions at the previously unattainable scale of single vines in a site-independent manner. With this information, irrigation systems could be designed that apply water to vines based on their needs, preventing over and underwatering. These results represent a major milestone in the development of the HRI method for single vine ET rate prediction, and will support further research aimed at developing technologies capable of addressing the problem of water scarcity while maintaining or improving grape quality.

The data presented in this manuscript is strong evidence that the area terms in the CMT and MB models for ET rate may be measured directly. Based on the multiple r-squared statistic value in both multiple linear regressions, it is clear that overall, the vine characteristics we measured explain much of the variability in both the CMT and MB model area terms. Also, results from both multiple linear regression as well as the individual linear regression analyses indicated a significant relationship between the superficial and polygon area vine characteristics

and the CMT and MB area terms. This relationship is corroborated by the PCA biplot analysis, which shows some collinearity between the superficial and polygon area vine parameters, as well as the CMT and MB area terms. While CMT theory does not predict a direct relationship between the superficial or polygon areas of a canopy and the CMT area term, it is possible these physical concepts could be related indirectly. MB theory, however, predicts the relationship between the superficial area of a canopy and the MB area term, and it is not unreasonable to expect this relationship to extend to the polygon area of a canopy, which is fundamentally related. The evidence supporting a relationship between leaf area and the CMT area term is limited to the results of the biplot analysis and p-value result in the individual linear regression. In the CMT biplot, the fPAR parameter is oriented in the opposite direction to the CMT area term, indicating a negative relationship between these concepts. Taken together, these results suggest there may be some quantitative relationship between the CMT and MB area terms and measurable vine physical parameters, but this relationship may not be straightforward and would likely include some error.

Often in order to inform downstream management practices requires first overcoming the challenge of quantifying plant size or vigor. The classic example is of the vineyard manager determining nitrogen fertilization rates for the upcoming season using pruning weights from the previous season. While this method may be effective in some cases, it does not consider factors such as the effect of rootstocks and soil variability on the mobility and uptake of nutrients (Lambert *et al.,* 2008). In some viticultural settings, LiDAR sensors are used to estimate vegetative matter for calculating spray rates, for example. There are many potential issues with the scanning process that often interfere with the quality of estimates. When triangulating point clouds into surfaces, error may arise because leaf edge effects can inadvertently connect the edges of adjacent leaves, or because noise in position measurements can result from leaf motion caused by wind. Error may also be due to erroneous classification of woody material as leaf material, which cannot be corrected without careful manual segmentation (Bailey and

Mahaffee, 2017). In large management areas, energy balance approaches along with satellite imagery may be used to estimate ET rates of groups of plants. While these approaches may be effective, they are sensitive to myriad sources of error. Many energy balance methods, for example, require clear skies, are highly sensitive to surface temperature errors and involve the simplification of many physical processes (Zhang *et al.,* 2016). Directly measuring ET with the Eddy Covariance method may provide the advantage of improved data quality over remotely sensed satellite imagery, but it comes with some limitations. In this method sensible heat flux density, the energy lost to the air from the plant, soil and cover crops via convection and conduction, is estimated. This term is sensitive to factors impacting the distribution of energy sources in the canopy including wind speed and surface roughness, and is therefore affected by canopy size, structure, trellising, plant phenological stage and even ground surface heterogeneity (Rienth *et al.,* 2019). Furthermore, this method is fundamentally an energy balance method and therefore requires a bounding area. While this area is often assumed to be constant, this is probably a highly variable area (Stanhill, 2019).

While the evidence presented here expands our understanding of how to use the HRI method for estimating single vine ET, there are some remaining questions which ought to be answered before this method is considered for commercial applications. First, even if a simple equation can be derived for estimating the A_s term in the CMT or MB model directly from vine physical parameter data, the challenge of collecting this data regularly throughout the season remains. An automated method for collecting and extracting vine measurements from images, light interception data, and LiDAR scans could be crucial to the viability of this technology at the scale of a modern commercial vineyard. Ideally this technology would be small, robust to normal spraying and other management activities and have minimal power requirements. The imaging component would also be designed for easy mounting on tractors or other farm equipment, so data can be recorded during normal farming operations, in a system similar to that used in Olensky *et al.,* 2022. Once collected, this data could be fed into an automated analysis pipeline

which returns the desired vine measurements. The design, testing and implementation of this hardware and software is a non-trivial addition to the core goals of this project and would represent a significant engineering effort.

In addition, implementation in a commercial vineyard presents other challenges. For example, it is possible that canopies with less radial symmetry, such as many common trellis systems in California, could render the methods used in this manuscript to measure vine parameters ineffective. It is also possible that certain cultivars, regions, topographical features, or other factors we have yet to consider could limit the performance of the models, even if an area term can be accurately calculated from observation. In addition, the sensors for capturing data, onboard computation, telemetry, data storage and retrieval will all need to be inexpensive, especially if every vine or a high density of vines is to be monitored, and robust in an agricultural environment–both topics of further research.

While further research is required to elucidate the equations for calculating the A_s terms directly from observations, the results presented here expand evidence that the HRI algorithms for prediction of ET rate of water from single vines can be used as an inexpensive and high resolution means of controlling irrigation. If canopy SArea, PArea, or fPAR can be measured, used to calculate model area terms, and appropriate biometeorological data collected, then the algorithms presented here provide an option to growers looking for greater efficiency of irrigation and improved crop quality. The methods used in this manuscript provide a theoretical and practical basis for researchers to design and test automated, high throughput methods for extracting vine parameters from images and LiDAR scan datasets, for use in making ET or other management decisions. Overall, if there is an inexpensive means of measuring vine parameters and biometeorological data, this project has the potential to provide ET data at the single vine level, more effectively than existing expensive or destructive methods or methods that require thousands of vines covering multiple acres.

Acknowledgments

The authors thank Leticia Chacon Rodriguez for viticultural guidance and access to vineyard facilities, Guillermo Federico Garcia Zamora and Gonzalo Ruiz Gonzalez for assistance with vine care and equipment installation at the RMI Vineyard. This work was made possible through financial support from Till Guldimann and the Ernest Gallo Endowed Chair in Viticulture and Enology.

Author contributions

K.M. and M.R.J. conceptualized the CMT model. D.E.B., S.N. and M.R.J. conceptualized the MB model. M.R.J. wrote all code for data capture, analysis and visualization. D.L. and F.C.L. captured and analyzed all field data. M.R.J. and D.E.B. wrote the paper with revisions from all authors. D.E.B., M.B., M.G. and M.R.J. provided funding and access to materials.

Chapter Three

Comparing novel single vine sensors and High Resolution Irrigation algorithms for ET to lysimetric and flux tower ET

Matthew Jenkins, Brian Johnson, Maria del Mar Alsina Marti, William P. Kustas, Joseph G. Alfieri, Shayla Nikzad, Konrad Miller, Mark Burns, David E. Block

Preface

To understand if the HRI method can be used in a commercial setting, and to see how it compares to other industry accepted methods for measuring ET, the third QE aim is to "evaluate the system performance in a commercial setting". This manuscript (**ready for submission**) first introduces new low-cost Cube biometeorological sensors then evaluates them in research and also commercial contexts.

Abstract

Testing the use of new low-cost sensors in conjunction with high resolution irrigation (HRI) models for calculating ET in a commercial viticulture setting will provide crucial footholds to the pioneering early adopters of these technologies. Currently, evapotranspiration (ET) is estimated at the scale of a full vineyard (e.g. 3-5 acres) or on the scale of a single vine, but at a cost that prohibits monitoring past a small number of representative vines. Previous results have shown HRI is possible and likely generalizable, but in order to make this technology useful in a commercial context the method needs to be tested in a representative setting. To better understand how the new Cube sensor performance compares to research grade biometeorological sensors, a potted Zinfandel vine was placed on a load cell to collect

continuous weights indicative of actual ET, and mounted with research grade sensors for humidity and temperature. Wind speed performance was analyzed separately in a wind tunnel experiment. To assess Cube sensor performance linear regression analysis was performed on all biometeorological data (r^2 0.84 - 0.99). The data from the Cube sensors was then used to make ET calculations with the three HRI models and these were compared to ground truth ET measured with the load cell (multiple r^2 0.44). After assessing the performance of Cube sensors in a research setting, Cube sensors were deployed in a commercial vineyard with a flux tower for two days during the 2022 growing season. The correlation between flux tower ET calculated with the eddy covariance method and Cube sensor ET calculated with the three HRI models was also evaluated (multiple r^2 0.051). Despite the lack of a correlation between eddy covariance and HRI calculated ET values, overall the results suggest the low cost Cube sensors are a functional alternative to expensive research grade sensors, and a significant relationship between HRI model estimates of ET and ground truth ET. These observations expand support for the HRI models for estimating ET at the single plant level.

Introduction

In key winegrowing regions such as California, South Australia and parts of Southern Europe, the rivalry for water resources among agricultural, urban and conservation sectors continues to grow. As a result of this competition, allocating water equitably is particularly challenging in these regions. Despite growing research questioning the sustainability of continued freshwater withdrawal from surface and subsurface water systems, and the fact that irrigation can account for more than 63% of overall global water use, California growers alone are still irrigating 300,000 hectares of vineyards (CDFA and USDA, 2022; Zhang *et al.,* 2022). The drip irrigation systems used in these cropping systems typically treat all plants in a management zone identically, even though it is clear all plants do not require the same amount

of water. Variability of water demand can arise from cultivar differences, complex topography, soil structure and composition, or roguing practices for disease control, as examples. Consequently, treating all plants in a single irrigation zone as identical will typically result in some excessively wet or dry soil conditions which can affect crop quality and yield, layering additional complexity into irrigation management. Even more, in some perennial woody crops like grapes and almonds, well-timed water stress can also help control vegetative vigor and may increase fruit quality (Chaves *et al.,* 2007; Van Leeuwan and Seguin, 2006). Stress caused by too much deficit irrigation, however, can lead to decreased yields and quality. Ideally, an irrigation system would allow the grower to maintain soil saturation in this narrow range of applied water, which would require understanding the spatially and temporally dynamic concept of individual plant water demand. New ways of monitoring water use, at previously unthinkable scales as small as individual plants, will be vital to bending the high value crop irrigation status quo towards more dynamic irrigation and water management infrastructure capable of achieving these ideals.

Low-cost single vine strategies such as the High Resolution Irrigation (HRI) method proposed in Jenkins *et al., 2023* enable growers to sense water use and water status at the level of individual plants, empowering growers to apply a unique water budget for each plant, curated to its individual needs. In Jenkins *et al.,* 2023 three new evapotranspiration (ET) models were introduced which along with low cost sensors empower growers to apply irrigation based on an individual plants' water use. Then, in Jenkins *et al.,* 2024 the generalizability of two of these models was explored. Specifically the physical meanings of the area terms in both the Convective Mass Transfer (CMT) and Mass Balance (MB) models were investigated, with results indicating significant relationships between model area terms and canopy superficial area, canopy polygon area and fraction of absorbed photosynthetically active radiation (fPAR). Though these results are promising, demonstrating the utility of the models in a research environment and exposing significant correlations between physical aspects of the vines and

model area terms, the models have yet to be tested in a commercial agriculture context. Despite this limitation, HRI is still a promising single plant irrigation tool.

Other low-cost options for estimating ET also have some significant limitations but have nevertheless seen widespread adoption. Most methods for sensing ET commercially require ownership of expensive equipment or subscription plans, but several methods for low-cost estimation of local crop ET are available including reference ET systems and the pan evaporation method. Reference ET systems and crop coefficients may be one of the least expensive methods for estimating ET but they are not ubiquitous, requiring a network of expensive and regularly maintained regional weather stations. Where these systems exists, such as in California, they are an important method for estimating ET, allowing regional growers to schedule irrigation based on proxy measurements along with correction factors known as crop coefficients, specific for the type of plant being grown nearby and management factors (Allan *et al.,* 1998; Behboudian and Singh, 1998). These proxy ET values, known as reference ET, are calculated at one of over 200 California Irrigation Management Information System (CIMIS) weather stations distributed throughout the state (LAWR-UC Davis, 2021). Some other states in the USA have similar systems including Florida (Jackson *et al.,* 2008), Colorado (Andales *et al.,* 2014), Arizona (Brown and Yitayew 1988), and Washington (Badr et al., 2015), as well as other countries including Australia (Webb, 2010), India (Wani *et al.,* 2016), and the United Kingdom (Hough and Jones, 1997); but the specific data types available from these systems may differ considerably from CIMIS. At each CIMIS station, meteorological data is collected at a weather station 2 meters above well-watered clipped grass, and then fed into a modified version of the original Penman-Monteith known as FAO56 Penman-Monteith because it was introduced in the Irrigation and Drainage Paper 56 from the United Nations Food and Agriculture Organization (Allan *et al.,* 1998). While FAO56 Penman-Monteith is generally used for CIMIS reference ET estimates, it is also possible to use the CIMIS-Penman model, a

modified version of the Pruitt/Doorenbus Penman-Monteith equation that includes wind speed and cloud cover parameters (Pruitt, 1977)

Once reference ET is known, it can be used to calculate true ET of crops grown nearby by multiplying by a scaling factor known as the crop coefficient. The crop coefficient is an experimentally derived value, specific to variety, seasonal canopy development and plant spacing, and sometimes adjusted for other management factors (Bravdo *et al.,* 1987). Other studies have explored a two part definition for the crop coefficient, splitting the coefficient into separate terms for the basal crop coefficient representing a factor for crop transpiration, and the soil evaporation coefficient representing a factor for evaporation from the soil surface.

Compared to the other approaches for ET estimation, this method has the distinct advantage of being virtually free for California growers and other growers in areas with similar programs. However, this approach is limited by its reliance on the assumptions of generalizable regional reference ET values and crop coefficients. As a result, this method can be quite effective at estimating regional reference ET but it can lack local specificity, not adequately accounting for or ignoring complex factors influencing slight differences in plant water demand such as management practices, phenological stage, topography, soil characteristics and many others (LAWR-UC Davis, 2021). In areas where reference ET estimates are not available or when more local specificity is required, the pan evaporation method may be a suitable option for estimating crop ET.

With the pan evaporation method it is possible to use nothing more than a standardized pan of open water, a scale and a watch to estimate local crop ET. While the most basic of pan evaporation approaches can achieve the aforementioned elegance of nearly optimal operational efficiency, modern examples of this method typically require the collection of supplemental meteorological data for model building purposes. Other approaches involve calculating a pan coefficient that when multiplied by pan evaporation yields an estimate of reference and then crop ET. The most widely used method for determining a pan coefficient value is a table from

the United Nations Food and Agriculture Organization which categorizes different values based on the composition of the ground surrounding the pan, the local climate type and the size and type of vegetation near the pan (Doorenbos and Pruitt, 1977).

The pan evaporation method is effective because it takes advantage of the correlation between pan evaporation and reference ET, which in turn has a known correlation with crop ET. To reduce error caused by differences between pans, there is a standard pan called the “class A evaporation pan” issued by the United States National Weather Service which allows for more accurate comparisons between sites. While the relationship between pan evaporation and reference ET is valid under many conditions, there can be conditions causing differences in energy fluxes and heat storage in an open water pan relative to vegetation. This effect is pronounced at night when energy stored in the pan during the day increases the overnight evaporation rate of water in the pan, while canopy resistance to transpiration will cause little to no nighttime ET (Snyder *et al.,* 2005).

In this manuscript new low-cost biometeorological sensors are introduced, then evaluated alongside the HRI method for ET calculation in a one-year trial at a commercial vineyard in the Central Valley of California, USA. Existing research grade biometeorological sensors are typically expensive for laboratories, costing around $500 to $4000 per sensor. New low-cost “Cube” sensors are first compared to high performance research-grade sensors, then HRI based ET predicted made using data from Cube sensors is compared to ground truth ET measured with a load cell. Finally, Cube sensors are mounted in a commercial vineyard and data is used to make HRI predictions of ET which are compared to ET estimates from a flux tower. Together these experiments suggest the HRI method may be a useful tool for irrigation managers looking for a better understanding of the water use of individual plants.

Material and methods

We have developed new low-cost Cube sensors that are small, about 3.5 cm^3 devices custom formed from thermoplastics 3D printed using the fused filament fabrication technique (Miller et al., 2023). Each cube contains a combination of sensors, all of which are used to sense the biometeorological metrics relevant to HRI modeling of ET. The version tested in this study includes a relative humidity sensor, configured to determine the relative humidity of the air (units %) and sense the temperature of the air (units ^oC), along with two custom heater circuits, each producing a temperature increase, the dissipation of which is a function of the wind speed (units $m \cdot s^{-1}$). The heater circuits measuring wind speed are each mounted in a slot oriented along one of the two horizontal axes of the Cube, allowing a vector-based measurement of horizontal wind speed, much like a cup anemometer. A Raspberry Pi single board computer, running Raspberry Pi OS and executing Python code, is used to control each Cube sensor via a customized electronic interface. Cube sensors and microcomputers are powered using a 5-volt, 2.1-amp USB power supply, in this case a 10000 mAh lithium ion battery unit.

Figure 3.1: An example of a 3D printed low-cost Cube sensor deployed in the field.

Cube sensor analysis experiments

To investigate whether or not the new low-cost Cube sensors are appropriate for research applications they were first compared to research grade sensors over a 10-day period using the lysimeter mounted grapevines in the Robert Mondavi Institute (RMI) vineyard in Davis, California. The vine used in this study was a head trained *Vitis vinifera* L. cv. Zinfandel vine grafted on St. George rootstock (*V. rupestris*), planted in a plastic container filled with Yolo County, CA sourced sandy loam; estimated available water holding capacity of about 10-15% by volume (Schwankl and Prichard, 2009). The Zinfandel scion was grafted onto rootstock in Davis, CA in 2009, then transplanted into a container in 2016. The vine was irrigated using a dedicated programmable drip irrigation and fertigation system, composed of 8 equally spaced 2 L/H Woodpecker pressure compensating drippers (Netafim, model 01WPC2) in a ring around the base of each vine. Irrigation events were programmed to occur before dawn every 24 to 72 hours during periods of normal irrigation. Vines received the same pest management and fertilizer regimen as other vines at RMI, per the direction of the vineyard manager.

For comparison to Cube sensors, also mounted on vines, and then to calculate single plant ET (units = kg), the air temperature and relative humidity were measured in vine canopies with a suite of research grade sensors. Temperature (units ^{o}C) and relative humidity (units %) were measured using HMP60L sensors (*Campbell Scientific*; Logan, UT) mounted both inside and outside of each vine canopy and recording instantaneous measurements at each 2-minute interval. All biometeorological data was filtered using a 3-hour moving average to remove noise without causing any significant over or under-approximation of daily maxima and minima. Cube wind speed (units $m \cdot s^{-1}$) sensor function was verified separately using a wind tunnel with an integrated anemometer, allowing a single axis of the multi-axis Cube wind speed sensor to be isolated for testing. Twelve measurements of Cube and reference anemometer were performed across a range of values from approximately 0.5 - 2.5 meters per second.

To further demonstrate the utility of the low-cost sensors and HRI method for ET estimation, ET estimates generated using data from Cube sensors and the HRI method were compared to ground truth ET measured with a load cell. The HRI models, including the CMT, MB and Empirical Model (EM) utilize a non-destructive, largely automated proximal sensing and a computation pipeline, feeding data from biometeorological sensors to the models (Jenkins *et al.,* 2023). In this process, wind speed, air temperature and relative humidity are measured in or near the plant canopy to calculate estimated ET rate per area ($\dot{m}_e$, units $kg \cdot s^{-1} \cdot m^{-2}$) for an individual plant. Hereafter ET rate per area is referred to as mass flux. The CMT model relates transpiration to theory describing the convective mass transfer from a flat surface of water into moving air. This theory is based on an application of the Reynolds analogy, which suggests a simple relationship between different transport phenomena (Cussler, 2009). In this case an analogy to the process of convective heat transfer from a flat solid plate into a fluid with laminar flow over its surface is applied. Using this analogy, transpiration is defined as convective mass transfer from a flat surface of liquid or a gas saturated with water vapor into a gas with laminar flow over its surface (Cussler, 2009). In this study, CMT model estimates were calculated using data from the Cube sensor mounted in the canopy of the vine. The Mass Balance (MB) model is based on the concept of conservation of mass. In the case of a plant canopy, this means the mass flow rate of water out of the canopy is equal to the mass flow rate of water into the canopy plus the mass flow rate from the plant. MB model estimates were calculated using data from the Cube sensors mounted in the canopy, and research grade sensors mounted outside the canopy. The EM is a purely statistical model, including only wind speed and air temperature, but may still prove useful as a tool and is therefore included in this study. EM model estimates were also calculated using only data from the Cube sensor mounted within the canopy.

Once mass flux has been calculated using one of the HRI models and A_s terms have been determined, it is possible to move on to ET calculation. Each HRI model generates an estimated instantaneous mass flux for every two minute interval. This mass flux is integrated

over time (t, units s) and multiplied by a plant scaling coefficient (A_s, units m^2), giving estimated ET_e. In this case, because the research grade anemometers failed during the initial 10-day measurement window, a subsequent 5-day observation was performed including a research grade cup anemometer in order to extract an experimentally derived plant scaling coefficient using the process presented Jenkins et al., 2023, and calculate model estimated ET. To measure ground truth ET (units kg), the potted vine and attached sensor suite was placed on a commercial load cell, model HFS 405 (2270 kg capacity, 0.01 kg resolution, *CAS Corporation*; Seoul, South Korea), which recorded instantaneous mass at each 2-minute interval. The load cell was calibrated annually using manufacturer guidelines.

All data collection at the RMI site was automated using a single CR1000 data logger (*Campbell Scientific*; Logan, UT) and custom CR1 program. A single 30W solar cell and 12V lead acid battery powered the entire vine-sensor system.

Commercial context experiment

After effectively exploring the function of the low-cost Cube sensor in a research setting, the performance of the Cube sensors and the HRI method were compared to an industry standard ET technology in a two day experiment in a commercial vineyard. Two *Vitis vinifera* L. cv. Merlot vines grafted on unknown rootstock, trained to quadrilateral cordons were used. Vines were planted at a within row density of 1.5 m and between row density of 3.3 m and located in a 21.5 hectare vineyard block in Sierra Loma, California, USA. Vines were irrigated per standard guidance from the vineyard manager using two 2 L/H Woodpecker pressure compensating drippers (Netafim, model 01WPC2) per vine. Importantly, each vine was located in a block with a flux tower including a suite of research grade sensors allowing for the calculation of ET estimates using the eddy covariance method.

Eddy covariance methods are considered one of the only ways to directly measure ET. In this method, a flux tower is used to measure changes in vertical air velocity while simultaneously measuring the concentrations of water vapor in air, in order to calculate the

vertical flux of water vapor, giving an estimate of ET (Tanny, 2013). This method is validated for open field crops, vineyards, open water bodies and grasslands (Kustas *et al.,* 2022; Tanny, 2013). While this theoretically limits the eddy covariance approach to open, flat and homogeneous vegetation canopies, an uncommon motif in agricultural settings, this method has still seen some adoption in commercial contexts.

The fluxes observed by sensors mounted on flux towers represent ET from a dynamic area that depends on wind and air stability. This area is called the “footprint” or “fetch” (Chu *et al.,* 2021; Zhang *et al.,* 2014). The uncertainty of the exact dimensions of this area propagates through calculations, contributing to the error observed in estimates of sensible heat flux and other parameters which often only account for 70-80% of total incident energy (Stoy *et al.,* 2013; Eshonkulov *et al.,* 2019). In the eddy covariance method, data were recorded at a high frequency, about 20 hertz. Data includes wind speed and direction, collected with a sonic anemometer; relative humidity and air temperature, recorded with research grade sensors; and gas concentrations in air, measured using an infrared gas analyzer. Once a predicted ET is generated using the eddy covariance method, using an energy balance calculation, these predictions were compared to ET estimates generated using the three HRI models.

Programming and data analysis

For the following results, we utilized R v3.5.1 for all analysis and visualization (R Core Team, 2018). Model statistics, including r^2 and p-value, were generated using the ‘stats’ package, a part of R. For all computation we used a 2021 Apple MacBook Pro with 16 gigabytes of random access memory.

Results

Cube sensor analysis experiments

Before testing the new Cube sensors in the context of ET estimation, the functionality of the chip mounted biometeorological sensors was evaluated (*Figure 3.2*). Over the course of 10

days in June, 2023 biometeorological data was collected from both the Cube integrated temperature and relative humidity sensors as well as a research grade HMP60L temperature and relative humidity sensor (*Figure 3.2, Panels A and B*). The Cube wind speed sensors were tested in a separate wind tunnel experiment at the University of Michigan (*Figure 3.2, Panel C*). When comparing the Cube temperature to the research grade sensors, the Cube sensors were found to generally measure values higher than those measured with the research grade sensors, despite sensors being placed as close as possible to one another within the vine canopy. The Cube measured relative humidity however was almost always lower than the humidity observed by the research grade sensors. The Cube wind speed sensor agreed very closely with the wind tunnel reference anemometer across the observed range.

In order to measure the agreement between the Cube sensor measurements and the research grade reference sensors, linear regression analyses were performed. All three Cube sensors were observed to have statistically significant relationships with their respective reference sensor, with p-values less than 0.05. Exploring the correlations reveals the Cube

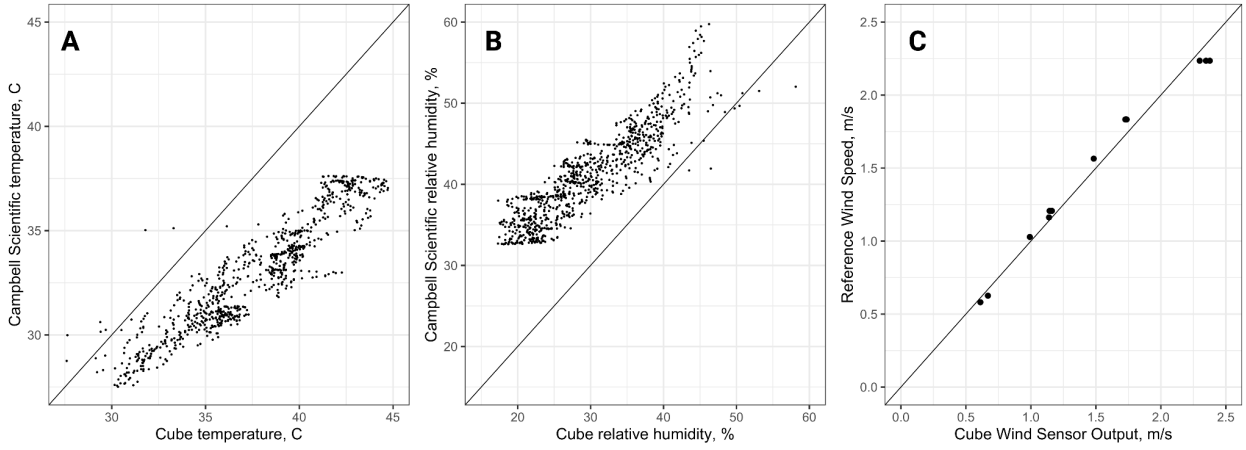

Figure 3.2: Biometeorological data measured with research grade and Cube sensors. Panel A is Cube versus Campbell Scientific temperature, observed over 10 days. Panel B is Cube versus Campbell Scientific relative humidity, also observed over 10 days. Panel C is Cube versus reference anemometer wind speed, observed in a single day wind tunnel experiment. 1:1 line is shown in black in all panels.

temperature sensors explained almost 93% of the variation in reference sensor variation, whereas the Cube relative humidity sensors only explained about 84% of the variation in reference sensor variation. The Cube wind speed sensors, on the other hand explained more than 99% of the variation in wind tunnel reference anemometer variation.

To better understand the performance of the Cube sensors in the context of measuring ET, one of the RMI lysimeter vines was used for the 10-day sensor verification experiment, giving the ability to measure ground truth water use. Daily throughout the experiment a Cube sensor was activated for a 6 hour span, from 4 hours before solar noon and until 2 hours after. The biometeorological data collected during these 6 hour windows, as well as experimentally determined area terms from the RMI lysimeter vine in August 2023, were used to make estimates of ET over a 1-hour window spanning solar noon using each of the three HRI models (*Figure 3.3*). Multiple linear regression analysis revealed a statistically significant relationship between the CMT and MB model estimates of ET and ground truth ET, with a p-value less than 0.05. Together the HRI models explained more than 43% of the variation in ground truth ET, despite no obvious visual trends.

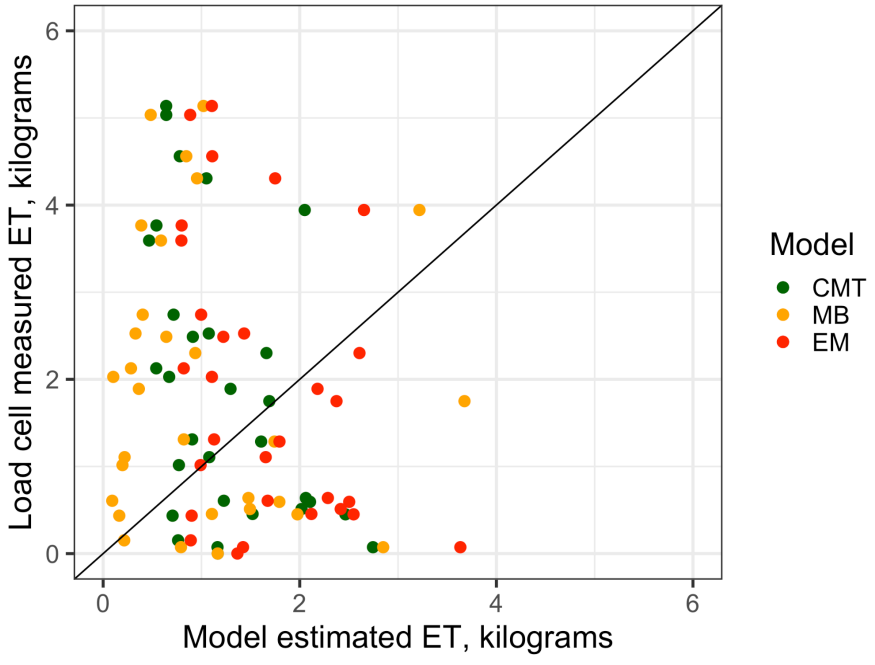

Figure 3.3: Estimates of ET over a 1-hour window spanning solar noon using each of the three HRI models and load cell ground truth ET.

Commercial context experiment

Over the course of two days in July and August, 2023 a similar ET experiment was performed again using Cube sensors to measure ET, but this time in a commercial vineyard with a flux tower. Each measurement day, researchers installed a Cube sensor about 4 hours before solar noon, and initiated a 6 hour measurement window. With data from the flux tower sensors reference ET was calculated using the eddy covariance method in units of equivalent depth. This was then compared to ET estimates from the Cube sensors calculated using the HRI method, using experimentally determined area terms from the RMI lysimeter vine in August 2023 (*Figure 3.4*). In Figure 3.4, ET estimates represent the cumulative water use in units of equivalent depth, over a single hour approximately spanning solar noon, each day. Multiple linear regression was performed to investigate the relationship between the HRI model estimates of ET and the eddy covariance estimates. In this case none of the HRI model estimates were observed to have relationships with eddy covariance ET with a p-value less 0.05, or even less 0.5. Also, the three models together only explained a little over 5% of the variation in eddy covariance ET.

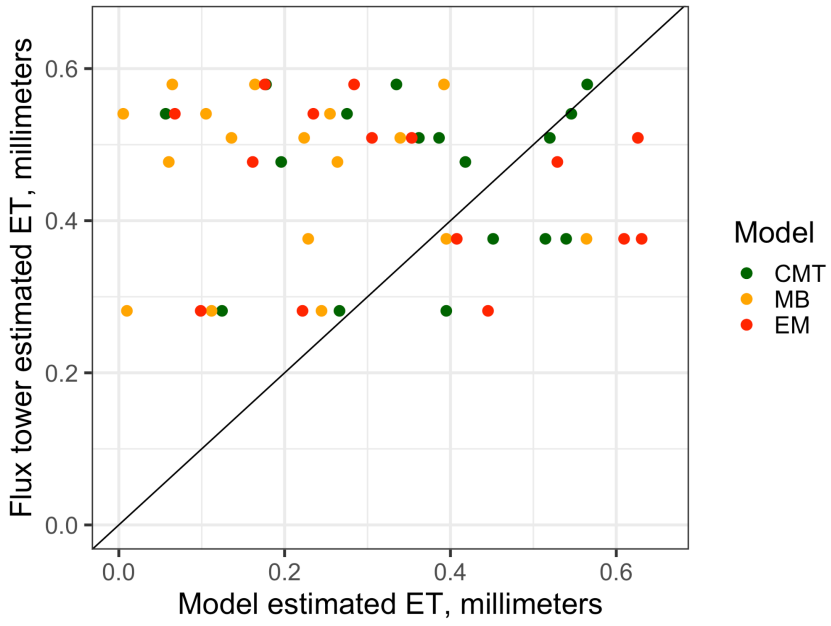

Figure 3.4: Estimates of ET over a 1-hour window spanning solar noon using each of the three HRI models and flux tower sensors with eddy covariance analysis.

These results suggest the Cube sensors can reasonably estimate the biometeorological values measured by research grade reference sensors, and these values can be used to make reasonable estimates of ground truth ET. Further research will be required to understand the lack of a significant relationship between the single vine ET values calculated by the HRI models and the more spatially coarse values generated by the eddy covariance method.

Discussion

The availability of low-cost Cube sensors for measuring key biometeorological parameters would empower growers to use the HRI method to make ET measurements at the previously unattainable scale of single vines. Information from these sensors could inform irrigation systems designed to apply water at this scale, delivering water to plants based on their needs and preventing over or underwatering. If results suggested that HRI models and Cube sensors could be used to estimate ET this would represent a major milestone in the development of the HRI method for single vine ET rate prediction, supporting further research aimed at developing technologies capable of addressing the problem of water scarcity while maintaining or improving grape quality. While we observed a relationship between Cube sensor data, the relationship was not as strong as the relationship observed with commercial sensors. This does not necessarily indicate the HRI method cannot be used with Cube sensor data, but that Cube sensors may need to be further optimized before they are ready for commercial applications.

The data presented in this manuscript is strong evidence that, with more research aimed at understanding the source of error in Cube based ET predictions, low-cost Cube sensors and HRI algorithms for ET measurement may be a useful tool for measuring single vine ET in commercial contexts. Importantly, the novel chip integrated biometeorological sensors in the Cube performed well. On average the wind speed, temperature and relative humidity explained 92% of the variability in reference sensor data, an important milestone, because these data are

then used to make HRI calculations of ET. When the Cube sensors were used to measure biometeorological data in a commercial vineyard in the Central Valley of California, USA, the results were promising. Though the relationship between the ET measured with the HRI method and Cube sensors (r^2 = 0.4384) was not as well correlated as the relationships observed with research grade sensors in previous studies (e.g. r^2 = 0.91; Jenkins *et al., 2023*) there were some challenges with this experiment that may have impacted this result. Principally, the area term was not derived from Cube data, but rather from research grade sensor data. This is due to the design of these early generation Cubes which did not allow for the continuous 24-hour measurements that were possible with the research grade sensors installed in the RMI vineyard. In order to experimentally derive an area term by the protocol given in Jenkins *et al., 2023*, two to three consecutive days of 24-hour biometeorological are used. This is because the full range of values for all parameters included in the HRI method for ET measurement need to be included in this calculation. If the data from the Cube sensors' daily 6 hour windows, always scheduled around solar, were used to calculate an area term, then this would lead to an area term that is not relevant to most of the day. This is because the range of values observed for each of the biometeorological parameters during this 6 hour window would include only the values occurring at this rather unique time of day when temperature is typically at its peak, relative humidity is at its nadir and wind speed tends to be high as well. Despite the challenges with extracting an area term, both the CMT and MB model estimates were observed to have significant relationships (p-value < 0.05) with ground truth ET. These two models happen to be the only two HRI models based on first principles, meaning the area terms associated with them have a putative physical meaning. Taken together, these results expand evidence supporting the use of the HRI method for estimating ET, though the transition from the research grade sensors used for model development to new low-cost Cube sensors will require further work.

The lack of a correlation between the single vine Cube sensor and HRI model predictions of ET and the larger area flux tower and eddy covariance data does not necessarily

indicate the HRI method is not useful. Other low-cost methods for estimating ET also involve error but have nevertheless seen widespread adoption in research and commercial contexts alike. For example, one study found the difference between crop coefficients recommended by FAO56 Penman-Monteith methods and locally observed data can be greater than 40% (Gharsallah *et al.,* 2013). Researchers in this study attributed the results to crop coefficients, which attempt to integrate several physical and biological concepts into one signal, leaving significant potential for error. Due to its Penman-Monteith origins, the reference ET approach is inherently sensitive to local climatic conditions at the reference ET measurement site which may differ from local conditions at the prediction site. When climatic variation exists between the reference and prediction site it may be possible to use direct measurements of stomatal and boundary layer resistance to calibrate estimates (Li *et al.,* 2019, Yan *et al.,* 2020). Pan evaporation is a nearly ubiquitously available method but relies heavily on the assumption that the reference pan used for evaporation studies is the “class A evaporation pan” issued by the United States National Weather Service, or a pan of nearly identical design. Though the relationship between pan evaporation and reference ET is valid under many conditions, some conditions such as night or prolonged cloud cover may violate this assumption. Additionally, the reference ET and pan evaporation methods do not perform well under deficit irrigation, when they cannot completely account for the response of plants to water stress (Hochberg *et al.,* 2017). Even the favored method of many commercial viticulturists, eddy covariance, has some significant limitations. The eddy covariance method, while valued by researchers for its ability to directly estimate ET, is very challenging to validate. The large scale and high variability of the flux footprint in this model, as well as the open boundary layer of the volume studied, both affected by the degree of advection, create issues for those seeking to make direct comparisons of other ET estimates to the estimates generated by eddy covariance methods (Kustas *et al.,* 2022; Stanhill, 2019). The issue of the flexible footprint, which results in energy imbalance between the total available energy and turbulent fluxes calculated by the eddy covariance

technique, can lead to overuse of water in agricultural settings. Different approaches for computationally distributing this imbalance to create pseudo-balance can lead to uncertainty in daily ET estimates up to 50% (Bambach *et al.,* 2022). The Bambach et al., 2022 team of researchers went on to show over the growing season this uncertainty can amount to up to a third of the total annual applied irrigation.

While the evidence presented here expands support for the utility of the HRI method for estimating ET, and provides early insight into the design of low-cost sensors that could allow this technology to scale, there are some remaining questions that need to be addressed before the method is considered for commercial applications. First, an improved method for regularly collecting vine physical data would allow for regular calculation of area terms and likely improve predictions of ET at specific sites and for specific plants. An automated method for collecting and extracting vine measurements from images, light interception data, and three-dimensional scans (e.g. LiDAR) could be crucial to the viability of this technology at the scale of a modern commercial vineyard. Ideally the imaging component would be designed for easy mounting on tractors or other farm equipment, so data can be recorded during normal farming operations, in a system similar to the methods in Olensky *et al.,* 2022. Once collected, this data could be fed into an automated analysis pipeline which returns the desired vine measurements. The design, testing and implementation of this hardware and software is a non-trivial addition to the core goals of this project and would represent a significant effort.

If a network of sensors is to be deployed in an agricultural context, then power and communication will also be challenges. As one example, the lithium ion batteries used in this study, while durable in many respects, lacked the ability to withstand the 10 ^{o}C or greater daily temperature fluctuations common in the Central Valley of California. In order for longer duration, multi-day studies to be conducted in the field with Cube sensors new batteries will need to be tested. Recent advances in lithium iron phosphate battery technology including improved thermal stability, long lifespan, and low risk of combustion, may mean longer duration studies

are a near term possibility (Hassoun *et al.,* 2014). It may also be possible to use an oversized power source such as a portable solar energy harvesting panel combined with a large capacity lead-acid battery; a strategy successfully employed in other studies (Kustas *et al.,* 2022; Jenkins *et al.,* 2023). Even if power is available, for irrigation equipment to function properly and deliver water only when conditions warrant, it is essential that spatially distributed devices can rapidly and reliably communicate with each other. Low power wide area networks are an ideal option for low power IoT devices in agricultural settings.

Several low power wide area networks have been investigated for their applicability to large scale deployment of networks of devices in rural settings. The Long Range Wide Area Network (LoRaWAN) is a low data rate communication protocol specifically designed for minimum energy budget applications and the longest range coverage for communication (Marini *et al.,* 2022). Another popular low power wide area network technology, called Narrowband IoT (NB-IoT), was developed for efficient connectivity in cellular IoT networks and to optimize for minimal power consumption (Marini *et al.,* 2022). A third option, Sigfox, was designed for IoT applications operating with only small infrequent data packets. This technology transmits in the sub-gigahertz range allowing for extremely low power consumption, and because sensor networks are managed by Sigfox, infrastructure management is relatively simple compared to other options (Lalle *et al.,* 2019; *Sigfox,* Labège, France). Overall, while each of these technologies show great potential to support development in different areas of IoT innovation, research has shown the NB-IoT option may be the most promising for agriculture applications. With NB-IoT there is the distinct advantage of being able to connect massive numbers of devices, more than fifty thousand, to a single node, whereas LoRaWAN and Sigfox are limited to thousands of connections per node (Liberg *et al.,* 2017).

While further research will be required to prepare the low-cost Cube sensors and HRI method for large scale applications in commercial agriculture, the results presented in this manuscript show strong promise that the remaining challenges can be overcome. If improved

sensor power systems can be developed along with methods for directly measuring the HRI model area terms from data captured at the growing site, then the novel sensors and algorithms presented here provide an option to growers looking for a better understanding of individual vine water use, information that can be used for fine-scale, demand based distribution of water.

Acknowledgements

The authors thank Leticia Chacon Rodriguez for viticultural guidance and access to vineyard facilities, Guillermo Federico Garcia Zamora and Gonzalo Ruiz Gonzalez for assistance with vine care and equipment installation at the RMI Vineyard. Additionally the authors thank E.J. Gallo Winery and the staff of the Winegrowing Research Division for providing access to data and facilities. This work was made possible through financial support from Till Guldimann and the Ernest Gallo Endowed Chair in Viticulture and Enology. Parts of this work were supported by Grant Case-48166 of the 21st Century Jobs Trust Fund received through the MSF from the State of Michigan.

Author contributions

K.M. and M.R.J. conceptualized the CMT model. D.E.B., S.N., and M.R.J. conceptualized the MB model. M.R.J. and B.J. wrote all code for data capture, analysis and visualization. B.J. and M.B. designed and developed the Cube sensor. M.M.A.M., W.P.K., J.G.A., D.E.B., and M.B. provided access to research consulting, data and facilities.

Chapter Four

Leaf Area Tool, open source pipeline for automated leaf area detection

Matthew Jenkins, Dylan Lenczewski-Jowers, Fabiola Chavez Lamas, David E. Block

Preface

In this manuscript (**ready for submission**) a new field ready, fast and accurate image analysis pipeline is introduced. With this new technology, images acquired with any digital camera can be used for the quantification of leaf area. This tool will improve the ability of researchers and other HRI users to capture important plant information, thereby supporting the core research goals of this dissertation.

Abstract

Across several scientific disciplines ranging from agronomy to ecology, the accurate measurement of leaf area serves as a cornerstone for understanding vital processes including photosynthesis, transpiration, and plant growth. This fundamental parameter, which has far-reaching implications for both research and practical applications, is currently constrained by available tools which often fall short of providing precise measurements or lack the robustness necessary for field deployment. The dichotomy between laboratory precision and real-world applicability has created a critical gap in methodologies, restricting advancements in our understanding of plant function and behavior. The Leaf Area Tool image analysis pipeline is a field ready, fast and accurate method for the quantification of leaf area from images acquired

with any digital camera, including smartphone cameras. Without adjusting for the error caused by shadow the Leaf Area Tool pipeline still explains more than 94% of the variation in ground truth leaf area, and with adjustments for shadow it explains more than 99%. Though further research will be required to add important features such as shadow mitigation, a non-destructive process, and to expand the library of extractables, overall the Leaf Area Tool performs well on broad leaves and has significant advantages compared to other existing methods.

Introduction

Across scientific disciplines ranging from agronomy to ecology, the accurate and rapid measurement of leaf area is vital to building our understanding of myriad biophysical processes at the level of the leaf and the whole plant, to characterizing differences between species or populations, and to inform large scale breeding projects (Osnas *et al.,* 2013; Díaz *et al.,* 2016; Kattge *et al.,* 2011; Furbank and Tester, 2011; Berger *et al.,* 2010; Borevitz, 2012; Albrecht and Bargmann, 2011). The utility of this fundamental parameter, which has far-reaching implications for both research and practical applications, is currently constrained by available tools that often fall short of providing precise measurements or lack the robustness necessary for field deployment. This dichotomy between laboratory precision and real-world applicability has created a critical gap in leaf area methodologies, restricting advancements in the understanding of plant function and behavior.

Large datasets are typically required in order to make accurate whole plant leaf area estimates, but as dataset size grows the practicality of manual segmentation methods diminishes. Most existing techniques for measuring leaf area, especially high-throughput options, require expensive equipment or common flatbed scanners and software (*Delta-T Devices*, Cambridge, UK; *LI-COR*, Lincoln, NE; *WinFOLIA*, Canada). Apart from leaf area meters (e.g. LI-3000, WinDIAS) or proprietary devices (e.g. WinFOLIA calibrated optical

scanner), existing pipelines start with the capture of leaf scans using a portable scanner then process scans using software. These algorithms extract leaf area from scanner images using pixel counts, scaling results using an object of known size (Bylesjö *et al.,* 2008; Weight *et al.,* 2008; Varma and Osuri, 2013; Maloof *et al.,* 2013). While some portable scanners have been developed and some leaf area methods have been developed for smartphones, these scanners are not robust enough to withstand long days in varied outdoor conditions (e.g. rain, snow) and current smartphone application workflows can be slow, requiring user input at multiple steps for each measurement. Despite these limitations, existing methods have been used to measure the area of broad leaves in many studies.

Existing methods for measuring area of broad leaves are generally either manual or semi-automated using software. The traditional manual method for determining leaf area is measurement of the maximum leaf blade width and leaf height from petiole to blade tip, then multiplying. While this method has the distinct advantages of being non-destructive and essentially free, requiring only a notepad, a fixed ruler or tape measure, and perhaps a calculator, it lacks the specificity of other methods and may under or over-estimate the area of some leaf shapes. When more specificity is needed but datasets are small enough for manual measurement, or when ground truth leaf area is needed for validation of new tools, leaf area is typically determined via destructive imaging using a common flatbed scanner and manual measurement using one of several software options (Gao *et al.,* 2011; Varma and Osuri, 2013). The most commonly used software for leaf analysis are Image J (Schneider *et al.,* 2012), GNU Image Manipulation Program (GIMP, 2019) and Photoshop CS (Adobe Inc., 2019). With each of these image processing software, users first set a scale based on an object of known size and the image pixel density, then use this scale to determine the true dimensions of the leaf via tracing. While manual tracing is accurate, it is only feasible when datasets are small. Therefore in some fields hand tracing is sufficient, but in other fields, such as community ecology, datasets routinely include hundreds to thousands of samples and extracting functional trait information is

not possible without leaf analysis (Kraft *et al.,* 2008; Katabuchi *et al.,* 2012; Fortunel *et al.,* 2012). In these situations, semi-automated leaf image analysis tools are the preferred option.

Software leaf analysis tools automate key aspects of the leaf analysis process, allowing users to rapidly extract measurements such as leaf area, width, length, fraction of diseased tissue and more. But before processing with software, users must first capture leaf images in a destructive process using either a digital camera or a common flatbed scanner, including portable models. Even more, existing methods for leaf area analysis using images captured with a digital camera are limited by the requirement of highly specific formatting of images for accurate analysis, or rely on assumptions that are violated in most cases.

One method, the Fast and Accurate Method for Leaf Area Measurement (FAMLAM), requires users to capture leaf images using a 16.1 megapixel resolution digital color camera on a completely white background except for a 2 cm by 2 cm black square, for calibration (Chaudhary *et al.,* 2012). Once images are acquired the software computes leaf area using a thresholding processing and grid count method. In this process a hole filling technique is automatically applied which may cause error in some cases where this is not desired, such as when herbivory is quantified. Another technology, Leaf-IT, is an Android smartphone application requiring users to capture photos on a completely white background, including a calibration shape of known size (Schrader *et al.,* 2017). Though image acquisition and processing can be slow, this software is favored in some cases because it uses a margin detection algorithm to find leaf edges, mitigating errors caused by shadows. Easy Leaf Area, released in 2014, is one of the only non-destructive options for measuring leaf area. In this software, users capture images of living *Arabidopsis thaliana* from directly above, including an object of known size for calibration (Easlon and Bloom, 2014). Though notable for being non-destructive, area measurements are rooted in the often false assumption that leaves do not occlude one another relative to camera position, and this approach was originally only validated for *A. thaliana*. Since

then, it has seen use in many other cropping systems including orchard crops, wheat, oak and tomato (Ganchev, 2023; Lama *et al.*, 2023; Rogers, 2022; Idowu *et al.*, 2023).

Leaf analysis software designed for images acquired in a destructive process involving removal and imaging with common flatbed scanners are more popular due to the uniformity and clarity of the images acquired. WinFOLIA (Regent Instruments Canada Inc., Quebec, Canada), perhaps the most widely known tool for analysis of scanner acquired leaf images, is based on pixel color analysis using three user programmed thresholds. With these values set properly metrics such as leaf area, length, width and even diseased tissue fraction can be extracted; and uniquely, petiole measurements can also be extracted. Another popular software option is LeafArea, an R package which allows users to run ImageJ within R, automating some otherwise tedious processes such as adding together several pieces of a larger leaf that was cut into pieces before scanning (Katabuchi, 2015). Other tools such as Compu Eye, Leaf & Symptom Area (CELSA), are less user friendly, requiring scanning and processing of leaf images one at a time, but are optimized for certain tasks. In this case, using user programmed thresholds can highlight areas of mite damage in addition to extracting leaf area and other metrics (Bakr, 2005). LeafAnalyser, another such example, is a tool optimized for analysis of leaf shape (Weight *et al.,* 2008). This software detects the leaf margin then places hundreds of evenly spaced arrows perpendicular to the surface around the perimeter of the leaf. The orientation of these arrows and other extracted data is provided in a format optimized for principal component analysis, which can help visualize group differences in size, width, and tip to base symmetry.

Other software options for leaf scan analysis were developed primarily for flexibility and user friendliness. One option, Black Spot, is a free software that lets users program thresholds for pixel based classification, but unlike others allows batch processing of scans (Varma and Osuri, 2013). Though this tool has been shown effective, with a reported 0.4% error rate compared to manual processing, it is not open source and therefore may be difficult to adapt to non-ideal use cases. Perhaps the most user experience driven software, Leaf Shape

Determination (LAMINA), is a standalone Java application including a graphical user interface that allows users to select multiple threshold levels for highlighting various objects in images (Bylesjö *et al.,* 2008). The results generated by this tool, including area, width, serration angles, and even levels of herbivory, are also optimized for use in association mapping with principal component analysis.

Digital camera and flatbed scanner image analysis pipelines may be popular options for measuring leaf area in research and industry contexts, but they all require some degree of technical expertise in either computing, imaging or both. To overcome these challenges, leaf area meters have been developed to provide out of box capabilities for measuring leaf area (*LI-COR BioSciences*, Lincoln, Nebraska, USA; *Delta-T Devices*, Cambridge, UK). Many features are shared between two of the most popular leaf area meters on the market, the *LI-COR* LI-3000 and *Delta-T* WinDIAS, but there are some significant differences as well. The LI-3000 measures leaves using a sensor absorbance signal and an array of narrow band light emitting diodes embedded in the portable handheld scanner head, minimizing error caused by shadows. Leaf width and length is sensed by the software as the user slides the device along the length of the leaf, then area is estimated by multiplying maximum width by length. While this process is non-destructive, it is restricted to leaves which fit inside the handheld device. When leaves are oversized or many leaves need to be measured quickly, leaves can be collected destructively then scanned using the LI-3000 conveyor belt accessory. If the conveyor belt is used, the LI-3000 which normally has a 16 hour field battery life, will need to have access to a grid power source. In either a field or lab setting, the LI-3000 provides data to the user immediately on a built-in screen displaying values as they are measured, as well as in an exportable format. The Delta-T WinDIAS, on the other hand, is a much larger device and is only suitable for use in a laboratory or similar setting where grid power is readily available. Users must also have access to a computer running a Windows (*Microsoft*; Redmond, Washington, USA) operating system in order to interface with the imaging hardware. Once images are

acquired, a destructive process in which users place leaves on a custom built 1000+ dpi optical scanner, leaf measurements are extracted using a thresholding process. The user can set multiple thresholds in the software, allowing for measurement of visually distinct areas such as diseased or variegated tissue. Due to the thresholding and pixel counting method for extracting leaf measurements, a more accurate area is generated as well as measurements of perimeter, length from blade tip to petiole, maximum width, object count and more. In situations where many leaves need to be measured, an optional conveyor belt accessory is available that increases the capacity to 800 leaves per hour, and also facilitates the measurement of very long leaves in a single scan. Though leaf area meters can provide useful and accurate estimates of leaf parameters they are expensive and still require operators to be knowledgeable or trained to some extent.

In an effort to address the gap between the relatively low throughput tools designed for accurate measurement of leaves, and the high throughput tools designed for rapid extraction of estimated or sensed leaf parameters, a new semi-automated leaf area tool has been developed which is accurate, high-throughput, and field ready. This method does not require any special equipment, such as digital cameras with specific resolution or custom calibrated optical scanners, nor does it require an additional calibration step. The new pipeline introduced in this manuscript is a simple, free, and open-source process for extraction of leaf area from images of leaves captured with any digital camera. The process is generally broken into two distinct phases, the field phase and the analysis phase.

In the field phase, the user captures a photo of a single leaf on a white background of known size. This procedure is specifically designed to be a single, fast and easy step even in difficult field settings. Once images are obtained in the field, the user can, at any later point, execute the analysis phase using any computer with Leaf Area Tool software installed. This free, open source software allows the user to batch process hundreds or thousands of leaf images in minutes with minimal computational effort.

In this manuscript the new Leaf Area Tool pipeline for leaf area extraction from digital images is introduced. To highlight the unique and powerful features of the tool, the design and user flow through the image processing pipeline is presented in detail. The performance of Leaf Area Tool is then tested with a dataset of 104 photos of broad leaves from 12 distinct species, comparing software estimates of leaf area to manually measured leaf area, as well as a manually measured estimate of leaf area, calculated from maximum width and length from petiole to blade tip. An investigation of the time required for processing images with each method is also reported. The observations and results reported here constitute strong evidence for the utility of the new Leaf Area Tool pipeline for extraction of leaf area from digital images.

Materials and methods

Leaf Area Tool software is written in Python and utilizes tools in several modules including Python Imaging Library (Pillow fork, version 9.2.0, https://pypi.org/project/Pillow/), Pandas (version 1.4.4, https://pandas.pydata.org/), scikit-image (version 0.19.3, https://scikit-image.org/; Walt *et al.,* 2014), OpenCV (version 4.6.0.66, https://pypi.org/project/opencv-python/), and imutils (version 0.5.4, https://pypi.org/project/imutils/). The software is designed to run in a Jupyter notebook, an operating system agnostic environment that opens in a web browser, with no internet connection required once the software is installed (Kluyver *et al.,* 2016). An in-depth user manual and codebase is available at https://github.com/mattjenkins3/Automated-Leaf-Area-Detection.

The full Leaf Area Tool pipeline incorporates field and analysis phases and is depicted in annotated images in Figure 4.1. In the field phase, the user will destructively obtain leaves, removing petiole unless this area should be included in leaf area. Then, the researcher will photograph individual leaves on a rigid, rectangular white background of known size. If individual leaf areas are not needed, such as when estimating whole plant leaf area, then

multiple leaves may be photographed simultaneously on a single background, though leaves cannot overlap and cannot extend beyond the edges of the white background. Any digital camera may be used for image acquisition, though accuracy of results may differ slightly from those reported here. It is important to consider the lighting of photos, as images with pronounced shadows or an uneven background may cause the software to measure leaf area inaccurately. An example of an acceptable image can be found in Figure 4.1.

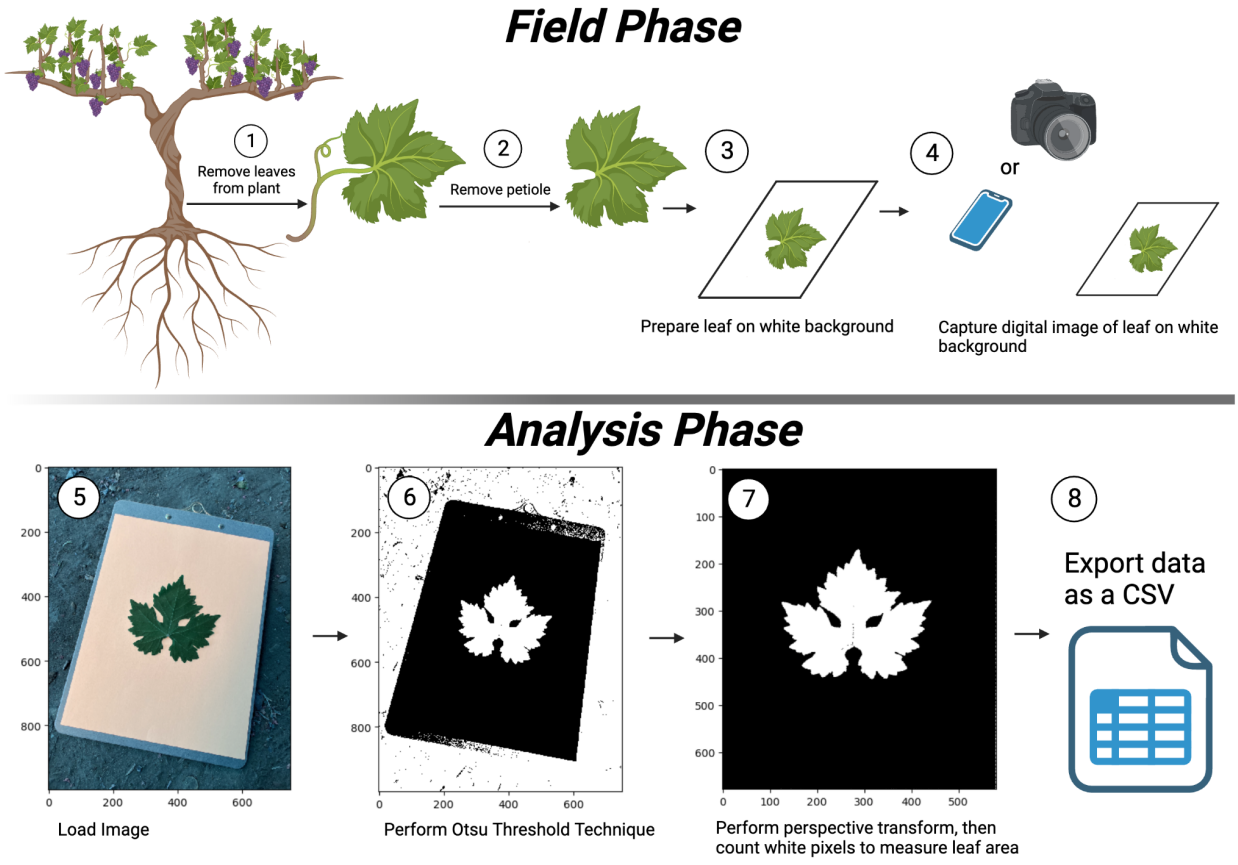

Figure 4.1: Diagram of the Leaf Area Tool pipeline for leaf image analysis. In the Field Phase leaves are removed from the plant, then petioles are removed and leaves are individually photographed on a white background of known size. Then, in the Analysis Phase the leaf images are loaded, thresholding is performed followed by a four point perspective transformation. Finally, leaf area is extracted using pixel counting and the data is exported as a CSV file.

Once Leaf Area Tool has been installed on a computer and leaf images have been exported from the camera to the computer, the user will populate a directory with the images

that are to be analyzed together. If images are logically grouped by any categorical concept such as plant, species, or row, as examples, then the user should create a unique directory for each group. Leaf Area Tool is then launched using a command line tool, opening a Jupyter notebook. In the notebook, the user will set the name and relative location of the directory containing the photos to be analyzed as well as the true size of the white background, using preferred units. The analysis pipeline is fully automated from this point forward. Looping over all the photos in the directory, the software first loads the images then performs Otsu's Thresholding technique, binarizing the image into two classes by calculating an optimal single threshold value (Otsu 1979). The mathematically chosen threshold selection is based on an exhaustive process of searching all possible values, then choosing the value that minimizes intraclass variance. Once a binarized image is obtained, such as in Step 6 of Figure 4.1, a contour search function is applied, finding the largest four sided object, the corners of which correspond to the corners of the white background. Using the locations of the corners of the white background, a perspective transform is then applied, yielding a binarized image of the leaf on a solid background, such as in Step 7 of Figure 4.1. At this point a simple pixel counting method is applied, using the user set background size as a scale for the extraction of leaf area. Finally, data is exported as a comma-separated value (.csv; CSV) file containing the image file name, the date and time of image creation, and the leaf area.

To assess the performance of the Leaf Area Tool pipeline for leaf area analysis a test dataset was created including 104 images of broad leaves from different deciduous trees, collected in Davis, California in May, 2023. Leaf images were captured using an iPhone 13 Pro (*Apple Inc*; Cupertino, CA) rear-facing 12 megapixel digital camera on a piece of standard USA "Letter" size printer paper mounted on a rigid clipboard to prevent curling of corners during the field phase of the experiment. Once images were acquired, they were subjected to three parallel analysis pipelines, the Leaf Area Tool method and two manual measurement methods: exact tracing and a width and length based estimate. Exact manual tracing, while time consuming, is a

widely accepted method for measuring ground truth leaf area values, and is also useful for the validation of new tools. The rough estimate, computed by multiplying width and length, is computed because manual measurements of width and length are commonly used as a proxy for true leaf area, and therefore serve as a reasonable benchmark for new leaf area tools. In this study, we compare Leaf Area Tool software estimates as well as rough estimates of leaf area to manually traced ground truth leaf area. To explore the weaknesses of Leaf Area Tool and explore areas of future improvement, a comparison between hand traced leaf area including shadows and Leaf Area Tool estimates is also presented. To conclude, and to emphasize the drastic reduction in human engagement achieved by using software to automate repetitive tasks, the time required to measure leaf area in one image is compared across manual tracing, manual rough estimation and automated estimation using Leaf Area Tool software.

For the following results, R v3.5.1 was utilized for all analysis and visualization (R Core Team, 2018). Statistical values including r^2, p-value and RMSE were generated using the 'stats' package, a part of R. A 2021 Apple Macbook Pro with 16 gigabytes of random access memory was used for all computation.

Results

Comparing software measurements to exact measurements and rough estimates

In order to understand the performance of the new Leaf Area Tool pipeline for leaf image analysis and a commonly used width and length based estimate, leaf area estimates generated by both methods are compared to ground truth leaf area determined using hand tracing (Figure 4.2). The Leaf Area Tool software measurement of leaf area is acquired using the process described in the Methods section of this manuscript. Both the ground truth leaf area and the rough width and length based estimates were measured by hand using ImageJ (Schneider *et al.,* 2012). Whether measuring ground truth or rough leaf area, the user must first set a pixel based scale using the known size of the white background and the 'set scale' function in

ImageJ. Ground truth leaf area is then measured using the polygon selection tool, tracing the outer edge of the leaf around the full perimeter of the leaf, as depicted in Panel B of Figure 4.3). Using the same scale and tools, the length from petiole to blade tip is measured (using the central leaflet if multiple leaflets are present) and the maximum leaf width is also measured.

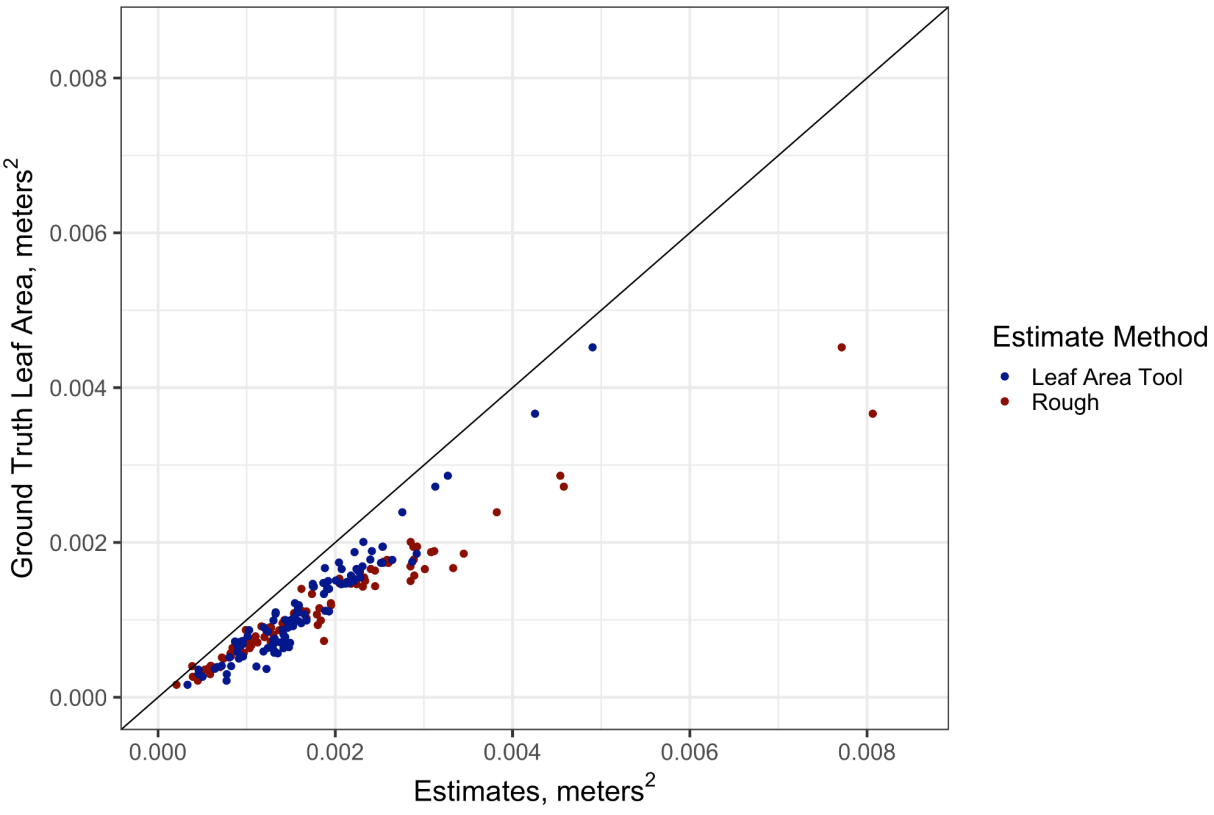

Figure 4.2: Leaf Area Tool and rough width and length based estimates of leaf area (units = m^2) are plotted against ground truth leaf area as determined by manual tracing.

In Figure 4.2, Leaf Area Tool software estimates as well as rough estimates are plotted against ground truth leaf area and linear regression analysis was performed between software estimates and ground truth; and between rough manual estimates and ground truth. Leaf Area Tool software estimates explained more than 94.4% of the variation in ground truth leaf area, while rough estimates based on length and width only explained 92.4% of the variation in ground truth leaf area. Though both the rough estimates and software estimates explained

much of the variation in leaf area, it is visually clear that at the higher end of the leaf area range, specifically above 0.004 m^2, the rough estimates of leaf area begin to overestimate the ground truth leaf area.

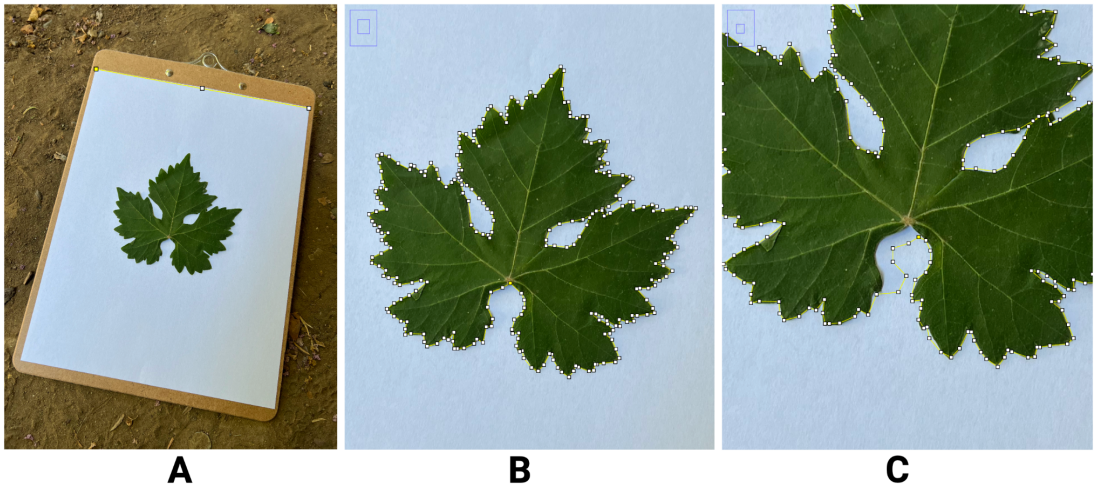

Figure 4.3: Panel A features an example of a suitable Leaf Area Tool leaf image, and also depicts in bright yellow the method used for manually setting the image scale in ImageJ with the Straight Line tool (Schneider *et al.,* 2012). Panel B depicts a zoomed in version of Panel A, and an example of ground truth leaf area tracing in ImageJ with the Polygon Selections tool. In Panel C, zooming slightly more, an example of the tracing of shadow is given on that same leaf.

While developing the Leaf Area Tool pipeline, we noticed Otsu thresholding would often erroneously include shadow areas as leaf area. To better understand the impact of shadows on leaf area estimates 13 images from the original dataset of 104 images were randomly selected. Researchers then analyzed the leaf area of these images using a method similar to the ground truth area method but now including shadows, as depicted in Panel C of Figure 4.3. These new "Ground Truth Leaf Area and Shadow" measurements were then plotted against Leaf Area Tool software estimates of leaf area (Figure 4.4). Another linear regression analysis is performed and this time the Leaf Area Tool estimates are observed to explain 99.4% of the variation in ground truth leaf area plus shadows. This result suggests some of the error in Leaf Area Tool software

estimates is caused by erroneous inclusion of shadows created by fresh leaves which do not naturally lay flat on the white background.

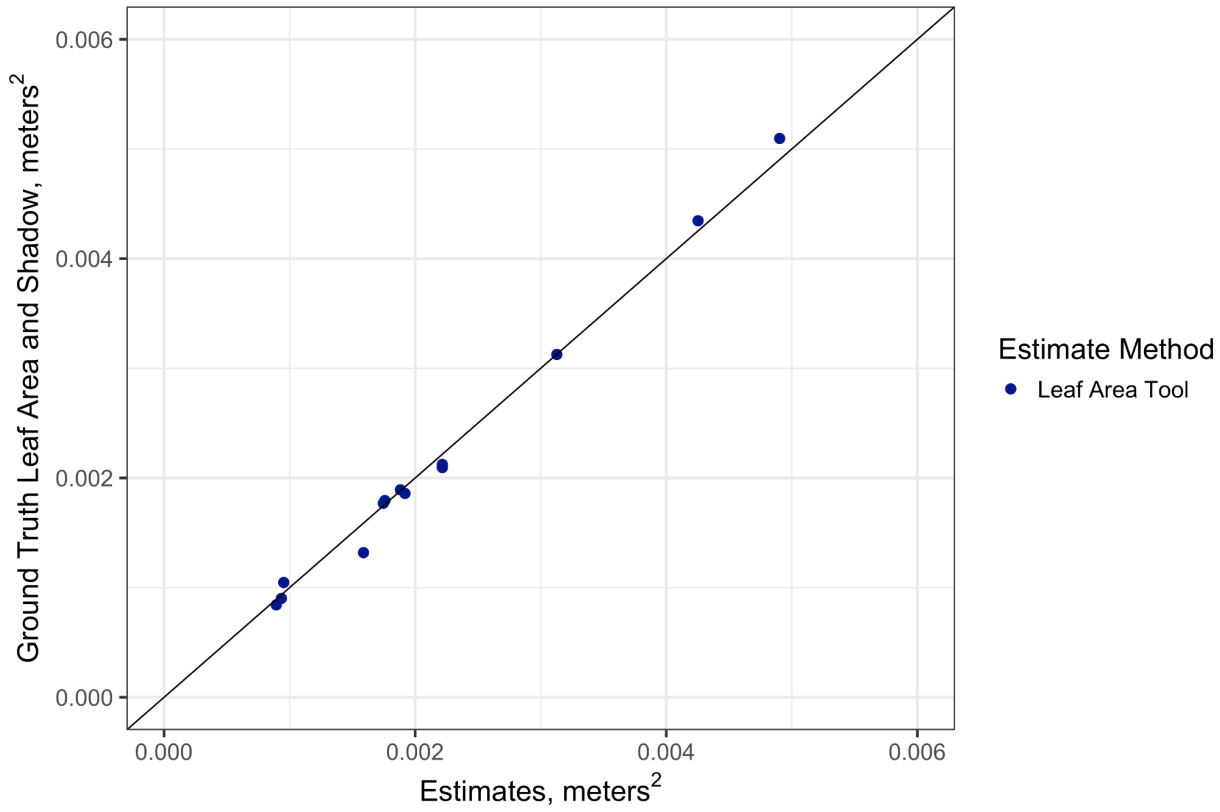

Figure 4.4: Leaf Area Tool estimates of leaf area (units = m^2) are plotted against ground truth leaf area, including shadows, as determined by manual tracing.

Quanitfiying the temporal efficiency of Leaf Area Tool

Temporal efficiency was one of the guiding principles in the design of the Leaf Area Tool image analysis pipeline. To demonstrate the difference in time required to analyze a single leaf image using different methods, several destructive leaf area methods are compared (Figure 4.5). The “ImageJ Trace” and the “ImageJ Rough” methods method in Figure 4.5 are the same methods used for ground truth leaf area and for width and length based estimates in previous figures. A third option, “manual rough” is added in this figure, and represents the process of manually estimating leaf area using a fixed edge ruler, measuring the length from petiole to blade tip and maximum width, much like the rough method in ImageJ but performed manually,

including the step of adding values to a database. The time required to multiply width and length values in a database was not included in measurement time as this is nearly instantaneous in most modern database software. The mean of 40 measurements performed with each process is plotted as bars in Figure 4.5, with standard deviation as brackets. The “Leaf Area Tool” category represents the mean time required to analyze a single photo using the Leaf Area Tool software pipeline. This number was calculated by dividing the total computation time for measuring leaf area in 104 images by the number of images. At 0.118718 seconds, compared to other mean leaf analysis times the Leaf Area Tool pipeline is between about 750 and 225 times faster than other options. Notably, the “Manual Rough” method was also between about 2 and 3.4 times faster than any of the manual methods requiring ImageJ.

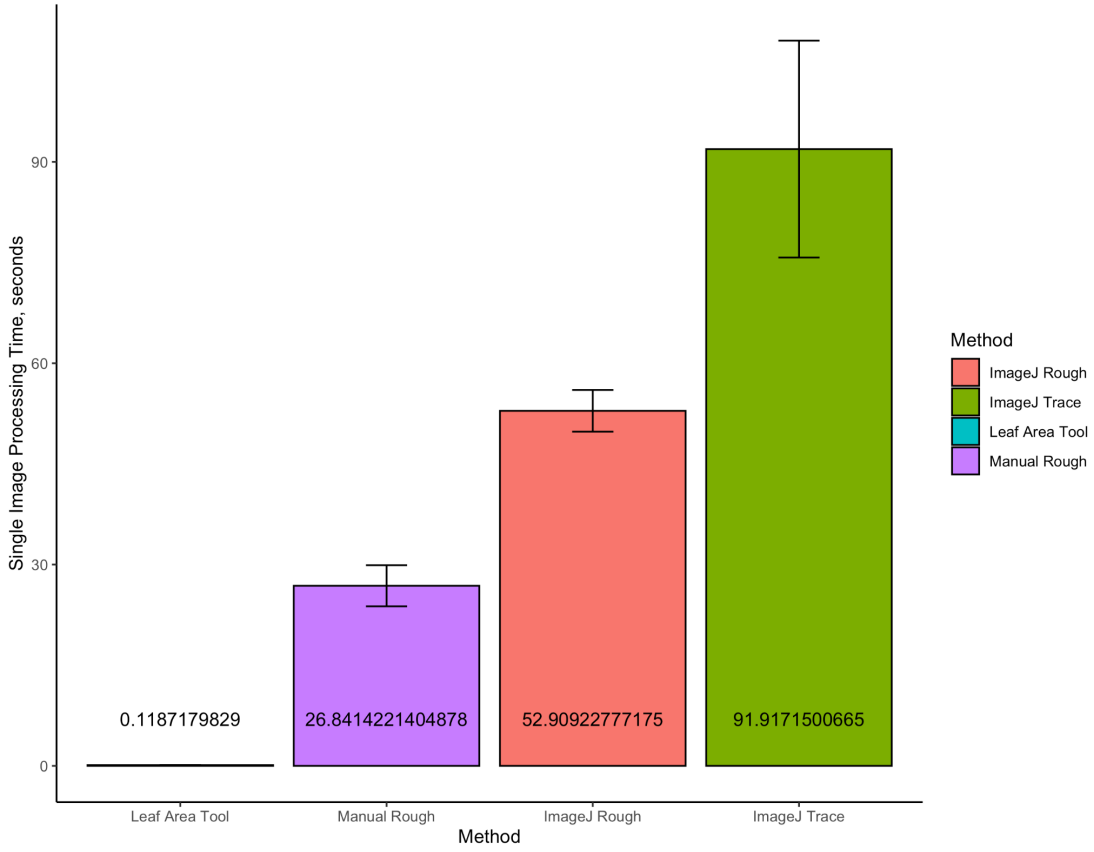

Figure 4.5: Image processing time (units = seconds) is plotted, with bars representing each leaf area measurement method. The numbers above or within bars are the mean single leaf measurement times; error bars represent standard error.

Taken together these results suggest the new Leaf Area Tool pipeline for leaf image analysis is a promising new option for rapidly extracting accurate leaf area values from hundreds or thousands of images.

Discussion

The generally good results when compared to ground truth leaf area, and in the vastly improved per leaf measurement times, are strong evidence the Leaf Area Tool is a suitable tool for measuring leaf area in field and laboratory settings. Tools for rapidly extracting accurate leaf traits will accelerate the characterization of functional differences between plants, improving our understanding of the impact of leaf traits on key ecological processes and expanding phenotyping capabilities in rapid breeding projects. To answer important plant and community level questions in topic areas ranging from ecology to astrobotany, large datasets will be required as well as the tools that can handle these datasets. The observations presented here suggest the Leaf Area Tool leaf image analysis pipeline is a performant tool for extracting leaf area from large collections of leaf images, and an important next step, simplifying both the image acquisition and image processing phases of leaf image analysis.

The data presented in this manuscript is strong evidence the Leaf Area Tool image analysis pipeline can be used to measure leaf area. Compared to rough estimates of leaf area based on length and width measurements, the Leaf Area Tool method explains more variation in ground truth leaf area (Figure 4.2). Rough length and width based estimates of leaf area, whether measured using image analysis software or in the field with a measurement device such as a ruler or tape measure, are commonly used as a proxy for ground truth leaf area (*LI-3000*; LI-COR BioSciences, Lincoln, Nebraska, USA). Based on observations in Figure 4.2, rough leaf area estimates may differ from ground truth especially when leaves are larger than 0.004 m^2, suggesting rough estimates of leaf area may be sufficient in some cases but perhaps

not when leaves are large. To maximize the performance of the Leaf Area Tool image analysis pipeline the effect of shadows should be minimized through additional lighting or mechanical flattening of leaves, if this is appropriate for the application. Temporal efficiency is often the most important factor, especially in large scale studies, and the Leaf Area Tool method was observed as orders of magnitude faster than any of the other methods measured in this study (Figure 4.5). Taken together, these results suggest the Leaf Area Tool method can be used to measure leaf area with accuracy and considerable speed.

Other methods designed for measuring leaf area, while effective and potentially more efficient for specific applications, have several limitations which could restrict their utility. For example, more than seven of the thirteen leaf area measurement methods discussed in this manuscript require flatbed scanners for capturing leaf images (Table 4.1). While these scanners are common and easily acquired in most regions, they are not as ubiquitous, durable or nearly as portable as other imaging devices such as smartphone cameras. Perhaps even more limiting, ten out of thirteen leaf area measurement methods are strictly destructive. In other words, in order to use these methods leaves must first be harvested from the subject plant, then scanned, imaged or manually measured. Though some leaf area meters can capture a non-destructive measurement of leaf area, this is time consuming and the required sensors are very expensive. Finding the true scale, or true distance per pixel dimension, of an image is a fundamental barrier to extracting accurate measurements. Many technologies and methods for leaf area measurement overcome this issue by asking users to include a separate object of known size for calibration (Table 4.1). Not only does this process slow the image acquisition process, but it increases the possibility of user error caused by overlapping of leaf margins and calibration objects or the possibility of incorrect calibration if the size of the calibration object is slightly off, as examples. Other leaf area measurement options include significant sources of known error which can limit their accuracy in certain applications. One example, the FAMLAM approach, includes a computational step of automatically correcting any holes in leaves by filling

Method	Flatbed Scanner images	Digital camera images	Calibration object in image	Destructive	Non destructive	Expertise required	High throughput	Open source	Free
Easy Leaf Area		x	x		x		x	x	x
Leaf-IT		x	x	x					
FAMLAM		x	x	x		x			
WinFOLIA	x		x	x		x			
LeafArea	x		x	x		x	x		x
CELSA	x		x	x		x			
LeafAnalyser	x			x		x	x		
Black Spot	x		x	x			x		x
LAMINA	x		x	x		x			
LI-COR LI-3000				x	x	x	x		
Delta-T WinDIAS	x			x		x	x		
Leaf Area Tool		x	x	x			x	x	x
Rough length x width estimate				x	x			x	x

Table 4.1: A table including all the leaf area measurement methods discussed in this manuscript, with categorical information describing the features associated with each method.

them with pixels of the same class as leaf tissue (Chaudhury *et al.,* 2012). This could be a useful feature in some cases but because FAMLAM software is not open source the hole filling process cannot be circumnavigated by the user in any way, and therefore this approach is limited to situations where leaf tissue damage is not present or ignoring it is reasonable. Though the Easy Leaf Area method is notable for being non-destructive, the quantification method used by the software requires leaves do not occlude one another (Easlon and Bloom, 2014). Even when plants are grown in laboratory conditions, as is often the case in the *Arabidopsis thaliana* studies Easy Leaf Area is most commonly used for, leaf occlusion is a common feature and thus this assumption introduces some error in leaf size estimation. Generally speaking, limitations and error are common features of all existing methods for leaf area measurement especially as dataset size increases.

Shadows pose a particularly significant challenge for several existing leaf area measurement methods and this is also the case for the Leaf Area Tool method (Varma and Osuri, 2013; Schrader *et al.,* 2017). When leaves do not lay flat on the reference surface a shadow can form, and due to the Otsu thresholding method employed during image processing, this shadow can cause error in area determination. While shadows were the only limitation investigated in this manuscript, it is also possible other challenges will arise as the Leaf Area Tool is brought into practice. For example, it is possible there is a maximum angle of image capture beyond which the four point perspective transform function may not perform reliably. Or perhaps users will find white backgrounds made from certain materials will create glare and a similar thresholding error. Even with these limitations, the Leaf Area Tool has significant advantages over existing methods for leaf area measurement especially if dataset sizes are large. One major advantage is no scanner is required for capturing leaf images. Instead any smartphone or digital camera can be used. Also, any rectangular white background of known size can be used for image background and calibration, eliminating the need for cutting up large leaves by simply using a larger background. Perhaps most importantly, with the Leaf Area Tool

data processing is achieved using fully customizable open source software that is very fast and simple to use. Once images are analyzed, data is generated in the widely used CSV format. Though an internet connection is required to download the software, once downloaded it can be run offline using a lightweight portable computer in the field.

With further research the Leaf Area Tool for leaf image analysis could be improved in some key ways, expanding its utility. Work is already underway on some improvements including a project aimed at solving the troublesome issue of shadows. In this beta version of the Leaf Area Tool software, a very similar automated workflow is employed to isolate the white background, but after the perspective transform step a color version of the image is reintroduced, allowing for the use of a margin detection algorithm that can more easily distinguish between shadow and leaf pixels. Leaf area is then determined using the detected leaf shape without shadow and a similar pixel counting method. Another ongoing investigation is aimed at developing a non-destructive Leaf Area Tool pipeline. In this alternate pipeline the user would still capture images of leaves on a white background of known size, but the petiole of the still living leaf would cross the margin of the white background. The current approach for detecting the white background requires all four sides are uninterrupted, so in order to detect the white background the section of the petiole that crosses the background edge would need to be ignored or a new method for detecting the vertices of the white background would need to be developed. Another important addition to Leaf Area Tool would be more automated extraction of leaf parameters, enriching datasets with minimal impact of computation time. Possible parameters that could also be extracted using the current workflow include leaf length from leaf tip to petiole, width, perimeter, and even shape quantification metrics. If image resolution is suitable it may also be possible to add analysis of leaf tissue type and serration at the leaf margin, extracting parameters such as percent of diseased tissue, average serration angle, serration depth and width from peak to peak. Another interesting feature in development is the addition of a bubble sheet feature integrated into the white background. Not only would this

feature not affect the measurement protocol, apart from leaves needing to not occlude the bubbles, but it would give users the ability to encode images with important information at the moment of capture, requiring only an implement for marking and erasing bubbles. In the early tested versions, four variables of categorical information were encoded with bubbles and automatically extracted from leaf photos.

Though further research will be required to expand its applicability, the results presented here are strong evidence Leaf Area Tool is an accurate and high-throughput method for measuring leaf area. If shadows can be mitigated the tool explains 99.4% of the variation in ground truth leaf area, but even without adjusting for error caused by shadow the Leaf Area Tool software explains 94.4% of the variation in ground truth leaf area. The pipeline presented in this manuscript provides a useful tool to researchers and other users seeking to understand the functional differences between species and other populations through leaf area studies. Using only readily available equipment such as a smartphone camera, a sheet of white printer paper and a laptop with Leaf Area Tool software installed, users can extract an accurate measurement of leaf area from hundreds or thousands of images in a small fraction of the time once required for such a monumental task. Overall, this pipeline represents an important next step and presents a useful tool to researchers and other users.

Acknowledgements

This work was made possible through financial support from Till Guldimann and the Ernest Gallo Endowed Chair in Viticulture and Enology.

Author contributions

M.R.J. and D.LJ. conceptualized and coded the software. D.L.J. and F.C.L collected and analyzed all field data. M.R.J. wrote the manuscript with edits from all authors. D.E.B. provided funding and access to materials.

Summary

With each of the preceding chapters a new set of significant experiments are introduced, with each set aimed at addressing one of the aims outlined in my Qualifying Exam (QE) proposal several years ago. The following is a thorough discussion synthesizing and connecting results from all chapters in the context of the research goals outlined in my QE, and an overview of possible future directions.

The first aim of my QE is stated as, “test the three existing and promising models using additional data". The term “additional data” is used because some early data had already suggested the three HRI models might be useful for estimating single vine ET. In “Novel algorithms for high resolution prediction of canopy evapotranspiration in grapevine”, the results of a multi-year trial at RMI vineyard are presented to illustrate the performance of each of the three HRI models over a variety of environmental conditions including prolonged drought conditions, thereby addressing the first QE aim. Results showed the three HRI algorithms consistently performed well, with single vine ET rate predictions showing a strong linear relationship with ground truth (range in r^2 over three seasons CMT r^2 = 0.61 - 0.86; MB r^2 = 0.07 - 0.91; EM r^2 = 0.57 - 0.92). Though results were generally reasonable, the MB approach which includes two measurements of relative humidity and temperature was the most variable, likely due to the impact of sensor placement. While not sharply focused on addressing the goals of QE aim 1, Chapter 3 provides additional examples of the HRI method being applied, including in a commercial context.

The second aim, “define the plant-dependent coefficient in each of the models”, is a slightly more enigmatic goal. Though all three HRI models include a plant-dependent coefficient, also known as an area term (or A_s), only two of these models have a physical basis–CMT and MB. The third model, EM, was developed using purely statistical reasoning and therefore the area term in this model has an unknown meaning. In Chapter 1, the experimentally derived

trend in the area term is reported for the CMT and MB models over three seasons (Figure 1.6), providing early insight into the seasonal trend in area terms for each model. These early observations inspired Chapter 2 of this dissertation, "Quantifying vine size and morphology for the High Resolution Irrigation evapotranspiration models", which dives deeper into QE aim 2. As the title reveals, this paper focuses on the development of methods for directly estimating vine scaling terms and specifically tries to understand which vine morphological features correlate with model area terms. In this study vine physical characteristics were measured on a weekly basis throughout the season, then experimentally derived area terms were calculated at a similar rate throughout the season using ground truth data and HRI model estimates of ET. Results showed a similar pattern in all the vine physical parameters and area terms over the season (multiple r^2 0.58 - 0.80). Perhaps more importantly, the combined results of multiple linear regression and principal component analysis suggest a significant relationship between the MB and CMT area terms and vine physical parameters including canopy superficial area, canopy polygon area, and fPAR. Despite these findings further investigation will be required to extract an equation for direct calculation of model area terms from vine observations.

The stated research goals in Chapter 4, "Leaf Area Tool, open source pipeline for automated leaf area detection", also support QE aim 2, though indirectly. Leaf Area Tool was designed to balance laboratory precision and real-world applicability, addressing a critical gap in existing methodologies for measuring leaf area. Accurate measurement of leaf area serves as a cornerstone for understanding vital processes including photosynthesis, transpiration, plant growth, and could prove useful in the HRI pipeline if leaf area correlates with model area terms. To determine if the Leaf Area Tool image analysis pipeline is a field ready, fast and accurate method for the quantification of leaf area from images acquired with any digital camera, a test dataset was created. With a 12 megapixel smartphone camera 104 images of broad leaves from 12 different species of deciduous trees were captured and analyzed with the Leaf Area Tool. Without adjusting for the error caused by shadow the Leaf Area Tool pipeline still explains

more than 94% of the variation in ground truth leaf area; and with adjustments for shadow it explains more than 99%. Despite these very promising results, further research will be required to add important features such as shadow mitigation, a non-destructive process, and to expand the library of extractables. Nevertheless the Leaf Area Tool performs well on broad leaves and has significant advantages compared to other existing methods. Also, the putative physical meaning of the area term in the MB model is directly related to leaf area, therefore, adding the Leaf Area Tool to the collective toolbox of modern agriculture means testing this hypothesis may be possible in the near future.

The third QE aim is to “evaluate the system performance in a commercial setting”, a goal designed to test the HRI method in an environment representing the conditions that would be experienced in real, highly productive agricultural settings. The stated research goals of Chapter 3, “Comparing novel single vine sensors and algorithms for ET to lysimetric and eddy covariance ET”, align well with the goals of the third QE aim. In this study, low-cost Cube biometeorological sensors were first tested and verified as reasonable alternatives to much more expensive research grade reference sensors. Linear regression analysis revealed a strong relationship between Cube sensor values and reference values (r^2 0.84 - 0.99). Then, real data from the new Cube sensors captured on the RMI lysimeter vines was used to make HRI model calculations of ET and these were compared to load cell ground truth data (multiple r^2 0.44). After assessing the performance of Cube sensors in a research setting, Cube sensors were deployed in a commercial vineyard with a flux tower for two days during the 2022 growing season. In this section which most directly relates to the third QE aim, the correlation between flux tower ET calculated with the eddy covariance method and Cube sensor ET calculated with the three HRI models was also evaluated with linear regression (multiple r^2 0.051). Despite the lack of a notable correlation between eddy covariance and HRI calculated ET values, overall the results of Chapter 3 suggest a significant relationship between HRI model estimates of ET and ground truth ET; further evidence supporting both QE aims 1 and 3. Though indirect, Chapter 4,

also supports QE aim 3. The commercial viability of HRI depends on full-pipeline scalability, not just the scalability of sensing or water delivery, but also every small step in between. To this end Chapter 4 gives early insight into the types of technology that would need to be developed to rapidly and accurately estimate plant area terms in a frequent and likely automated process.

The three QE aims were meant to address the core research goal originally stated as "the development of a comprehensive single plant water use sensing and delivery system". Though the preceding dissertation chapters present the results of experiments designed to address these QE aims, and in doing so cover the development of a comprehensive water use *sensing* system, the results here fall short in terms of the development of novel water *delivery* systems. Chapters 1-4 cover the HRI water sensing system quite completely, with Chapter 1 introducing the three HRI models for calculating ET from simple biometeorological measurements. Then in the second chapter, the area terms in the MB and CMT models were examined more closely, expanding the generalizability of these models to other plants and potentially other plant types as well. Then, in Chapter 3 a new low-cost sensor system called the Cube is introduced and tested along with the HRI models in a commercial context, providing even more evidence to support the use of HRI for sensing single vine water use. Finally, with Chapter 4 a new tool is introduced that can help make measurements of leaf area faster and more accurate, improving the efficiency of the HRI method for sensing water use. Despite all of this progress, there is very little mention in the area of water *delivery* systems in this body of work. This can be largely attributed to events early in the history of the HRI project, when opportunities for a collaborative effort with Mark Burns' Lab at the University of Michigan-Ann Arbor allowed for the active development of water delivery systems to shift almost entirely to the Burns Lab. There, trained engineers with experience innovating in the flow sensor and flow control space could advance this aspect of the project more effectively. The Burns Lab had already collaborated with us, building all iterations of the Cube sensor, including the designing of a novel circuit with embedded biometeorological sensors and a custom 3D printed body. We

also submitted a US patent application together in 2022, with assistance from both University of Michigan and UC Davis technology transfer legal representatives and a law firm in Chicago, Illinois.

When the circumstances to continue working together on water delivery technology presented themselves, they were viewed as a welcome opportunity by those involved and were a natural fit in terms of expertise. This opportunity grew out from my interactions with ag-tech professionals at multiple conferences in 2022 and 2023. Sponsored by the UC Davis Innovation Institute in Food and Health fellowship program (cohort 9 alumni, 2021 Winter and Spring quarters), I was able to attend several major ag-tech events and generate 75+ customer discovery interactions, each focused on finding pathways to commercialization for the technology related to the HRI project. One of these interactions germinated into a healthy business relationship that has since sprouted into a presently ongoing collaboration, with regular meetings between all parties, and signed legal disclosures, all in an effort to fund a multi-year product development program for single plant irrigation hardware. Importantly, if the results from this multi-year partnership yield functional single plant irrigation hardware systems, and if the HRI models and Cube sensors continue to be improved along with automated water status sensing technologies such as sap flow (Lakso *et al.,* 2022b), then a closed-loop HRI system could be tested. In this ultimate HRI automation challenge, water use and plant water status information would flow directly from sensors to a computation unit that can control the flow of water to individual plants based on user programmed thresholds, thereby eliminating direct human interaction from the irrigation process.

In addition to the future goals mentioned in the Discussion section of Chapter 4 which relate specifically to the Leaf Area Tool software, the future research goals for the HRI project are important to continuing to ripen this promising technology. Generally speaking, these goals can be broken into two broad categories, (1) expanding the scope and understanding of the HRI method and (2) improving the commercial viability of the HRI method including Cube sensors. In

the former category, the first priority for future work would be to repeat an area term study using the four research lysimeter vines at RMI. The goal of this project would be to extract an equation for direct calculation of the area term in each HRI model from raw data such as digital images or 3D point clouds. In this expanded study focused on the parameters already found to have significant relationships with the MB and CMT model area terms, ideally a larger number of vines would be included, images would be collected at a higher frequency and other types of data would also be included, such as some third party LiDAR sensing and analysis pipelines (e.g. cite AgerPoint). In a separate effort but of perhaps equal or greater interest from the scientific community, the HRI method ought to be tested on other crops with structured canopies such as almonds or other nut crops. If the results of Chapters 1 and 2 were reproduced in another crop this would demonstrate the utility of the HRI approach outside of grapevine applications, and begin to shed light on the area term associations for a different cropping system. These experiments could, for example, be conducted using the lysimeter mounted almond trees currently operated by the Isaya Kisekka Lab at UC Davis. If these trees were mounted with Cube sensors or similar research grade biometeorological sensors, and lysimeter values were recorded over time, then multi-year HRI trials in almond could commence immediately.

Despite being rather unorthodox, the design of this dissertation project was guided by both scientific *and* commercial goals. Therefore the other major category for future research relates to the commercial viability of the HRI approach. If the HRI method is ever to be applied to any major crop, then a large number of water use sensors, water status sensors, water flow sensors and water valves will need to work in a seamlessly coordinated manner, all sharing power and communicating as needed. To have any chance of achieving this lofty vision in the near term, the issues of power and communications need to be addressed as soon as possible. As discussed in the introductory chapter, “A review of evapotranspiration estimation methods for high-value crop applications”, there are several options for providing power to large groups of

sensory or irrigation hardware 24 hours a day in harsh conditions. One potential option would be solar energy harvesting panels with lead-acid batteries, or alternatively smaller, more densely distributed lithium-iron-phosphate batteries. The potential for irrigation line integrated low power connected to the grid is also an attractive option, because a constant supply of power could be provided without any additional equipment.

However, even if power is available to all the irrigation equipment, in order for this equipment to function properly, delivering water only when conditions warrant, it is essential that spatially distributed devices can rapidly and reliably communicate with each other. In the case of powering irrigation valves with wires embedded in tubing, it would be possible to also include communication wiring in this tubing. This method would ensure devices communicate with each other and any central nodes, and data could be sent from any central nodes to control each device or many simultaneously. However, in the absence of irrigation tubing with embedded wires or a similar wired solution, low power wide area networks may provide the best option. Low power wide area networks are an ideal option for low power IoT devices in agricultural settings. Fortunately, power and communication will be thoroughly investigated in the ongoing collaboration between UC Davis, the University of Michigan-Ann Arbor and a commercial partner.

Assuming the collaboration is fruitful, a field ready single plant irrigation system will be developed and with this comes the possibility of a significant milestone in irrigation automation. That is, a closed loop system could be used to irrigate a crop, and even more to irrigate this crop in a spatially dynamic way that allows for all plants to maintain a more optimal water status throughout the entire lifecycle than similar crops irrigated with a standard block-level irrigation system. Testing a system exemplifying this zenith of operational autonomy in which crops thrive via irrigation controlled independent of human consultation, would set an important precedent for future innovation in irrigation technology. To achieve this test would require the integration of some method for measuring ground truth ET, likely lysimeter mounted plants, along with a low

cost water use sensing system such as Cube sensors and the HRI models, and also a method for measuring water status autonomously such as sap flow sensors. If lysimeters are used, not only can the accuracy of HRI model ET estimates be assessed, but also the accuracy of irrigation hardware in terms of water dispensing, allowing the quantification of any over or under watering. Though this hypothetical experiment would be an impressive proof of concept, the most exciting test of the HRI method will be the real users who may someday soon choose to start using this method in high-productivity agriculture contexts.

Bibliography

Adobe Inc. (2019). Adobe Photoshop. Retrieved from https://www.adobe.com/products/photoshop.html

AL-agele HA, Jashami H, Nackley L, Higgins C. A Variable Rate Drip Irrigation Prototype for Precision Irrigation. Agronomy. 2021; 11(12):2493. https://doi.org/10.3390/agronomy11122493

Albrecht, D. R., Bargmann, C. I. High-content behavioral analysis of Caenorhabditis elegans in precise spatiotemporal chemical environments. Nat. Methods, 8, 599-605 (2011).

Alfieri, J.G., Kustas, W.P., Prueger, J.H. et al., The vertical turbulent structure within the surface boundary layer above a Vineyard in California's Central Valley during GRAPEX. Irrig Sci 40, 481–496 (2022). https://doi.org/10.1007/s00271-022-00779-x

Allan, R.; Peirera, L.S.; Raes, D.; Smith, M. (1998). Crop Evapotranspiration—Guidelines for Computing Crop Water Requirements; FAO—Food and Agriculture Organization of the United Nations: Rome, Italy. ISBN 92-5-104219-5.

Allen, L. H. (1990). Plant responses to rising carbon dioxide and potential interactions with air pollutants. Journal of Environmental Quality, 19, 15–34.

Allison, G. B., Barnes, C. J., & Hughes, M. W. (1983). The distribution of deuterium and 18O in dry soils. Journal of Hydrology, 64, 377-379.

Anapalli, S. S., Ma, Y., Marek, G. W., Porter, D. O., Gowda, P. H., Howell, T. A., & Moorhead, J. E. (2018). Application of an energy balance method for estimating evapotranspiration in cropping systems. Agricultural Water Management, 204, 107–117.

Andales, A. A., Bauder, T. A., & Doesken, N. J. (2014). The Colorado Agricultural Meteorological Network (CoAgMet) and Crop ET Reports. Retrieved from www.ext.colostate.edu

Arrobas, M., Ferreira, I. Q., Freitas, S., Verdial, J., & Rodrigues, M. . (2014). Guidelines for fertilizer use in vineyards based on nutrient content of grapevine parts. Scientia Horticulturae, 172, 191–198. https://doi.org/10.1016/j.scienta.2014.04.016

Badr, G., Hoogenboom, G., Davenport, J., & Smithyman, J. (2015). Estimating growing season length using vegetation indices based on remote sensing: A case study for vineyards in Washington State. Transactions of the ASABE, 58(3), 551-564.

Bailey, B. N., & Mahaffee, W. F. (2017). Rapid measurement of the three-dimensional distribution of leaf orientation and the leaf angle probability density function using terrestrial LiDAR scanning. Remote Sensing of Environment, 194, 63–76. https://doi.org/10.1016/j.rse.2017.03.011

Bakr, E.M. (2005), A new software for measuring leaf area, and area damaged by Tetranychus urticae Koch. Journal of Applied Entomology, 129: 173-175. https://doi.org/10.1111/j.1439-0418.2005.00948.x

Baldocchi, D. D. (1997). Flux footprints within and over forest canopies. Boundary-Layer Meteorology, 85, 273-292.

Balendonck, J., Sapounas, A. A., Kempkes, F., Van Os, E. A., Van Der Schoor, R., Van Tuijl, B. A. J., & Keizer, L. C. P. (2014). Using a wireless sensor network to determine climate heterogeneity of a greenhouse environment. Acta Horticulturae, 1037, 539–546. https://doi.org/10.17660/ActaHortic.2014.1037.67

Bambach, N., Kustas, W., Alfieri, J., et al., (2022). Evapotranspiration uncertainty at micrometeorological scales: The impact of the eddy covariance energy imbalance and correction methods. Irrigation Science. https://doi.org/10.1007/s00271-022-00783-1

Bambach, N., Kustas, W., Alfieri, J., et al., (2022b). Inter-annual variability of land surface fluxes across vineyards: The role of climate, phenology, and irrigation management. Irrigation Science. https://doi.org/10.1007/s00271-022-00784-0

Bastiaanssen, W. G. M., Menenti, M., Feddes, R. A., & Holtslag, A. A. M. (1998). A remote sensing surface energy balance algorithm for land (SEBAL): 1. Formulation. Journal of Hydrology, 212–213, 198–212.

Behboudian, M. H., & Singh, Z. (2001). Water Relations and Irrigation Scheduling in Grapevine. In Horticultural Reviews (pp. 189–225). John Wiley & Sons, Ltd. https://doi.org/10.1002/9780470650813.ch5

Berger, B., Parent, B., Tester, M. High-throughput shoot imaging to study drought responses. J. Exp. Bot., 61, 3519-3528 (2010).

Berti, A., Tardivo, G., Chiaudani, A., Rech, F., & Borin, M. (2014). Assessing reference evapotranspiration by the Hargreaves method in north-eastern Italy. Agricultural Water Management, 140, 20–25.

Bird, R. B., Stewart, W. E., & Lightfoot, E. N. (2006). Transport Phenomena. John Wiley & Sons. https://doi.org/10.1002/aic.690070245

Blanco, V., & Kalcsits, L. (2021). Microtensiometers Accurately Measure Stem Water Potential in Woody Perennials. Plants, 10(12), 2780. MDPI AG. Retrieved from http://dx.doi.org/10.3390/plants10122780

Borevitz, J. O. Natural genetic variation for growth and development revealed by high-throughput phenotyping in Arabidopsis thaliana. G3 (Bethesda), 2, 29-34 (2012).

Bramley, R. G. V., Proffitt, A. P. B., Hinze, C. J., Pearse, B., & Hamilton, R. P. (2005). Generating benefits from precision viticulture through selective harvesting. In J. V. Stafford (Ed.), Proceedings of the 5th European Conference on Precision Agriculture (pp. 891–898). Wageningen Academic Publishers.

Bravdo, B. (1986). Water management and effect on fruit quality in grapevines. Proceedings of the 6th Australian wine industry technical conference, 1(9), 150-158. https://awitc.com.au/program/proceedings/sixth-australian-wine-industry-technical-conference/

Brown, P. W., & Yitayew, M. (1988). Near-real time weather information for irrigation management in Arizona. In Planning Now for Irrigation and Drainage in the 21st Century (pp. 708-715). ASCE.

Brillante, L., Bois, B., Lévêque, J., & Mathieu, O. (2016). Variations in soil-water use by grapevine according to plant water status and soil physical-chemical characteristics—A 3D spatio-temporal analysis. European Journal of Agronomy, 77, 122–135. https://doi.org/10.1016/j.eja.2016.04.004

Burchard-Levine, V., Nieto, H., Kustas, W. P., et al., (2022). Application of a remote-sensing three-source energy balance model to improve evapotranspiration partitioning in vineyards. Irrigation Science, 40, 593–608. https://doi.org/10.1007/s00271-022-00787-x

Bylesjö M, Segura V, Soolanayakanahally RY, Rae AM, Trygg J, Gustafsson P, Jansson S, Street NR (2008) LAMINA: a tool for rapid quantification of leaf size and shape parameters. BMC Plant Biol 8:82–89. doi:10.1186/1471-2229-8-82

California Department of Food and Agriculture in cooperation with USDA National Agricultural Statistics Service. (2021). Grape Acreage Report 2021. 34(1). 2-4. https://www.nass.usda.gov/Statistics_by_State/California/Publications/Specialty_and_Other_Releases/Grapes/Acreage/2022/2021gabtb.pdf

California Department of Food and Agriculture in cooperation with USDA National Agricultural Statistics Service. (2022). Grape Acreage Report 2022. 34(1). 2-4. https://www.nass.usda.gov/Statistics_by_State/California/Publications/Specialty_and_Other_Releases/Grapes/Acreage/Reports/2022GrapeAcreageReport.pdf

Cabibel, B., & Isberie, C. (1997). Flux de sève et alimentation hydrique de cerisiers irrigués ou non en localisation. Agronomie, 17, 97–112.

Chaudhary, P., Godara, S., Cheeran, A. N., & Chaudhari, A. K. (2012). Fast and accurate method for leaf area measurement. Int. J. comput. appl, 49(9), 22-25.

Chaves, M. M., Santos, T. P., Souza, C. R., Ortuño, M. F., Rodrigues, M. L., Lopes, C. M., Maroco, J. P., & Pereira, J. S. (2007). Deficit irrigation in grapevine improves water use efficiency while controlling vigour and production quality. Annals of Applied Biology, 150(2), 237-252. https://doi.org/10.1111/j.1744-7348.2006.00123.x

Chu, H., Luo, X., Ouyang, Z., et al., (2021). Representativeness of Eddy-Covariance flux footprints for areas surrounding AmeriFlux sites. Agricultural and Forest Meteorology, 301–302, 108350. https://doi.org/10.1016/j.agrformet.2021.108350

Cleugh, H. A., Leuning, R., Mu, Q., & Running, S. W. (2007). Regional evaporation estimates from flux tower and MODIS satellite data. Remote Sensing of Environment, 106, 285–304.

Cohen, M., Goldhamer, D., Fereres, E., Girona, J., & Mata, M. (2001). Assessment of peach tree responses to irrigation water deficits by continuous monitoring of trunk diameter changes. Journal of Horticultural Science & Biotechnology, 76, 55–60.

Cussler, E. L. (2009). Diffusion: Mass Transfer in Fluid Systems. Cambridge University Press. https://doi.org/10.1017/CBO9780511805134

Datta, S., Taghvaeian, S., & Stivers, J. (2017). Understanding Soil Water Content and Thresholds for Irrigation Management. Oklahoma Cooperative Extension Service: Stillwater, OK, USA.

Dayer, S., Reingwirtz, I., McElrone, A. J., & Gambetta, G. A. (2019). Response and Recovery of Grapevine to Water Deficit: From Genes to Physiology. In D. Cantu & M. A. Walker (Eds.), The Grape Genome (pp. 223–245). Springer International Publishing. https://doi.org/10.1007/978-3-030-18601-2_11

Díaz, S., Kattge, J., Cornelissen, J. H. C., Wright, I. J., Lavorel, S., Dray, S., … Gorné, L. D. (2016). The global spectrum of plant form and function. Nature, 529, 167–171.

Diffenbaugh, N. S., Swain, D. L., & Touma, D. (2015). Anthropogenic warming has increased drought risk in California. Proceedings of the National Academy of Sciences, 112(13), 3931–3936. https://doi.org/10.1073/pnas.1422385112

Documentation Lysimeter Station Michalovce. Groundwater Principle Michalovce. Umwelt-Geräte-Technik GmbH: Müncheberg. 2014. Available online: http://www.ugt-online.de (accessed on 5 July 2023).

Donatelli, M., Bellocchi, G., & Carlini, L. (2006). Sharing knowledge via software components: Models on reference evapotranspiration. European Journal of Agronomy, 24, 186–192.

Donovan, L., Linton, M., & Richards, J. (2001). Predawn plant water potential does not necessarily equilibrate with soil water potential under well-watered conditions. Oecologia, 129, 328–335. https://doi.org/10.1007/s004420100738

Doorenbos, J., & Pruitt, W. O. (1977). Crop evapotranspiration. FAO Irrigation and Drainage Paper No. 24, FAO, Rome, Italy.

Easlon, H.M. and Bloom, A.J. (2014), Easy Leaf Area: Automated digital image analysis for rapid and accurate measurement of leaf area. Applications in Plant Sciences, 2: 1400033. https://doi.org/10.3732/apps.1400033

Eshonkulov, R., Poyda, A., Ingwersen, J., et al., (2019). Evaluating multi-year, multi-site data on the energy balance closure of eddy-covariance flux measurements at cropland sites in southwestern Germany. Biogeosciences, 16, 521–540. https://doi.org/10.5194/bg-16-521-2019

Ewaid, S. H., Abed, S. A., & Al-Ansari, N. (2019). Water footprint of wheat in Iraq. Water, 11(3), 535.

FAO – Food and Agriculture Organization of the United Nations. (2014). Did you know …? Facts and figures about. http://www.fao.org/nr/water/aquastat/didyouknow/index3.stm (last access: 24 November 2016).

Fernández, E., & Testi, L. (2017). Methods to Estimate Sap Flow. ISHS Working Group on Sap Flow, 9(1). Article 09. https://www.ishs.org/sites/default/files/documents/methods_0.pdf

Fisher, J. B., Tu, K. P., & Baldocchi, D. D. (2008). Global estimates of the land-atmosphere water flux based on monthly AVHRR and ISLSCP-II data, validated at 16 FLUXNET sites. Remote Sensing of Environment, 112, 901–919.

Foley, J. A., Ramankutty, N., Brauman, K. A., Cassidy, E. S., Gerber, J. S., Johnston, M., et al., (2011). Solutions for a cultivated planet. Nature, 478(7369), 337–342. https://doi.org/10.1038/nature10452

Fortunel C, Fine PV, Baraloto C (2012) Leaf, stem and root tissue strategies across 758 neotropical tree species. Funct Ecol 26:1153–1161. doi:10.1111/j.1365-2435.2012.02020.x

Fulton, A., Grant, J., Buchner, R., & Connell, J. (2014). Using the pressure chamber for irrigation management in Walnut, Almond and Prune. UC ANR. https://doi.org/10.3733/ucanr.8503

Fulton, J., Norton, M., & Shilling, F. (2019). Water-indexed benefits and impacts of California almonds. Ecological Indicators, 96, 711–717. https://doi.org/10.1016/j.ecolind.2017.12.063

Furbank, R. T., Tester, M. Phenomics--technologies to relieve the phenotyping bottleneck. Trends Plant Sci., 16, 635-644 (2011)

Fynn, R. P., Al-shooshan, A., Short, T. H., & McMahon, R. W. (1993). Evapotranspiration Measurement and Modeling for a Potted Chrysanthemum Crop. Transactions of the ASAE, 36, 1907–1913.

Ganchev, D. (2023). A Rapid Measurement Method for Canopy Porosity of Orchard Crops. International Journal of Agriculture and Animal Production(IJAAP) ISSN 2799-0907, 3(05), Article 05. https://doi.org/10.55529/ijaap.35.1.7

Gatti, M., Garavani, A., Squeri, C., et al., (2022). Effects of intra-vineyard variability and soil heterogeneity on vine performance, dry matter and nutrient partitioning. Precision Agriculture, 23, 150–177. https://doi.org/10.1007/s11119-021-09831-w

Gatti, M., Garavani, A., Vercesi, A., & Poni, S. (2017). Ground-truthing of remotely sensed within-field variability in a cv. Barbera plot for improving vineyard management. Australian Journal of Grape and Wine Research, 23(3), 399–408. https://doi.org/10.1111/ajgw.12286

Gao, J., Guo, G., Guo, Y., & Wang, X. (2011). Measuring plant leaf area by scanner and ImageJ software. China Vegetables, (2), 73-77.

Geisel, P., Farnham, D., & Vossen, P. (2002). California Master Gardener Handbook (3338th ed.). University of California, Division of Agriculture and Natural Resources.

Gharsallah, O., Facchi, A., & Gandolfi, C. (2013). Comparison of six evapotranspiration models for a surface irrigated maize agro-ecosystem in Northern Italy. Agricultural Water Management, 130, 119–130.

Ghiat, I., Mackey, H. R., & Al-Ansari, T. (2021). A Review of Evapotranspiration Measurement Models, Techniques and Methods for Open and Closed Agricultural Field Applications. Water, 13, 2523. https://doi.org/10.3390/w13182523

Gómez-Candón, D., Bellvert, J., & Royo, C. (2021). Performance of the Two-Source Energy Balance (TSEB) Model as a Tool for Monitoring the Response of Durum Wheat to Drought by High-Throughput Field Phenotyping. Frontiers in Plant Science, 12. https://www.frontiersin.org/articles/10.3389/fpls.2021.658357

Granier, A. (1985). Une nouvelle méthode pour la mesure du flux de sève brute dans le tronc des arbres. Annales des Sciences Forestières, 42(2), 193–200. https://doi.org/10.1051/forest:19850204

Green, S. R., & Clothier, B. E. (1988). Water use of kiwifruit vines and apple trees by the heat-pulse technique. Journal of Experimental Botany, 39, 115–123.

Hargreaves, G. H., & Allen, R. G. (2003). History and Evaluation of Hargreaves Evapotranspiration Equation. Journal of Irrigation and Drainage Engineering, 129, 53–63.

Hargreaves, G. H., & Samani, Z. A. (1985). Reference Crop Evapotranspiration From Ambient Air Temperature. Paper presented at the American Society of Agricultural Engineering Annual International Meeting, Chicago, IL, USA, 96–99.

Hassoun, J., Bonaccorso, F., Agostini, M., Angelucci, M., Betti, M. G., Cingolani, R., ... & Scrosati, B. (2014). An advanced lithium-ion battery based on a graphene anode and a lithium iron phosphate cathode. Nano letters, 14(8), 4901-4906.

Herman, M.R.; Nejadhashemi, A.P.; Abouali, M.; Hernandez-Suarez, J.S.; Daneshvar, F.; Zhang, Z.; Anderson, M.C.; Sadeghi, A.M.; Hain, C.R.; Sharifi, A. Evaluating the role of evapotranspiration remote sensing data in improving hydrological modeling predictability. J. Hydrol. 2018, 556, 39–49.

Hirschi, M., Michel, D., Lehner, I., & Seneviratne, S. I. (2017). A site-level comparison of lysimeter and eddy covariance flux measurements of evapotranspiration. Hydrology and Earth System Sciences, 21, 1809–1825. https://doi.org/10.5194/hess-21-1809-2017

Hochberg, U., Herrera, J., Degu, A., Castellarin, S. D., Peterlunger, E., Alberti, G., & Lazarovitch, N. (2017). Evaporative demand determines the relative transpirational sensitivity of deficit-irrigated grapevines. Irrigation Science, 35. https://doi.org/10.1007/s00271-016-0518-4

Hough, M. N., & Jones, R. J. A. (1997). The United Kingdom Meteorological Office rainfall and evaporation calculation system: MORECS version 2.0-an overview. Hydrology and Earth System Sciences, 1(2), 227-239.

Howitt, R. E., MacWan, D., Medellin-Azuara, J., Lund, J. R., & Sumner, D. A. (2015). Economic analysis of the 2015 drought for California agriculture. Center for Watershed Sciences, University of California–Davis. Retrieved from: https://watershed.ucdavis.edu/files/biblio/DroughtReport_23July2014_0.pdf

Hu, X., Shi, L., Lin, G., & Lin, L. (2021). Comparison of physical-based, data-driven and hybrid modeling approaches for evapotranspiration estimation. Journal of Hydrology, 601, 126592.

Huguet, J. G., Li, S. H., Lorendeau, J. Y., & Pelloux, G. (1992). Specific micromorphometric reactions of fruit trees to water stress and irrigation scheduling automation. Journal of Horticultural Science, 67, 631–640.

Idowu, O., Ndede, E. O., Kurebito, S., Tokunari, T., & Jindo, K. (2023). Effect of the Interaction between Wood Vinegar and Biochar Feedstock on Tomato Plants. Journal of Soil Science and Plant Nutrition, 23(2), 1599–1610. https://doi.org/10.1007/s42729-023-01227-1

Jackson, J. L., Morgan, K. T., & Lusher, W. R. (2008, December). Citrus cold weather protection and irrigation scheduling tools using Florida automated weather network data. In Proceedings of the Florida State Horticultural Society (Vol. 121, pp. 75-80).

Jägermeyr, J., Pastor, A., Biemans, H., & Gerten, D. (2017). Reconciling irrigated food production with environmental flows for sustainable development goals implementation. Nature Communications, 8(1), 15900. https://doi.org/10.1038/ncomms15900

Jenkins, M. R., Lenczewski-Jowers, D., Chavez Lamas, F., Miller, K., Nikzad, S., Gilbert, M., Burns, M., & Block, D. E. (2024). The impact of size and morphology on single vine evapotranspiration predictions. Ready For Submission.

Jenkins, M. R., Mannsfeld, A., Nikzad, S., Lambert, J.-J., Miller, K., Burns, M., Earles, J. M., & Block, D. E. (2023). Novel algorithms for high resolution prediction of canopy evapotranspiration in grapevine. OENO One.

Kandra, B., Tall, A., Gomboš, M., & Pavelková, D. (2023). Quantification of Evapotranspiration by Calculations and Measurements Using a Lysimeter. Water, 15(2), 373. https://doi.org/10.3390/w15020373

Katabuchi M, Kurokawa H, Davies SJ, Tan S, Nakashizuka T (2012) Soil resource availability shapes community trait structure in a species-rich dipterocarp forest. J Ecol 100:643–651. doi:10.1111/j.1365-2745.2011.01937.x

Katabuchi, M. LeafArea: an R package for rapid digital image analysis of leaf area. Ecol Res 30, 1073–1077 (2015). https://doi.org/10.1007/s11284-015-1307-x

Katsoulas, N., & Stanghellini, C. (2019). Modelling crop transpiration in greenhouses: Different models for different applications. Agronomy, 9, 392.

Kattge, J., Díaz, S., Lavorel, S., Prentice, I. C., Leadley, P., Bönisch, G., … Wright, I. J. (2011). TRY - A global database of plant traits. Global Change Biology, 17, 2905–2935.

Kisekka, I. (2023). Orchard Water Management. In S. G. Vougioukas & Q. Zhang (Eds.), Advanced Automation for Tree Fruit Orchards and Vineyards (pp. 3). Agriculture Automation and Control. Springer, Cham. https://doi.org/10.1007/978-3-031-26941-7_3

Kluyver, T., Ragan-Kelley, B., Fernando Pérez, Granger, B., Bussonnier, M., Frederic, J., … Willing, C. (2016). Jupyter Notebooks – a publishing format for reproducible computational

workflows. In F. Loizides & B. Schmidt (Eds.), Positioning and Power in Academic Publishing: Players, Agents and Agendas (pp. 87–90).

Kogan, F., Guo, W., & Yang, W. (2019). Drought and food security prediction from NOAA new generation of operational satellites. Geomatics, Natural Hazards and Risk, 10(1), 651–666. https://doi.org/10.1080/19475705.2018.1541257

Ko-Madden, C. T., Upadhyaya, S. K., Kizer, E. E., Drechsler, K. M., Rojo, F., Meyers, J. N., & Schramm, A. E. (2017). Precision irrigation in wine grape using a proximal leaf monitor system for measuring plant water status. In 2017 ASABE Annual International Meeting (p. 1). American Society of Agricultural and Biological Engineers.

Kraft NJB, Valencia R, Ackerly DD (2008) Functional traits and niche-based tree community assembly in an Amazonian forest. Science 322:580–582. doi:10.1126/science.1160662

Kumari, N., & Srivastava, A. (2020). An Approach for Estimation of Evapotranspiration by Standardizing Parsimonious Method. Agricultural Research, 9, 301–309.

Kustas, W. P. (1990). Estimates of evapotranspiration with a one-layer and 2-layer model of heat-transfer over partial canopy cover. Journal of Applied Meteorology, 29, 704–715.

Kustas, W., & Anderson, M. (2009). Advances in thermal infrared remote sensing for land surface modeling. Agricultural and Forest Meteorology, 149(12), 2071–2081. https://doi.org/10.1016/j.agrformet.2009.05.016

Kustas, W. P., McElrone, A. J., Agam, N., et al., (2022). From vine to vineyard: the GRAPEX multi-scale remote sensing experiment for improving vineyard irrigation management. Irrigation Science, 40, 435–444. https://doi.org/10.1007/s00271-022-00816-9

Kustas, W., Nieto, H., Garcia-Tejara, O., et al., (2022b). Impact of advection on two-source energy balance (TSEB) canopy transpiration parameterization for vineyards in the California Central Valley. Irrigation Science. https://doi.org/10.1007/s00271-022-00778-y

Kyaw Tha Paw U, Qiu, J., Su, H.-B., Watanabe, T., & Brunet, Y. (1995). Surface renewal analysis: A new method to obtain scalar fluxes. Agricultural and Forest Meteorology, 74(1), 119–137. https://doi.org/10.1016/0168-1923(94)02182-J

Lakso, A. N., Santiago, M., & Stroock, A. D. (2022). Monitoring Stem Water Potential with an Embedded Microtensiometer to Inform Irrigation Scheduling in Fruit Crops. Horticulturae, 8, 1207. https://doi.org/10.3390/horticulturae8121207

Lakso, A. N., Zhu, S., Santiago, M., Shackel, K., Volkov, V., & Stroock, A. D. (2022b). A microtensiometer sensor to continuously monitor stem water potentials in woody plants – design and field testing. Acta Hortic, 1335, 317-324. DOI: 10.17660/ActaHortic.2022.1335.39

Lalle, Y., Fourati, L. C., Fourati, M., & Barraca, J. P. (2019). A comparative study of LoRaWAN, SigFox, and NB-IoT for smart water grid. Proc. Global Inf. Infrastruct. Netw. Symp. (GIIS), pp. 1-6.

Lama, S., Leiva, F., Vallenback, P., Chawade, A., & Kuktaite, R. (2023). Impacts of heat, drought, and combined heat–drought stress on yield, phenotypic traits, and gluten protein traits: Capturing stability of spring wheat in excessive environments. Frontiers in Plant Science, 14. https://www.frontiersin.org/articles/10.3389/fpls.2023.1179701

Lambert J, Anderson M, Wolpert J. 2008. Vineyard nutrient needs vary with rootstocks and soils. Calif Agr 62(4):202-207. https://doi.org/10.3733/ca.v062n04p202.

Lascano, R. J. (2000). A General System to Measure and Calculate Daily Crop Water Use. Agronomy Journal, 92(5), 821–832. https://doi.org/10.2134/agronj2000.925821x

Lascano, R. J., Goebel, T. S., Booker, J., Baker, J. T., & Iii, D. C. G. (2016). The Stem Heat Balance Method to Measure Transpiration: Evaluation of a New Sensor. Agricultural Sciences, 07(09), Article 09. https://doi.org/10.4236/as.2016.79057

Lauridsen, M., Nguyen, H., Vejlgaard, B., Kovacs, I. Z., Mogensen, P., Sorensen, M. (2017). Coverage comparison of GPRS, NB-IoT, LoRa, and SigFox in a 7800 km area. Proc. IEEE 85th Veh. Technol. Conf., pp. 1-5.

Lavoie-Lamoureux, A., Sacco, D., Risse, P.-A., & Lovisolo, C. (2017). Factors influencing stomatal conductance in response to water availability in grapevine: A meta-analysis. Physiologia Plantarum, 159(4), 468–482. https://doi.org/10.1111/ppl.12530

Lhomme, J. P. (1997). A theoretical basis for the Priestley-Taylor coefficient. Boundary-Layer Meteorology, 82, 179–191.

Li, S., Kang, S., Li, F., & Zhang, L. (2008). Evapotranspiration and crop coefficient of spring maize with plastic mulch using eddy covariance in northwest China. https://doi.org/10.1016/j.agwat.2008.04.014

Li, X., Kang, S., Niu, J., Huo, Z., & Liu, J. (2019). Improving the representation of stomatal responses to CO2 within the Penman–Monteith model to better estimate evapotranspiration responses to climate change. Journal of Hydrology, 572, 692–705.

Li, Z., Roy, D., Zhang, H., Vermote, E., & Huang, H. (2019b). Evaluation of Landsat-8 and Sentinel-2A Aerosol Optical Depth Retrievals across Chinese Cities and Implications for Medium Spatial Resolution Urban Aerosol Monitoring. Remote Sensing, 11(2), 122.

Liberg, O., Sundberg, M., Johan, E. W., & Sachs, B. J. (2017). Cellular Internet of Things: Technologies Standards and Performance. Elsevier, Amsterdam, The Netherlands.

Llamas, M. R., & Martínez-Santos, P. (2005). Intensive Groundwater Use: Silent Revolution and Potential Source of Social Conflicts. Journal of Water Resources Planning and Management, 131(5), 337–341. https://doi.org/10.1061/(ASCE)0733-9496(2005)131:5(337)

Long, D., Longuevergne, L., & Scanlon, B. R. (2014). Uncertainty in evapotranspiration from land surface modeling, remote sensing, and GRACE satellites. Water Resources Research, 50, 1131–1151.

Malik, A., Kumar, A., & Kisi, O. (2017). Monthly pan-evaporation estimation in Indian central Himalayas using different heuristic approaches and climate-based models. Computers and Electronics in Agriculture, 143, 302–313. https://doi.org/10.1016/j.compag.2017.11.008

Maloof JN, Nozue K, Mumbach MR, Palmer CM (2013) LeafJ: an ImageJ plugin for semi-automated leaf shape measurement. JoVE. doi:10.3791/50028

Mancha, L., Uriarte, D., & Prieto, M. (2021). Characterization of the Transpiration of a Vineyard under Different Irrigation Strategies Using Sap Flow Sensors. Water, 13(20), 2867. MDPI AG. Retrieved from http://dx.doi.org/10.3390/w13202867

Marini, R., Mikhaylov, K., Pasolini, G., & Buratti, C. (2022). Low-Power Wide-Area Networks: Comparison of LoRaWAN and NB-IoT Performance. IEEE Internet of Things Journal, 9(21), 21051-21063. doi: 10.1109/JIOT.2022.3176394.

Martínez-Maldonado, F. E., Castaño-Marín, A. M., Góez-Vinasco, G. A., & Marin, F. R. (2022). Upscaling Gross Primary Production from Leaf to Canopy for Potato Crop (Solanum tuberosum L.). Climate, 10(9), 127. https://doi.org/10.3390/cli10090127

Matese, A., & Di Gennaro, S. F. (2015). Technology in precision viticulture: A state of the art review. International Journal of Wine Research, 7, 69–81. https://doi.org/10.2147/IJWR.S69405

Meier, J., Zabel, F., & Mauser, W. (2018). A global approach to estimate irrigated areas – a comparison between different data and statistics. Hydrology and Earth System Sciences, 22, 1119–1133. https://doi.org/10.5194/hess-22-1119-2018

Mikhailova, A., & Friedman, D. (2018). Partner Pen Play in Parallel (PPPiP): A New PPPiParadigm for Relationship Improvement. Arts, 7(3), 39. MDPI AG. Retrieved from http://dx.doi.org/10.3390/arts7030039

Miller, K., Jenkins, M. R., Nikzad, S., Block, D. E., Mannsfeld, A., Nadra, I., Pritchard, Z., Lin, W.-C., Burns, M., & Johnson, B. (2023). Apparatus and Method for Detecting Evapotranspiration (PCT Patent Application).

Monteith, J. L., Szeicz, G., & Waggoner, P. E. (1965). The Measurement and Control of Stomatal Resistance in the Field. Journal of Applied Ecology, 2, 345.

Mu, Q., Heinsch, F. A., Zhao, M., & Running, S. W. (2007). Development of a global evapotranspiration algorithm based on MODIS and global meteorology data. Remote Sensing of Environment, 111, 519–536.

Mullins, C. (2001). Matric potential. In Soil and environmental analysis: Physical methods (2nd ed., pp. 17-30). Marcel Dekker. https://doi.org/10.1201/9780203908600.ch2

Netzer, Y., Yao, C., Shenker, M., Bravdo, B.-A., & Schwartz, A. (2009). Water use and the development of seasonal crop coefficients for Superior Seedless grapevines trained to an open-gable trellis system. Irrig. Sci., 27, 109–120. https://doi.org/10.1007/s00271-008-0124-1

Nobel, P. S. (2005). Physicochemical and Environmental Plant Physiology. Academic Press.

Norman, J. M., Kustas, W. P., & Humes, K. S. (1995). A two-source approach for estimating soil and vegetation energy fluxes from observations of directional radiometric surface temperature. Agricultural and Forest Meteorology, 77, 263–293.

Ohana-Levi, N., Gao, F., Knipper, K., et al., (2022). Time-series clustering of remote sensing retrievals for defining management zones in a vineyard. Irrigation Science, 40, 801–815. https://doi.org/10.1007/s00271-021-00752-0

Olenskyj, A., Sams, B., Fei, Z., Singh, V., Raja, P., Bornhorst, G., & Earles, J. M. (2022). End-to-end deep learning for directly estimating grape yield from ground-based imagery. arXiv. https://arxiv.org/abs/2208.02394

Orlando, F., Movedi, E., Coduto, D., Parisi, S., Brancadoro, L., Pagani, V., Guarneri, T., & Confalonieri, R. (2016). Estimating Leaf Area Index (LAI) in Vineyards Using the PocketLAI Smart-App. Sensors (Basel, Switzerland), 16(12). https://doi.org/10.3390/s16122004

Ortega-Farias, S., Poblete-Echeverrıa, C., & Brisson, N. (2010). Parameterization of a two-layer model for estimating vineyard evapotranspiration using meteorological measurements. Agricultural and Forest Meteorology, 150, 276–286.

Ortuño, M. F., García-Orellana, Y., Conejero, W., et al., (2006). Stem and leaf water potentials, gas exchange, sap flow, and trunk diameter fluctuations for detecting water stress in lemon trees. Trees, 20, 1–8. https://doi.org/10.1007/s00468-005-0004-8

Osnas JLD, Lichstein JW, Reich PB, Pacala SW (2013) Global leaf trait relationships: mass, area, and the leaf economics spectrum. Science 340:741–744. doi:10.1126/science.1231574

Otsu, Nobuyuki (1979). "A threshold selection method from gray-level histograms". IEEE Transactions on Systems, Man, and Cybernetics. 9 (1): 62–66. doi:10.1109/TSMC.1979.4310076

Pagay, V. (2022). Evaluating a novel microtensiometer for continuous trunk water potential measurements in field-grown irrigated grapevines. Irrigation Science, 40, 45–54. https://doi.org/10.1007/s00271-021-00758-8

Parkinson, K. J., Day, W., & Leach, J. E. (1980). A Portable System for Measuring the Photosynthesis and Transpiration of Graminaceous Leaves. Journal of Experimental Botany, 31(5), 1441–1453. https://doi.org/10.1093/jxb/31.5.1441

Penman, H. L. (1948). Natural evaporation from open water, bare soil and grass. Proceedings of the Royal Society of London. Series A. Mathematical and Physical Sciences, 193, 120–145.

Pereira, A. R., & Villa Nova, N. A. (1992). Analysis of the Priestley-Taylor parameter. Agricultural and Forest Meteorology, 61(1), 1–9. https://doi.org/10.1016/0168-1923(92)90021-U

Persia, S., Carciofi, C., & Faccioli, M. (2017). NB-IoT and LoRA connectivity analysis for M2M/IoT smart grids applications. Proceedings of the IEEE AEIT International Annual Conference, pp. 1-6.

Pokovai, K.; Fodor, N. (2019). Adjusting Ceptometer Data to Improve Leaf Area Index Measurements. Agronomy, 9, 866.

PP Systems. (n.d.). CIRAS-4 Portable Photosynthesis System. Available online: https://ppsystems.com/ciras4-portable-photosynthesis-system/ (accessed on 22 July 2023).

Prenger, J., Fynn, R., & Hansen, R. (2002). A comparison of four evapotranspiration models in a greenhouse environment. Transactions of the ASAE, 45, 1779.

Priestley, C. H. B., & Taylor, R. J. (1972). On the assessment of surface heat flux and evaporation using large-scale parameters. Monthly Weather Review, 100, 81–92.

Pruitt, W. O., & Doorenbos, J. (1977). Empirical calibration, a requisite for evapotranspiration formulae based on daily or longer mean climatic data? ICID Conference on Evapotranspiration, Budapest, Hungary, 20 pp.

R Core Team. (2018). R: A language and environment for statistical computing. R Foundation for Statistical Computing. https://www.r-project.org/

Reyes-González, A., Kjaersgaard, J., Trooien, T., Reta-Sánchez, D. G., Sánchez-Duarte, J. I., Preciado-Rangel, P., & Fortis-Hernández, M. (2019). Comparison of Leaf Area Index, Surface

Temperature, and Actual Evapotranspiration Estimated Using the METRIC Model and In Situ Measurements. Sensors, 19, 1857.

Ribeiro, L., Tokikawa, D., Rebelatto, J., & Brante, G. (2020). Comparison between LoRa and NB-IoT coverage in urban and rural Southern Brazil regions. Annals of Telecommunications, 75, 755-766.

Rienth, M., & Scholasch, T. (2019). State-of-the-art of tools and methods to assess vine water status. OENO One, 53.

Rogers, G. K. (2023). Comparative ecology of two closely associated scrub-dominating oaks in South Florida: Quercus myrtifolia and Q. geminata (Fagaceae). Flora, 298, 152201. https://doi.org/10.1016/j.flora.2022.152201

Safre, A., Nassar, A., Torres-Rua, A., et al., (2022). Performance of Sentinel-2 SAFER ET model for daily and seasonal estimation of grapevine water consumption. Irrigation Science. https://doi.org/10.1007/s00271-022-00810-1

Salmon, J. M., Friedl, M. A., Frolking, S., Wisser, D., & Douglas, E. M. (2015). Global rain-fed, irrigated, and paddy croplands: A new high-resolution map derived from remote sensing, crop inventories, and climate data. International Journal of Applied Earth Observation and Geoinformation, 38, 321-334.

Salter, W. T., Gilbert, M. E., & Buckley, T. N. (2018). A multiplexed gas exchange system for increased throughput of photosynthetic capacity measurements. Plant Methods, 14, 80. https://doi.org/10.1186/s13007-018-0347-y

Saugier, B., Granier, A., Pontailler, J. Y., Dufrene, E., & Baldocchi, D. D. (1997). Transpiration of a boreal pine forest measured by branch bag, sap flow, and micrometeorological methods. Tree Physiology, 17, 511-519.

Schaap, M. G., Leij, F. J., & Van Genuchten, M. T. (2001). Rosetta: A computer program for estimating soil hydraulic parameters with hierarchical pedotransfer functions. Journal of Hydrology, 251, 163-176.

Schindelin, J., Arganda-Carreras, I., Frise, E., Kaynig, V., Longair, M., Pietzsch, T., … Cardona, A. (2012). Fiji: an open-source platform for biological-image analysis. Nature Methods, 9(7), 676–682. doi:10.1038/nmeth.2019

Schneider, C. A., W. S. Rasband, and K. W. Eliceiri. 2012. NIH Image to ImageJ: 25 years of image analysis. Nature Methods 9: 671–675.

Schrader, J, Pillar, G, Kreft, H. Leaf-IT: An Android application for measuring leaf area. Ecol Evol. 2017; 7: 9731–9738. https://doi.org/10.1002/ece3.3485

Schwankl, L. J., & Prichard, T. (2009). Understanding Water Holding Characteristics. University of California Drought Management Web Site. http://UCManageDrought.ucdavis.edu

Schwankl, L., Prichard, T., & Fulton, A. (2020). Almond Irrigation Improvement Continuum (p. 3). Almond Board of California.

Senay, G., Budde, M., Verdin, J., & Melesse, A. (2007). A coupled remote sensing and simplified surface energy balance approach to estimate actual evapotranspiration from irrigated fields. Sensors, 7, 979-1000.

Shackel, K. A., Ahmadi, H., Biasi, W., Buchner, R., Goldhamer, D., Gurusinghe, S., ... & Yeager, J. (1997). Plant Water Status as an Index of Irrigation Need in Deciduous Fruit Trees. HortTechnology, 7(1), 23-29. https://doi.org/10.21273/HORTTECH.7.1.23

Shuttleworth, W. J., & Wallace, J. S. (1985). Evaporation from sparse crops-an energy combination theory. Quarterly Journal of the Royal Meteorological Society, 111, 839-855.

Siebert, S., Burke, J., Faures, J. M., Frenken, K., Hoogeveen, J., Döll, P., & Portmann, F. T. (2010). Groundwater use for irrigation—A global inventory. Hydrology and Earth System Sciences, 14(10), 1863–1880. https://doi.org/10.5194/hess-14-1863-2010

Smith, M. (2012). Yield response to water: the original FAO water production function. In P. Steduto, T. C. Hsiao, E. Fereres, & D. Raes (Eds.), Crop Yield Response to Water (pp. 19-32). Food and Agriculture Organization of the United Nations.

Snyder, R. L. (2005). Humidity Conversion. UC Davis Biometeorology Group, 2(1), 2-5. https://www.slideshare.net/AliAli127/hum-con

Snyder, R. L., Orang, M., Matyac, S., & Grismer, M. E. (2005). Simplified Estimation of Reference Evapotranspiration from Pan Evaporation Data in California. Journal of Irrigation and Drainage Engineering, 131(3), 249-253. https://doi.org/10.1061/(ASCE)0733-9437(2005)131:3(249)

Srivastava, A., Sahoo, B., Raghuwanshi, N. S., & Chatterjee, C. (2018). Modelling the dynamics of evapotranspiration using Variable Infiltration Capacity model and regionally calibrated Hargreaves approach. Irrigation Science, 36, 289-300.

Stanghellini, C. (1987). Transpiration of Greenhouse Crops: An Aid to Climate Management (PhD Thesis). Wageningen University, Wageningen, The Netherlands.

Stanhill, G. (2019). Evapotranspiration. In Reference Module in Earth Systems and Environmental Sciences. Elsevier.

Stéfan van der Walt, Johannes L. Schönberger, Juan Nunez-Iglesias, François Boulogne, Joshua D. Warner, Neil Yager, Emmanuelle Gouillart, Tony Yu and the scikit-image contributors. scikit-image: Image processing in Python. PeerJ 2:e453 (2014) https://doi.org/10.7717/peerj.453

Steiner, J. L., Howell, T. A., & Schneider, A. D. (1991). Lysimetric Evaluation of Daily Potential Evapotranspiration Models for Grain Sorghum. Agronomy Journal, 83, 240-247.

Steppe, K., Vandegehuchte, M., Tognetti, R., & Mencuccini, M. (2015). Sap flow as a key trait in the understanding of plant hydraulic functioning. Tree Physiology, 35(4), 341–345. https://doi.org/10.1093/treephys/tpv033

Stewart, W., Fulton, A., Krueger, W., Lampinen, B., & Shackel, K. (2011). Regulated deficit irrigation reduces water use of almonds without affecting yield. California Agriculture, 65(2), 90-95.

Still, C. J., Sibley, A., Page, G., Meinzer, F. C., & Sevanto, S. (2019). When a cuvette is not a canopy: A caution about measuring leaf temperature during gas exchange measurements. Agricultural and Forest Meteorology, 279, 107737.

Stoy, P. C., Mauder, M., Foken, T., et al., (2013). A data-driven analysis of energy balance closure across FLUXNET research sites: The role of landscape scale heterogeneity. Agricultural and Forest Meteorology, 171-172, 137-152. https://doi.org/10.1016/j.agrformet.2012.11.004

Subedi, A., & Chávez, J. L. (2015). Crop Evapotranspiration (ET) Estimation Models: A Review and Discussion of the Applicability and Limitations of ET Methods. Journal of Agricultural Science, 7, 50.

Tabari, H., & Talaee, P. H. (2011). Local Calibration of the Hargreaves and Priestley-Taylor Equations for Estimating Reference Evapotranspiration in Arid and Cold Climates of Iran Based on the Penman-Monteith Model. Journal of Hydrologic Engineering, 16, 837-845.

Talsma, C. J., Good, S. P., Jimenez, C., Martens, B., Fisher, J. B., Miralles, D. G., ... & Purdy, A. J. (2018). Partitioning of evapotranspiration in remote sensing-based models. Agricultural and Forest Meteorology, 260-261, 131-143.

Tanny, J. (2013). Microclimate and evapotranspiration of crops covered by agricultural screens: A review. Biosystems Engineering, 114, 26-43.

Tarnopolsky, M., & Seginer, I. (1999). Leaf temperature error from heat conduction along thermocouple wires. Agricultural and Forest Meteorology, 93, 185-194.

The GIMP Development Team. (2019). GIMP. Retrieved from https://www.gimp.org

Théroux-Rancourt, G., Jenkins, M. R., Brodersen, C. R., McElrone, A., Forrestel, E. J., & Earles, J. M. (2020). Digitally deconstructing leaves in 3D using X-ray microcomputed tomography and machine learning. Applications in Plant Sciences, 8(7), e11380. https://doi.org/10.1002/aps3.11380

Tiezen, L. L., Johnson, D. A., & Caldwell, M. M. (1974). A portable system for the measurement of photosynthesis using carbon-14 dioxide. Photosynthetica, 8, 151-160.

Tolk, J. A. (2003). Soils, Permanent Wilting Points. In Encyclopedia of Water Science. Taylor & Francis.

Tolk, J. A., Evett, S. R., & Howell, T. A. (2006). Advection Influences on Evapotranspiration of Alfalfa in a Semiarid Climate. Agronomy Journal, 98, 1646-1654.

Townend, J., Reeve, M., & Carter, A. (2001). Water release characteristics. In Soil and environmental analysis: Physical methods (2nd ed.). Marcel Dekker. https://doi.org/10.1201/9780203908600.ch3

Turan, M. A., Hassan, A., Elkarim, A., Taban, N., & Taban, S. (2009). Effect of salt stress on growth, stomatal resistance, proline and chlorophyll concentrations on maize plant. African Journal of Agricultural Research, 4, 893-897.

Van Leeuwen, C., & Seguin, G. (2006). The concept of terroir in viticulture. Journal of Wine Research, 17(1), 1-10. https://doi.org/10.1080/09571260600633135

Van Lier, Q. d. J. (2017). Field capacity, a valid upper limit of crop available water? Agricultural Water Management, 193, 214-220.

Varma V, Osuri AM (2013) Black Spot: a platform for automated and rapid estimation of leaf area from scanned images. Plant Ecol 214:1529–1534. doi:10.1007/s11258-013-0273-z

Vejlgaard, B., Lauridsen, M., Nguyen, H., Kovacs, I. Z., Mogensen, P., & Sorensen, M. (2017). Coverage and capacity analysis of Sigfox LoRa GPRS and NB-IoT. In IEEE 85th Vehicular Technology Conference, pp. 1-5.

Villarreal-Guerrero, F., Kacira, M., Fitz-Rodríguez, E., Kubota, C., Giacomelli, G. A., Linker, R., & Arbel, A. (2012). Comparison of three evapotranspiration models for a greenhouse cooling strategy with natural ventilation and variable high-pressure fogging. Scientia Horticulturae, 134, 210-221.

Wani, S. P., Anantha, K. H., Garg, K. K., Joshi, P. K., Sohani, G., Mishra, P. K., & Palanisami, K. (2016). Pradhan Mantri Krishi Sinchai Yojana: Enhancing Impact through Demand Driven Innovations, Research Report IDC-7.

Water Balance Irrigation Scheduling Using CIMIS ETo: Department of Land, Air, and Water Resources—UC Davis. (n.d.). Retrieved May 17, 2021, from https://lawr.ucdavis.edu/cooperative-extension/irrigation/drought-tips/water-balance-irrigation-scheduling-using-cimis-eto

Webb, C. P. (2010). Bureau of meteorology reference evapotranspiration calculations.

Weight C, Parnham D, Waites R (2008) LeafAnalyser: a computational method for rapid and large-scale analyses of leaf shape variation. Plant J 53:578–586. doi:10.1111/j.1365-313X.2007.03330.x

Williams, D. G., Cable, W., Hultine, K., Hoedjes, J. C. B., Yepez, E. A., Simonneaux, V., Er-Raki, S., Boulet, G., de Bruin, H. A. R., Chehbouni, A., Hartogensis, O. K., & Timouk, F. (2004). Evapotranspiration components determined by stable isotope, sap flow, and eddy covariance techniques. Agricultural and Forest Meteorology, 125(3), 241-258.

Williams, L. E., & Fidelibus, M. W. (2016). Measured and estimated water use and crop coefficients of grapevines trained to overhead trellis systems in California's San Joaquin Valley. Irrigation Science, 34(6), 431-441.

Wilson, K. B., Hanson, P. J., & Baldocchi, D. D. (2000). Factors controlling evaporation and energy partitioning beneath a deciduous forest over an annual cycle. Agricultural and Forest Meteorology, 102, 83-103.

Xue, J., Anderson, M. C., Gao, F., et al., (2022). Improving the spatiotemporal resolution of remotely sensed ET information for water management through Landsat, Sentinel-2, ECOSTRESS, and VIIRS data fusion. Irrigation Science. https://doi.org/10.1007/s00271-022-00799-7

Yan, H., Huang, S., Zhang, C., Gerrits, M. C., Wang, G., Zhang, J., Zhao, B., Acquah, S. J., Wu, H., & Fu, H. (2020). Parameterization and Application of Stanghellini Model for Estimating Greenhouse Cucumber Transpiration. Water, 12, 517.

Yu, L., Wang, W., Zhang, X., & Zheng, W. (2016). A Review on Leaf Temperature Sensor: Measurement Methods and Application. In Computer and Computing Technologies in Agriculture IX; Li, D., Li, Z., Eds.; Springer: Cham, Switzerland, Volume 478, pp. 216-230.

Yuan, Q., Shen, H., Li, T., Li, Z., Li, S., Jiang, Y., Xu, H., Tan, W., Yang, Q., Wang, J., et al., (2020). Deep learning in environmental remote sensing: Achievements and challenges. Remote Sensing of Environment, 241, 111716.

Zhang, K., Kimball, J. S., Mu, Q., Jones, L. A., Goetz, S. J., & Running, S. W. (2009). Satellite-based analysis of northern ET trends and associated changes in the regional water balance from 1983 to 2005. Journal of Hydrology, 379, 92-110.

Zhang, K., Kimball, J. S., Nemani, R. R., & Running, S. W. (2010). A continuous satellite-derived global record of land surface evapotranspiration from 1983 to 2006. Water Resources Research, 46, W09522.

Zhang, K., Kimball, J. S., & Running, S. W. (2016). A review of remote sensing based actual evapotranspiration estimation. WIREs Water, 3, 834-853. https://doi.org/10.1002/wat2.1168

Zhang, K., Li, X., Zheng, D., Zhang, L., & Zhu, G. (2022). Estimation of global irrigation water use by the integration of multiple satellite observations. Water Resources Research, 58, e2021WR030031. https://doi.org/10.1029/2021WR030031

Zhang, Z., Tian, F., Hu, H., & Yang, P. (2014). A comparison of methods for determining field evapotranspiration: photosynthesis system, sap flow, and eddy covariance. Hydrology and Earth System Sciences, 18, 1053-1072. https://doi.org/10.5194/hess-18-1053-2014